A GRAVITATIONAL INVESTIGATION OF THE SCIPIO OIL FIELD IN HILLSDALE COUNTY, MICHIGAN, WITH A RELATED STUDY FOR OBTAINING A VARIABLE ELEVATION FACTOR

Thesis for the Degree of Ph. D.
MICHIGAN STATE UNIVERSITY
DONALD WARREN MERRITT
1968





This is to certify that the

thesis entitled

A GRAVITATIONAL INVESTIGATION OF THE SCIPIO OIL FIELD IN HILLSDALE COUNTY, MICHIGAN, WITH A RELATED STUDY FOR OBTAINING A VARIABLE ELEVATION FACTOR

presented by

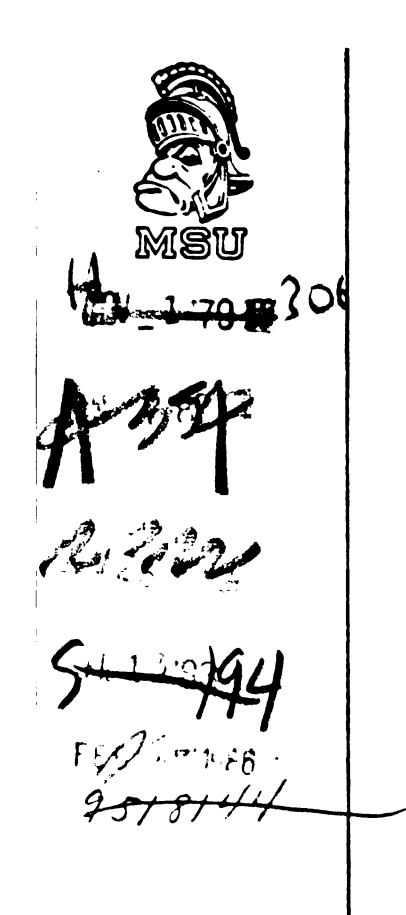
Donald Warren Merritt

has been accepted towards fulfillment of the requirements for

Ph.D. degree in Geology

Dato Major professor

Dato Major professor



ABSTRACT

A GRAVITATIONAL INVESTIGATION OF THE SCIPIO OIL FIELD IN HILLSDALE COUNTY, MICHIGAN, WITH A RELATED STUDY FOR OBTAINING A VARIABLE ELEVATION FACTOR

by Donald Warren Merritt

A detailed gravity survey was conducted in the north central portion of Hillsdale County, Michigan for the purpose of delineating gravity anomalies associated with the Scipio Oil Field. The error in the Bouguer gravity reduction caused by near surface density variations in the glacial drift was minimized by a method developed for obtaining an individual station elevation factor from the elevation and observed gravity values of surrounding stations.

Fourier analysis involving band pass filters is successful in isolating elongate positive anomalies which are associated with the geographical location of the Scipio Field. These anomalies have a magnitude in excess of 0.2 mgal and are similar to those theoretically calculated from a geologic model of the producing zone based on porosity values obtained from core analysis.

The complexity of the Bouguer surface in the study area precludes the objective use of polynomial and double Fourier series analysis for delineating anomalies associated with the production.

A regional gravity profile striking northeast into the Michigan Basin reveals a displacement in the uniform gravity gradient. This displacement, which occurs along the Albion-Scipio Oil Field is interpreted to originate from basement topographic relief in the form of a fault-line scarp. Renewed activity along the fault associated with the scarp may have established the conditions necessary for the development of the linear Albion-Scipio Oil Field.



A GRAVITATIONAL INVESTIGATION OF THE SCIPIO OIL FIELD IN HILLSDALE COUNTY, MICHIGAN, WITH A RELATED STUDY FOR OBTAINING A VARIABLE ELEVATION FACTOR

Ву

Donald Warren Merritt

A THESIS

Submitted to

Michigan State University
in partial fulfillment of the requirements
for the degree of

DOCTOR OF PHILOSOPHY

Department of Geology

Copyright by
DONALD WARREN MERRITT
1969

ACKNOWLEDGMENTS

The author wishes to express his sincere thanks to the following individuals and organizations.

To Dr. W. J. Hinze for his deep interest and guidance throughout the project.

To Dr. H. B. Stonehouse, Dr. J. W. Trow, and the late Dr. J. Zinn for their active participation on the guidance committee.

To the McClure Oil Company, Alma, Michigan, for financial assistance in the gathering of the data, and to Messers F. P. Hurry and W. K. Roth for providing geological insight into the problem.

To Messers G. D. Ells and F. Layton of the Michigan Geological Survey, Department of Conservation, for fruitful discussions concerning the regional aspect of the study.

To Messers J. Roth, R. G. Geyer, R. Ehlinger, and S. Wilke whose hard work made the gathering of the data possible.

To Michigan State University for the free use of the C. D. C. 3600 computer.

TABLE OF CONTENTS

																Page
ACKNO	WLE	DGM	ENTS	3.	•	•	•	•	•	•	•	•	٠	•	•	iii
LIST	OF	TAB	LES	•	•	•	•	•	•	•	•	•	•	•	•	vi
LIST (OF	FIG	URES	S .	•	•	•	•	•	•	•	•	•	•	•	vii
INTRO	DUC	TIO	N.	•	•	•	•	•	•		•	•	•		•	1
	Ap Lo	pro cat	tive ach ion ogra	of	the	Sti	ady	Are	· ea	•	•	•	•	•	•	1 3 4 4
GEOLO	GIC	AL	SETI	INC	·	•	•	•	•	•	•	•	•	•	•	7
FIELD	ME	THO	DS.	•	•	•	•	•			•	•	•	•	•	11
DATA 1	RED	UCT	ION	•	•	•	•	•	•	•	•	•		•	•	12
	La	tit	ved ude tior	Cor	rec	tion		•	•		•	•	•	•	•	12 12 13
		Pr	nera evic	us	Wor	k.	•		•	•	•	•	•		•	13 14
		Th	proa Ele eory evat	vat	ion.	Fac	tor.	·	•		•	•	•	•	•	18 19 20
					y M y M										•	21
			Gra		l Be y M						cia	•	rif	t.	•	24
			Gra	and vit	Re y M	ef S	Strı L of	cti A	ire ll t	the	So	urc	• es	•	•	36 44
			1110		hin	_										53

		Pa	ge
Decreasing the Station Spacing . Altering the Elevation Datum		•	53 57
Summary of the Model Studies	•	•	59
Elevation and Mass Correction for the Field Data	•	•	61
METHODS OF DATA ANALYSIS	•	•	68
Polynomial Approximations to the Bougue Surface	er	•	69
Double Fourier Series Analysis	•	•	70
Linear Filtering Methods	•	•	74
Theory	•	•	77 80
Regional	•	•	82
Regional		•	92 92
INTERPRETATION	•	. 1	.01
Model Study of the Scipio Oil Field . Geological Factors Which Will Distort	•	. 1	.01
the Anomaly	•		.02 .07
Least Squares Residuals		. 1	.07 .07 .08 .08
Regional Interpretation	•		.09 .13
Residual	•		.13 .14
CONCLUSIONS	•	. 1	.15
REFERENCES		. 1	18

LIST OF TABLES

Table								Page
1.	Porosity Analys	Values			•	•	•	104

LIST OF FIGURES

Figure	e	P	age
	GENERAL		
1.	Trenton-Black River Annual Oil Production	•	2
2.	Location of the Survey	•	5
3.	Geologic Column of Michigan	•	8
4.	Trenton Structure Map	•	9
5.	Elevation Factor Chart	•	15
	MODEL STUDIES		
6.	Plan View Map of the Sources of Anomalies	•	22
7.	Model Study Elevations	•	23
	MODEL INVOLVING THE GLACIAL DRIFT		
8-a.	Graph of the Error in the Calculated Density Values-5th Degree	•	25
8-b.	Graph of the Error in the Calculated Gravity Values-5th Degree	•	25
9.	Map of the Individual Station Density Error-5th Degree	•	26
10.	Map of the Individual Station Gravity Error-5th Degree	•	27
	GRAVITY MODEL INVOLVING THE GLACIAL DRIFT AND RIVER CHANNEL		
11.	Calculated Gravity Effect of the Buried River Channel	•	28
12 - a.	Graph of the Error in the Calculated Density Values-3rd Degree	•	30
12 - b.	Graph of the Error in the Calculated Gravity Values-3rd Degree	•	30

Figure		Page
13-a.	Graph of the Error in the Calculated Density Values-5th Degree	31
13-b.	Graph of the Error in the Calculated Gravity Values-5th Degree	31
14.	Map of the Individual Station Density Error-3rd Degree	32
15.	Map of the Individual Station Density Error-5th Degree	33
16.	Map of the Individual Station Gravity Error-3rd Degree	34
17.	Map of the Individual Station Gravity Error-5th Degree	35
	GRAVITY MODEL INVOLVING THE GLACIAL DRIFT AND REEF STRUCTURE	
18.	Calculated Gravity Effect of the Reef Structure	37
19-a.	Graph of the Error in the Calculated Density Values-3rd Degree	38
19-b.	Graph of the Error in the Calculated Gravity Values-3rd Degree	38
20 - a.	Graph of the Error in the Calculated Density Values-5th Degree	39
20-b.	Graph of the Error in the Calculated Gravity Values-5th Degree	39
21.	Map of the Individual Station Density Error-3rd Degree	40
22.	Map of the Individual Station Gravity Error-3rd Degree	41
23.	Map of the Individual Station Density Error-5th Degree	42
24.	Map of the Individual Station Gravity Error-5th Degree	43

Figure		Page
	GRAVITY MODEL INVOLVING ALL THE SOURCES	
25.	Gravity Effect of the Combined Sources	45
26-a.	Graph of the Error in the Calculated Density Values-3rd Degree	46
26-b.	Graph of the Error in the Calculated Gravity Values-3rd Degree	46
27-a.	Graph of the Error in the Calculated Density Values-5th Degree	47
27-b.	Graph of the Error in the Calculated Gravity Values-5th Degree	47
28.	Map of the Individual Station Density Error-3rd Degree	48
29.	Map of the Individual Station Gravity Error-3rd Degree	49
30.	Map of the Individual Station Density Error-5th Degree	50
31.	Map of the Individual Station Gravity Error-5th Degree	51
	COMPARISON OF ALL THE MODELS	
32 - a.	Graph of the Error in the Calculated Density Values-5th Degree	52
32-b.	Graph of the Error in the Calculated Gravity Values-5th Degree	52
	INCREASED DENSITY CONTRAST IN THE GLACIAL DRIFT	
33-a.	Graph of the Error in the Calculated Density Values-5th Degree	54
33-b.	Graph of the Error in the Calculated Gravity Values-5th Degree	54
34.	Map of the Individual Station Density Error-5th Degree	5 5

Figure		Page
35.	Map of the Individual Station Gravity Error-5th Degree	56
	DECREASED STATION SPACING	
36.	Map of the Individual Station Density Values-1st Degree	58
	ELEVATION DATUM ALTERED	
37.	Map of the Elevations After Raising the Elevation Datum	60
	FIELD STUDIES	
38.	Contour Map of the Survey Elevations	62
39.	Map of the Residual Elevations from a Third Degree Polynomial Approximation to the Elevation Surface	63
40.	Variable Density Map	64
41.	Profile of the Residual Elevations- Density Values-Bouguer Gravity	66
42.	Map of the Bouguer Gravity	67
	POLYNOMIAL APPROXIMATIONS	
43.	Profile of the Bouguer Gravity and the Residual Values from the 7th Degree Polynomial Approximation	71
44.	Map of the Residual Values from the 7th Degree Polynomial Approximation to the Bouguer Surface	72
	DOUBLE FOURIER SERIES APPROXIMATIONS	
45.	Profile of the Bouguer Gravity and the Residual Values	75
46.	Map of the Residual Values from the Double Fourier Series Approximation to the Bouguer Surface	76

Figure		Page
	BAND PASS FILTERING	
47.	Frequency Response of Band Pass and Low Pass Filters	81
48.	Profile of the Bouguer Gravity and Residual Values from the Band Pass Filters	83
49.	Residual Map of Half Wavelengths from 10,000 to 30,000 Feet	84
50.	Residual Map of Half Wavelengths from 5,000 to 15,000 Feet	85
51.	Residual Map of Half Wavelengths from 2,500 to 7,500 Feet	86
	LOW PASS FILTERING	
52.	Profile of the Bouguer Gravity and Residual Values from the Low Pass Filters	87
53.	Residual Map of Half Wavelengths from Infinity to 20,000 Feet	88
54.	Residual Map of Half Wavelengths from Infinity to 10,000 Feet	89
55.	Residual Map of Half Wavelengths from Infinity to 5,000 Feet	90
56.	Residual Map of Half Wavelengths from Infinity to 2,500 Feet	91
	HIGH PASS FILTERING	
57.	Profile of the Bouguer Gravity and Residual Values from the High Pass Filters	93
58.	Residual Map of Half Wavelengths Less Than 20,000 Feet	94
59.	Residual Map of Half Wavelengths Less Than 10,000 Feet	95
60.	Residual Map of Half Wavelengths Less Than 5,000 Feet	96

Figure		Page
	COMBINED HIGH AND LOW PASS FILTERING	
61.	Profile of the Bouguer Gravity and Residual Values from the Combined High and Low Pass Filters	97
62.	Residual Map of Half Wavelengths from 10,000 to 20,000 Feet	98
63.	Residual Map of Half Wavelengths from 5,000 to 20,000 Feet	99
64.	Residual Map of Half Wavelengths from 2,500 to 20,000 Feet	100
	MODEL STUDY OF THE SCIPIO OIL FIELD	
65.	Calculated Gravity Anomaly of the Scipio Oil Field for a Density Contrast of 0.05 gm/cc Between the Dolomite and Dolomitic Limestone	103
66.	Calculated Gravity Anomaly of the Scipio Oil Field for a Density Contrast of O.125 gm/cc Between the Dolomitic Lime- stone and Dolomite	106
	REGIONAL GRAVITY STUDY	
67.	Regional Gravity Profile Through Berry, Hillsdale, and Jackson Counties, Michigan	110

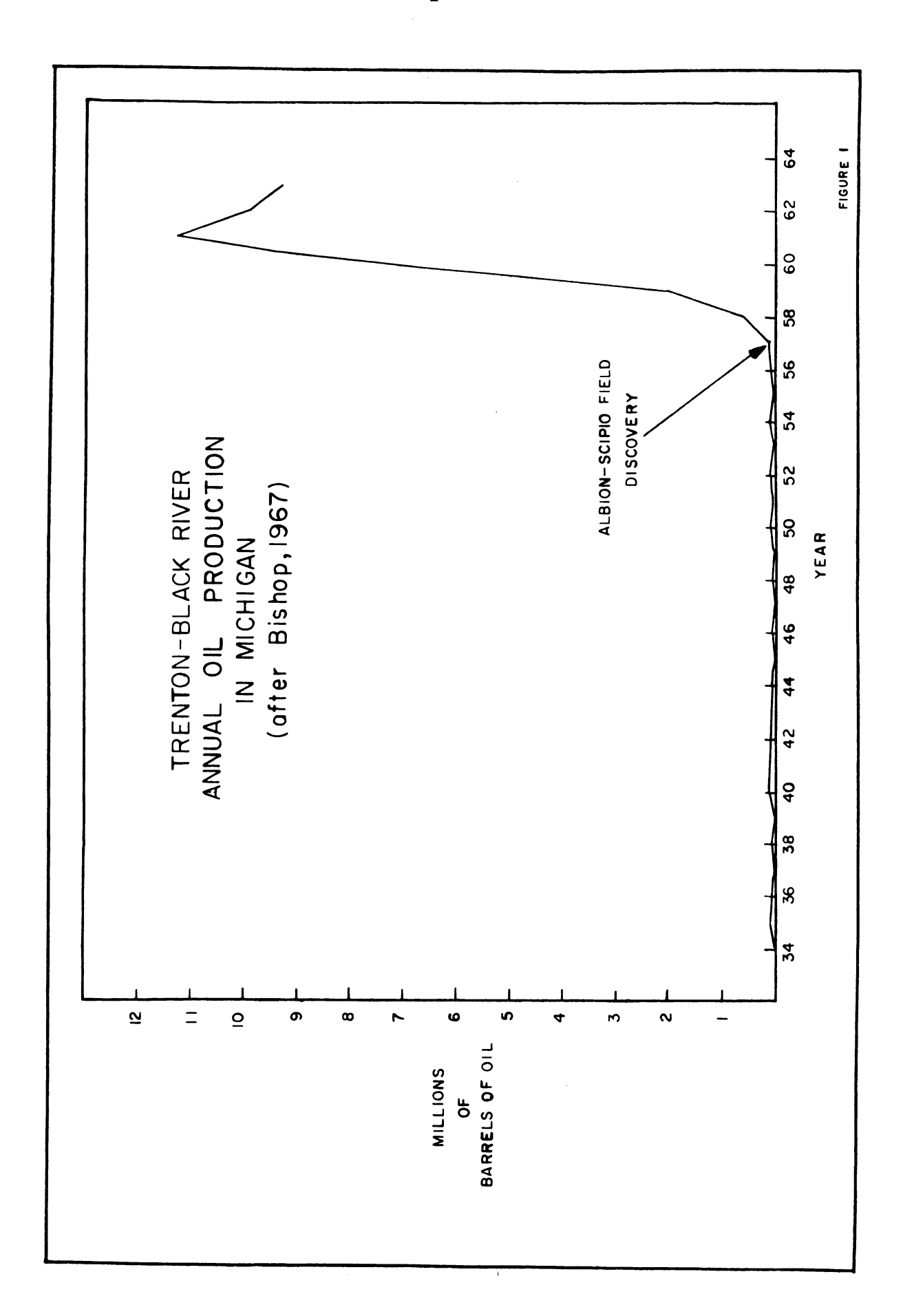
INTRODUCTION

Objective

The 1957 discovery of oil in an anomalous dolomite zone in the Middle Ordovician rocks of Hillsdale County, Michigan, led to the eventual development of the Albion-Scipio Oil Field. Preceding the discovery, the annual production from the Trenton and Black River Formations in Michigan was slightly in excess of 10,000 barrels. By 1961, the annual production approached the 12 million mark as shown in Figure 1. The Albion-Scipio Field is located in Hillsdale, Jackson, and Calhoun Counties and, although the length exceeds 35 miles, the average width is less than one mile.

Geological exploration methods used for extending the production proved unsatisfactory, resulting in a large increase in geophysical activity involving both seismic and gravity methods. The confidential nature of these company conducted investigations has resulted in a paucity of published information on the applicability of the geophysical approach to delineating the geographical location of the production.

The lack of published information, other than the results of an isolated gravity profile across the area by



Ferris (1962), provided the incentive for conducting a gravity investigation in the north central portion of Hillsdale County. The threefold purpose of the investigation was to develop a method of minimizing the error in the Bouguer gravity reduction due to near surface density variations, study the applicability of representative gravity anomaly enhancement methods for isolating the anomaly directly or indirectly associated with the Scipio Oil Field, and ascertain the geological source of the gravity anomaly associated with the Scipio Oil Field.

Approach

A generalized three dimensional geological model of the producing structure was constructed from subsurface geological data. Appropriate density contrasts between the productive dolomite and the non-productive dolomitic limestone host rock were assigned to the model, and the gravity effect of the structure calculated at the surface elevations. This study provided limits on the magnitude and configuration of the associated gravity anomaly.

The error in the assumed density value used on the Bouguer gravity reduction may mask the small magnitude geologically significant gravity anomalies. This problem is common to gravity surveying throughout Michigan, but is particularly pronounced in the area of the Scipio Field. The marked surface topography, and the abrupt

horizontal changes in the composition of the glacial drift precluded the use of a single density value. As a result, a method was developed and evaluated through the use of model studies by which a near surface representative density value is obtained from the gravity data for each station in the survey.

The field data was corrected with individual station elevation factors, and the Bouguer gravity was analyzed with polynomial, double Fourier series and linear filtering methods.

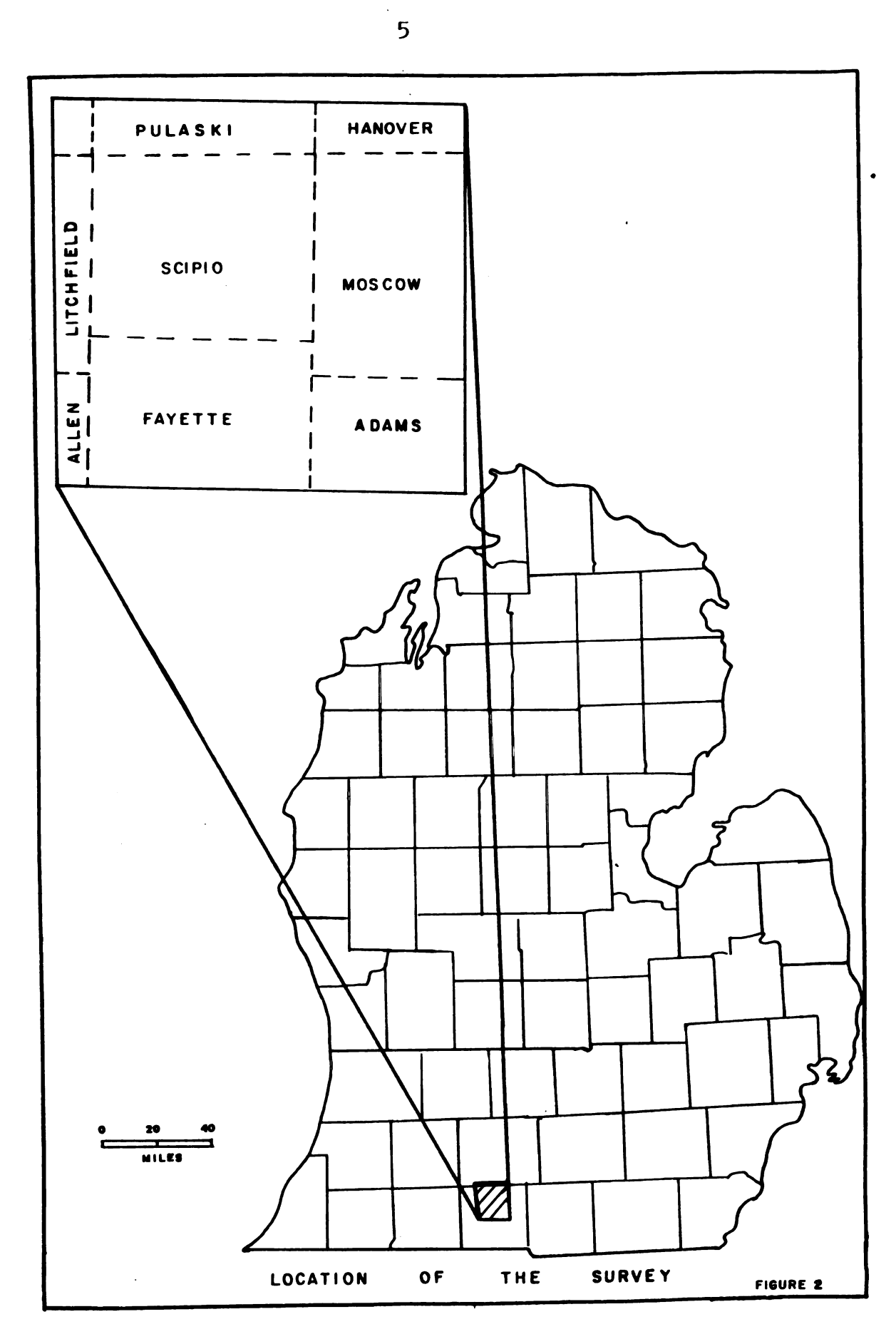
Location of the Study Area

The geographical location of the area of investigation includes portions of Allen, Litchfield, Scipio,
Fayette, Moscow, and Adams Townships in Hillsdale
County, and small portions of Pulaski and Hanover Townships in Jackson County, Michigan. Figure 2 is a location map of the area of investigation.

Physiography of the Study Area

The physiographic character of the county is appropriately described by Veatch (1924) in the statement that,

... the relief is largely constructional, due mainly to the uneven disposition of a thick layer of glacial material. The county has the rolling or billowy surface, smooth rounded slopes, sandy and gravelly knobs and ridges, numerous lakes and swampy depressions, sandy and gravelly plains, and nearly level clay plains characteristic of land of glacial origin.



The elevations in the survey area range from 1,000 to 1,300 feet.

GEOLOGICAL SETTING

In 1957, random drilling resulted in commercial production from the Middle Ordovician carbonates in Hillsdale County, with subsequent drilling resulting in the development of the Albion-Scipio Field. The production comes from the Trenton-Black River Formations (Figure 3) and is confined to an anomalous dolomite zone formed in the regionally dolomitic limestone province. The vertical extent of the dolomite zone is not defined due to the lack of drilling below the oil-water contact, but is at least 610 feet thick.

A structure contour map on top of the Trenton Formation is shown in Figure 4, illustrating the northwest regional dip that controls the -2750 foot gas-oil contact datum and the -2920 foot oil-water contact datum in the Scipio Field (Bishop, 1967).

Bishop concludes from his Albion-Scipio Field study that it,

... exhibits a northwest-southeast trending syncline developed on the Middle Ordovician Trenton limestone. This northwest plunging syncline has approximately 30 feet of relief, and is directly associated with fracturing, solution activity, dolomitization, and the development of a porosity oil trap in the Trenton-Black River limestones. The Albion-Scipio Field was formed in Devonian time by a movement along lines of pre-existing weakness

STRATIGRAPHIC SUCCESSION IN MICHIGAN PALEOZOIC THROUGH RECENT SYSTEM CENOZOIC COCHERCISES County with the second of schapes in the department, the U I flow legared former. Makingar's automation, other man Contegue former, and produces within Makingar's of and part relation. In Armad 1 County, Department of Goodage, Makingar San-County, Sandard of Tourney, Sandard of County, Sandard of County, Sandard of County, Sandard of San SUBSURFACE NOMENCLATURE OUTCROP NOMENCLATURE FORMATION MEMBER Grand River In. Square Bay La _ Opper part of Transmit Group in Wastern Michigan MISSISSIPPIAN DEVON Region City In ___ ~ Part of Salma Group I Unit __ Garobare Fin. Ferrum Robb Fin. Bradgoot Charry Le. Bad Sh. Bragers City Le. Dander Le. Anderdon Fin. MIS SLANES Pa au Chron Si RIAN Cardell Del. Schoolcraft Del. Mandricks Del. Byron Del. Lime Island Del. BACK BMB 3 TOTAL TOTA

FIGURE 3 .-- Geologic Column of Michigan

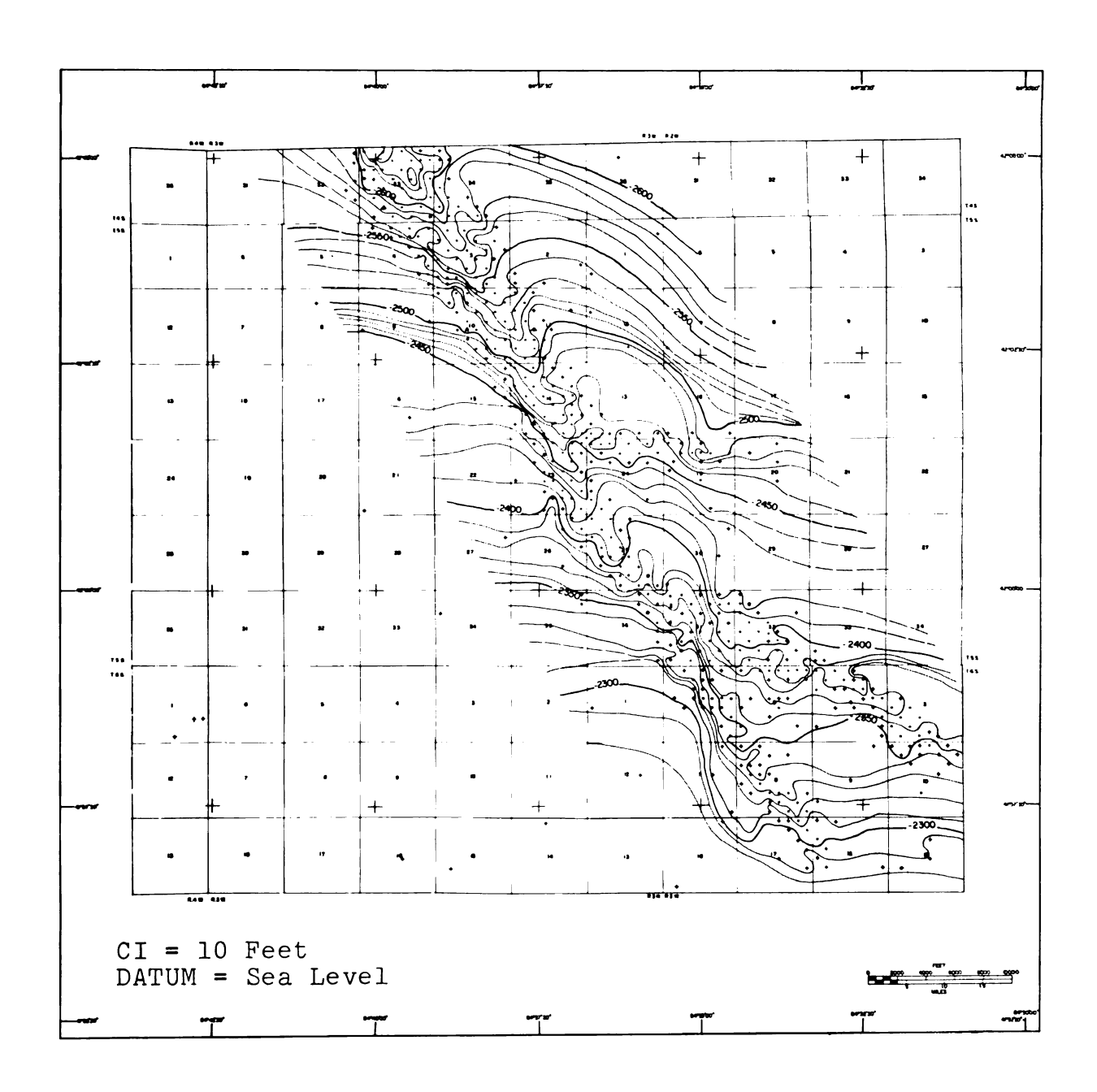


FIGURE 4.--Structure map on top of the Trenton Formation.

in the basement complex. The movement was reflected in the tilted Trenton-Black River limestones not as a single continuous fracture, but as a system of fractures trending northwest-southeast. These fractures served as a channel way for solutions that dissolved the calcium carbonate and provided sufficient additional magnesium ions to make possible the precipitation of dolomite. This solution activity created an approximate 8-9% loss of volume of the Trenton-Black River Formations. Devonian sedimentation filled the subsiding depression and it was no longer present after Devonian time. . .

FIELD METHODS

Gravity readings were taken along all available roads at approximate 500 foot intervals. Additional traverses were run cross-country where the road system failed to provide uniform coverage in the area, and where it was desirable to have additional coverage across the production. Regional coverage was extended through the use of gravity readings from a previous quarter mile station spacing survey. Accuracy of the meter readings was maintained by taking repeat observations at each station until duplication was obtained within 0.2 scale divisions (sd.). World Wide Meter number 45 (calibration constant of 0.10093 mgal/sd) was used throughout the survey.

Station elevations were established by leveling. Elevation control was maintained by tying to U. S. Geological Survey bench marks and closing all traverse lines. The largest closure error throughout the survey was less than 0.25 feet.

DATA REDUCTION

Observed Gravity

Base ties were made on an hourly interval and the mid-hour station reoccupied immediately after the base tie. Drift curves were used to eliminate meter drift and tidal effects. The drift rate between base ties was checked by the mid-hour repeat reading. If the drift rate exceeded a scale division per hour, or the mid-hour repeat reading did not check within 0.2 sd., the stations observed within that hour were reoccupied. After correcting the station readings for meter drift, they were multiplied by the meter constant to obtain the station observed gravity.

Latitude Correction

Station distances were calculated from the stadia intervals and plotted on 7-1/2 minute U. S. Geological Survey topographic sheets. The station coordinates were taken from the topographic sheets in reference to the Michigan Coordinate System, East Zone, established by the U. S. Coast and Geodetic Survey.

Latitude corrections were made by rotating out of this system into the latitude and longitude system and applying a correction factor of 0.0002474 mgal/ft.

Elevation and Mass Correction

General Statement

The elevation correction compensates for the normal vertical gradient of gravity by applying a correction factor to the difference in elevation between the station and a reference datum. The mass correction compensates for the mass of a horizontal sheet of infinite extent and thickness equal to this same elevation difference.

Because both corrections are linear functions of the elevation, they can be combined and expressed as

$$g(em) = (0.09406 - 0.01276 \sigma) h$$
 (1)

where h is the elevation difference in feet between the station and the datum, and σ is the density in cgs units assumed for the material within this interval. Throughout the remainder of this report, the combined correction will be referred to as the elevation factor.

The small magnitude (generally less than 0.3 mgals) of the geologically significant anomalies in the survey area combined with the pronounced surface topography and abrupt horizontal changes in the glacial drift composition precludes the use of a single density value for the entire area. The use of a single density value and the ensuing errors for other geological conditions are presented in an excellent review of the subject by Vajk (1956).

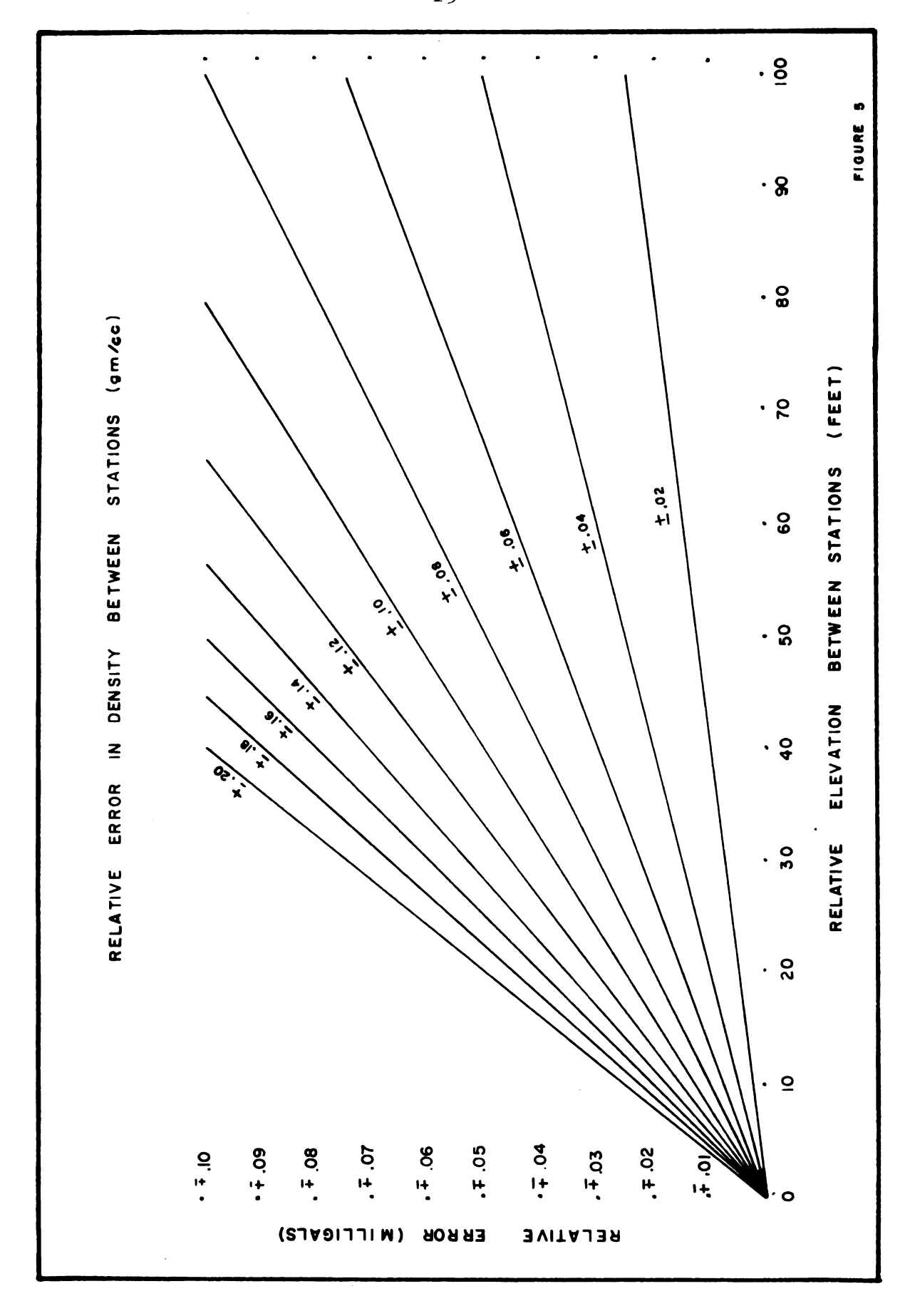
The relative error in gravity between two stations for a relative error in density is shown in Figure 5 as a function of the elevation differences. This graph, modified from Ivanhoe (1957), provides an easy method for checking the feasibility of a suspected correlation between an anomaly and the corresponding topographic feature. For example, a 0.1 mgal anomaly would be created by a 40 foot high topographic feature if the density assumed in the Bouguer reduction was 0.2 gm/cc too low.

Previous Work

The importance of the elevation factor in gravity surveying has been stressed in many published papers and a variety of techniques have been developed to minimize this error in the reduction of gravity data. The most significant of these methods are reviewed to provide background for the method developed in this study.

Nettleton (1939) was the first to publish a method for obtaining a local representative elevation factor from the gravity data. His approach involved

. . . making a special traverse of gravimeter stations across a topographic feature, reducing these stations for several different densities, and finding the density value for which the reduced curve had a minimum correlation with the topography. In this method, the sample is an entire topographic unit and the value obtained is the average density of all material within the elevation range of the gravity traverse.



Nettleton's method was later put into a computational form by Jung (1953).

Siegert (1942) assumes the gravity in the profile varies linearly with distance. He draws straight lines through the gravity and elevation values of the stations on either side of a station, and interpolates the gravity and elevation for that station from the straight lines. This process is repeated for all stations in the profile. For each station, the difference between the actual gravity and elevation value and the interpolated value will satisfy the equation

$$g = -kh \tag{2}$$

where g = the difference between the actual and interpolated gravity.

h = the difference between the actual and interpolated elevation, and

k = the elevation factor.

The quantity

$$\Sigma(g + kh)^2 \tag{3}$$

is minimized and the representative elevation factor for the entire profile is obtained.

The use of gravity profiles for determining a local elevation factor is limited to areas where there is no correlation between the gravity values and the

topographic features, there are no density changes within the length of the profile, and the gravity anomalies are smooth in comparison to the topographic relief. Another severe limitation of the profile method is the amount of field work required to establish the areal limits for which an elevation factor will apply.

In an attempt to circumvent some of the limitations of profile methods, Grant and Elsaharty (1962) extended the principles of profiling to include all of the data in the survey area. After reducing the gravity data with an arbitrary constant density value, they digitized both the elevation and Bouguer gravity maps onto a grid base. Both of these gridded maps are subjected to a least squares trend removal process to obtain the residual values. The true gravity residual (g) is then represented by the equation

$$g = rg + k(x, y) h (4)$$

where rg = residual gravity values

h = residual elevation values, and

k(x,y) = the elevation factor to be determined as some polynomial function of the coordinates.

The coefficients for the elevation factor are obtained by using the least squares method to minimize the function (g), and are used to alter the original density value to produce the optimum density value for a given set of coordinates.

Legge (1944) suggested using a polynomial function of the elevation and station coordinates to represent the Bouguer gravity in the area. The difference between the polynomial representation and the actual values is minimized by the least squares method to produce an elevation factor for a data set. This method is developed here to produce an elevation factor for each station in the survey, based on the observed gravity values and elevation differences of the immediately surrounding stations. The method has the advantage of requiring no preliminary data reduction, and eliminates the need for determining the areal limits for which a given density value should apply.

Approach for Obtaining a Variable Elevation Factor

The data set to be used for obtaining an elevation factor for a given station is composed of observed gravity and elevation values of all stations which fall within a predetermined radius of the station. The coordinates of the stations in the data set are made relative to the coordinates of the center station and the observed gravity values of the data set are approximated with a polynomial equation. The equation is a first degree function of the station elevations, and a first, third, or fifth degree function of the station coordinates.

The least squares process produces a set of coefficients for the polynomial equation. The coefficient
associated with the elevation term is the desired elevation
factor for the center station and is based on the observed
gravity and elevation values of the immediately surrounding stations.

Theory

The first degree polynomial equation can be expressed as

$$Ogp = Ko + Kl \Sigma x (i) + K2 \Sigma y (i) - K3 \Sigma h(i) (5)$$

where Ogp = the predicted observed gravity,

K(i) =the coefficients (i = 0,1,2,3)

The function Ogp is chosen such that

$$F(K) = \Sigma (Og - Ogp)^2$$
 (6)

is a minimum, where Og is the measured observed gravity.

The coefficients of Ogp are found by solving the equations obtained by setting the first partial derivatives of F equal to zero. These equations may be expressed in matrix form as:

$$\begin{bmatrix} N & \Sigma X & \Sigma Y & -\Sigma h \\ \Sigma X & \Sigma X^2 & \Sigma XY & -\Sigma h X \\ & & & & \\ \Sigma Y & \Sigma XY & \Sigma Y^2 & -\Sigma h Y \\ & -\Sigma h & -\Sigma Xh & -\Sigma Yh & \Sigma h^2 \end{bmatrix} \cdot \begin{bmatrix} K_0 \\ K_1 \\ K_2 \\ K_3 \end{bmatrix} = \begin{bmatrix} \Sigma O_g X \\ \Sigma O_g Y \\ \Sigma O_g Y \\ \Sigma O_g h \end{bmatrix}$$
(7)

or symbolically as

$$[A] \cdot [B] = [C]$$
 . (8)

The values in the coefficient matrix are obtained by multiplying both sides of the equation by the inverse of the A matrix to give

$$[B] = [A]^{-1} \cdot [C]$$
 (9)

The last term in the coefficient matrix is the elevation factor obtained from the data set. Higher order polynomials in x and y require expanding the matrix equations.

Elevation of the Proposed Method

The accuracy of the proposed method was evaluated through the use of gravity models. Geological conditions, ring size, and degree of approximating polynomial were varied in these models to determine their effect on the accuracy of the method. The accuracy is determined by comparing the known density and Bouguer gravity values

with the values obtained through the use of the calculated elevation factor. The Bouguer gravity was calculated by the equation

$$GBA_{c} = Og + Ef x h$$
 (10)

where GBA = calculated Bouguer gravity

Og = measured observed gravity and not the predicted

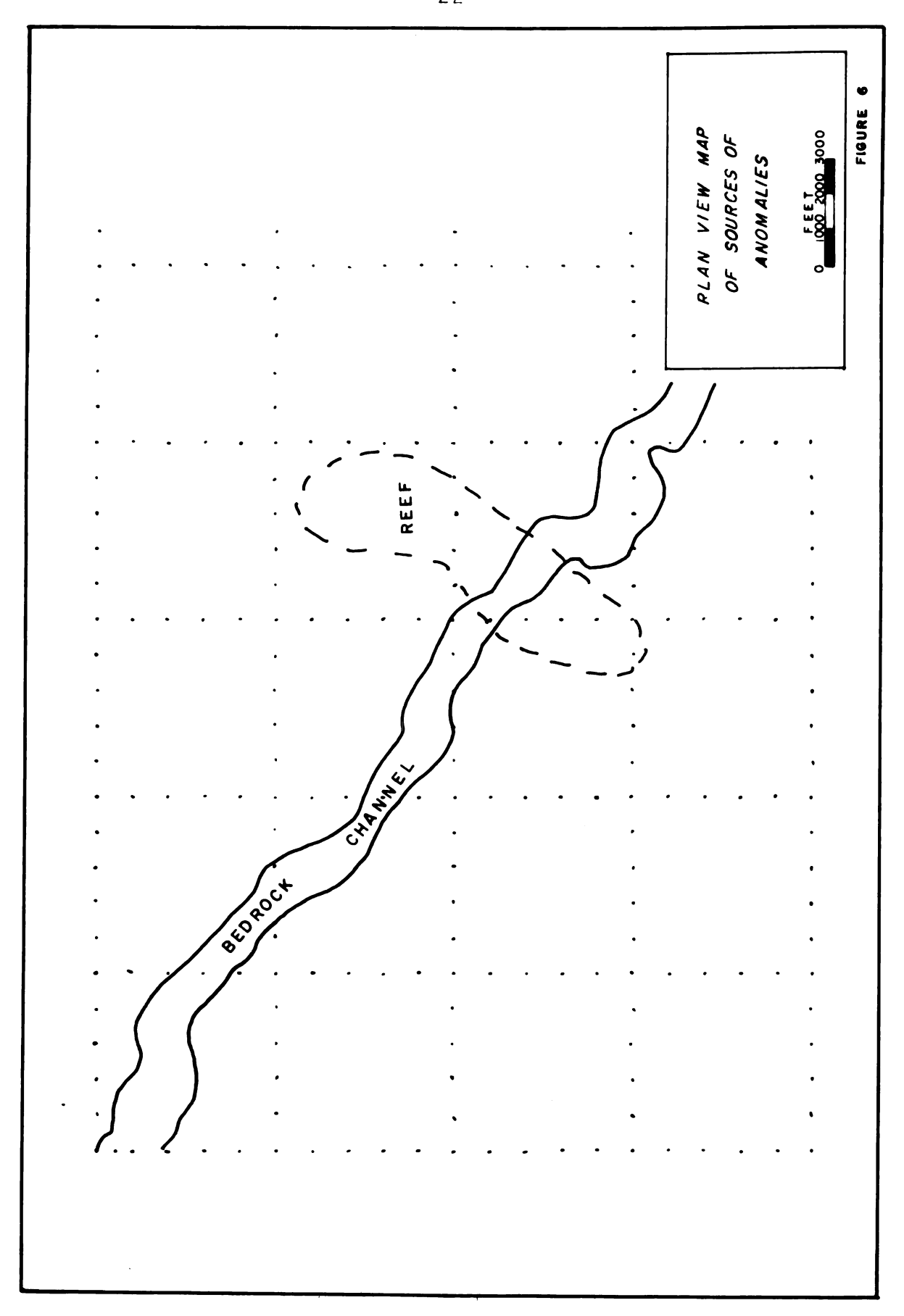
Ef = calculated elevation factor

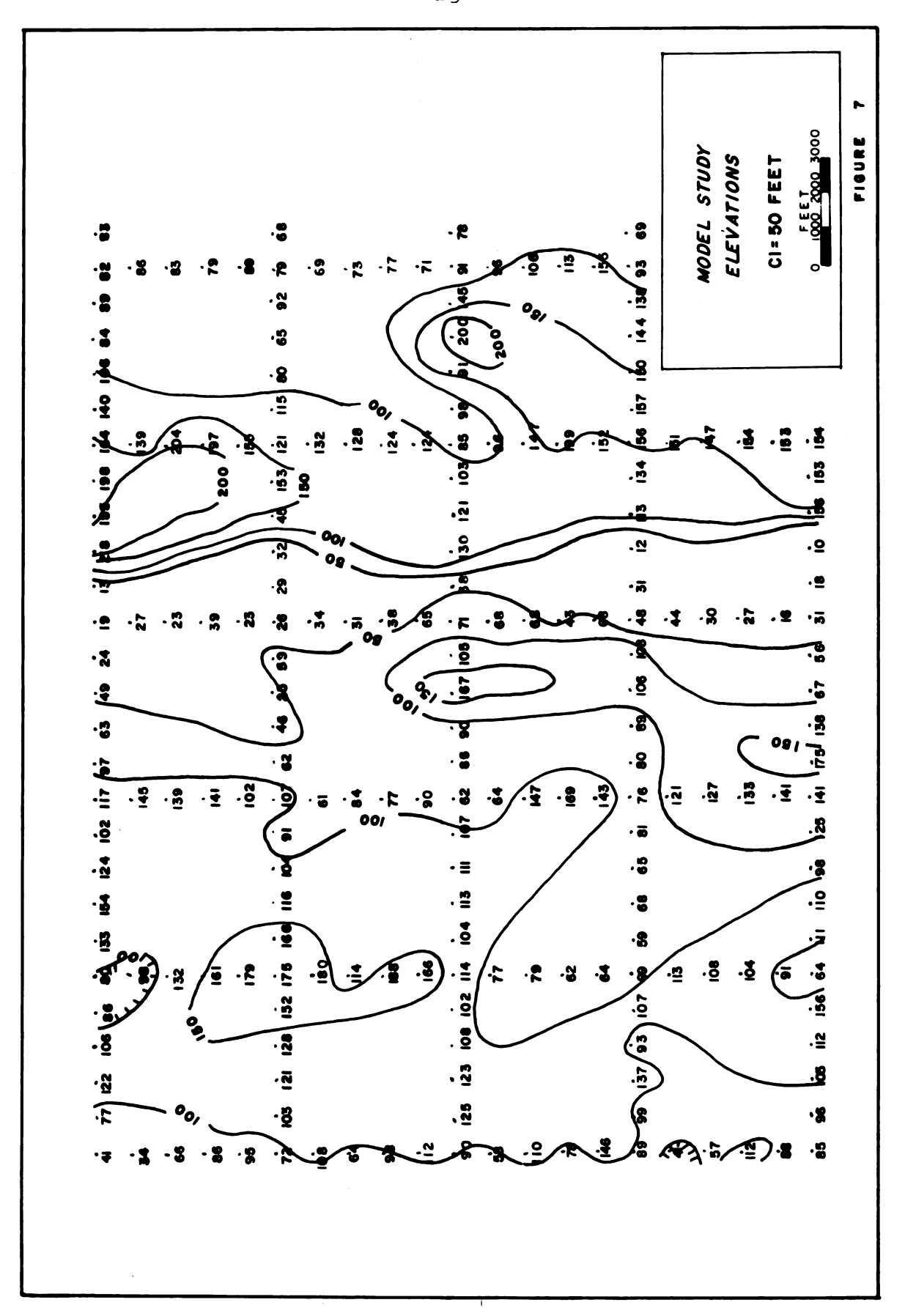
h = station elevation.

The observed gravity values from three subsurface sources were calculated at the surface elevations. The gravity stations are at 1,000 foot intervals on grid lines 5,000 feet apart. The sources include a glacial drift layer of varying thickness and density, a model of an actual buried bedrock river channel, and a reef structure modeled after the Bell River Mills reef in St. Clair County, Michigan.

The spatial relationship of the reef and the bedrock channel are shown in Figure 6, while the station locations and elevations are displayed in Figure 7.

Gravity Model of the Glacial Drift. -- The glacial drift thickness is equal to the magnitude of the station elevation. A density change within the drift was obtained by calculating the observed gravity values at the station elevations using a density of 2.1 gm/cc and 2.2





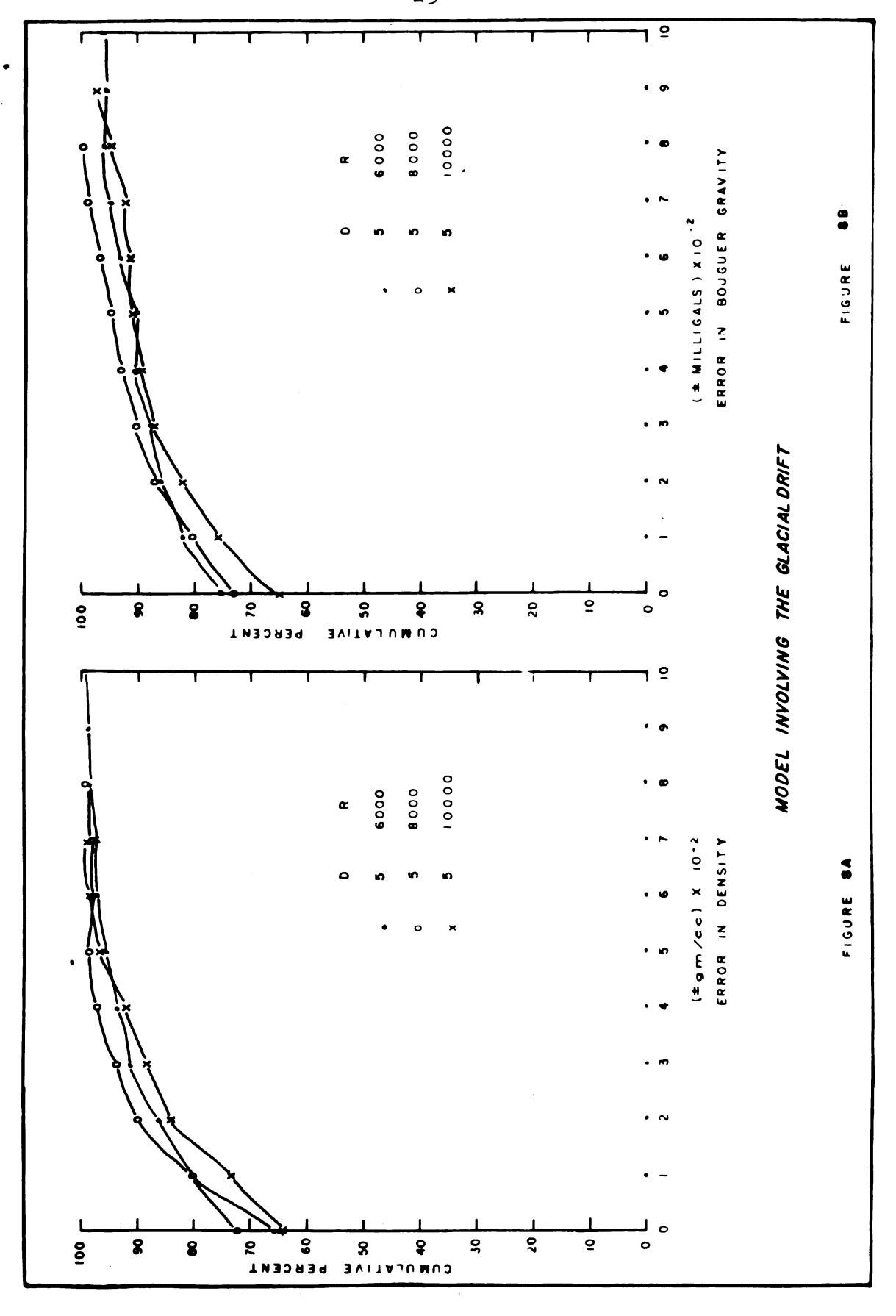
gm/cc. The areal limits for each density are shown at the top of each map.

The observed gravity values were processed with a fifth degree polynomial and ring sizes of 6, 8, and 10 thousand feet. The graphs in Figures 8-a and 8-b show the percentage difference between the known and calculated density and Bouguer gravity values. The error in individual station density and station gravity for a 10,000 foot radius is shown in Figures 9 and 10.

The graphs show that an 8,000 foot ring radius produces the most accurate results for both the density and gravity values. The maps of the density and gravity errors show the major differences are associated with the density contrast zone and not with the sharp elevation changes displayed in Figure 7.

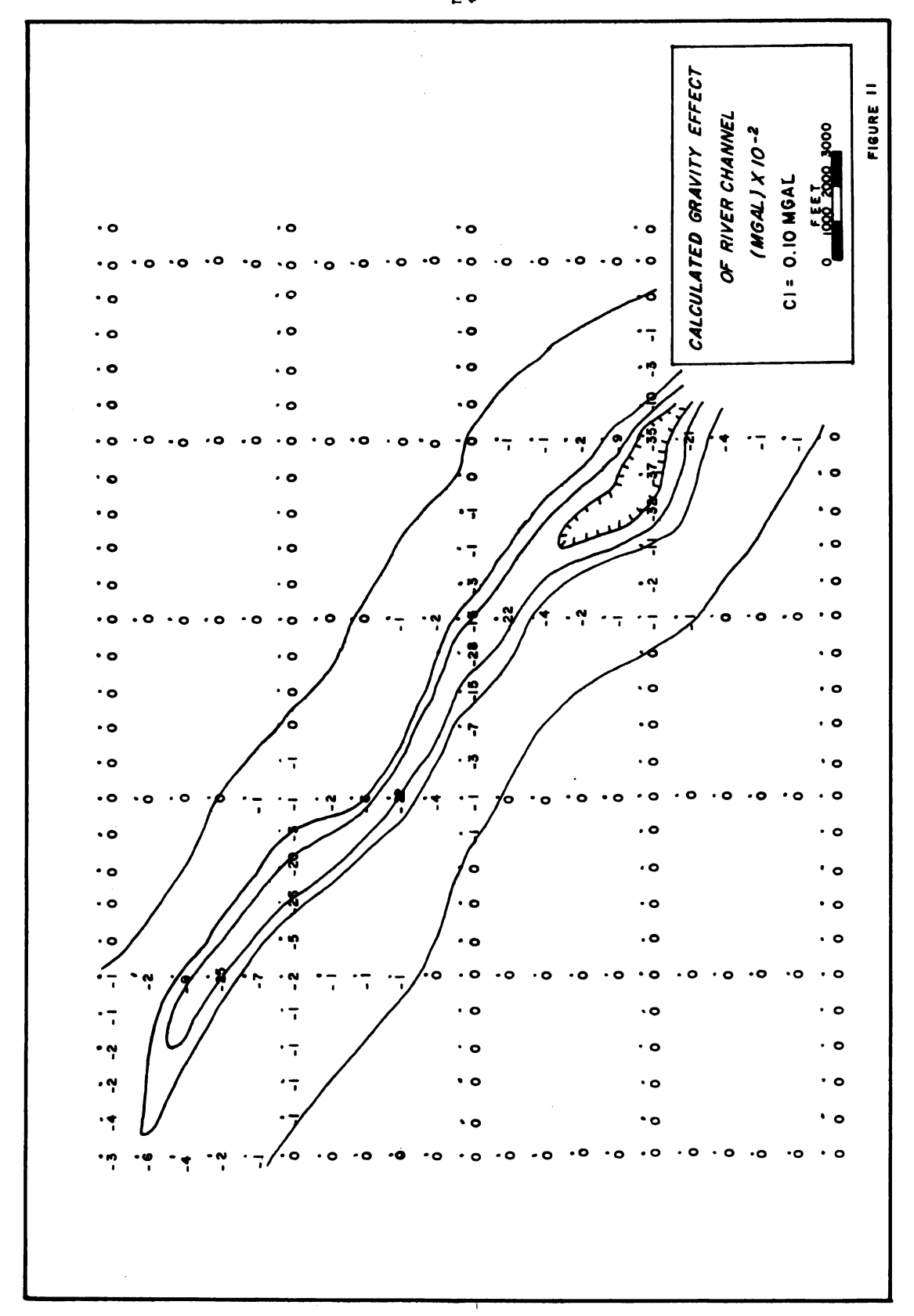
Channel. -- The bedrock channel, approximately 1,000 feet wide and 150 feet thick, extends across the map area and is buried immediately beneath the base of the drift. The gravitational attraction of this feature was calculated at the surface elevations using a negative density contrast of 0.3 gm/cc. The calculated effect, using the method described by Talwani and Ewing (1960), is presented in Figure 11.

These station values were algebraically combined with the glacial drift values and the model processed



																		STATION DENSITY ERROR	<i>3-01</i>	BING RADIUS = 10000 DEGREE POLYNOMIAL=5	000	FIGURE 9
Ā	۰0					۰.					۰.					. 0		DENSIT	(gm/cc) x10-2	ADIUS POLYN	FEET 1000 200	
	••	٠ ۰	٠0	٠.	••	۰.	. •	۰ ۰	. 0	٠0	۰۰	• •	.0	٠0	• 0	••	l	Ø	È	REE	•	
	٠.					٠.					٠ ٥					••		747	J	RIN		
	٠0					۰۰					٠ ٥					.0		S				
	۰۰					٠.					٠.					•0	L					j
	۰.					٠.					٠.					• •						
	. 0	٠.	٠.	۰.	٠.	. 0		. 0	٠.	. 0	٠.	٠.	٠_	. 0	٠.	٠.	. –	۰۰	. –			1:
2	••					٠.					•-										• 7	DRIFT
2.2 gm/cc	٠.					٠.					•-					٠.					. 0	
2.5	••					٠,										. 0						ACI,
l ï	••										. 4											છ
	• -			٠.	. 0	•-	• -		٠ ~	. 4	• ю	٠.		• -		. 4	۰ ۵	٠ ،			٠.	INVOLVING THE GLACIAL
	• •					. 5					, 10					٠ %					. 10	/NG
	• ~					. 10					. •					. ~					. m	770
	• ~					· m										٠,					. 4	<u>×</u>
																, ю					, w	
¥	• 10								. •		. •	. 🕶	. 10		. 10			. 10		10		MODEL
1 1	٠,	7	٠,٠	٠,٠	. 17	. 17	. 10		:1	. RÚ		Ÿ	7	, iů	. 9	• •	. 10	ï	• 15	• 10	.3 - 7	
	• •										. 4.											
	• •					. 17										• •					. 17	
	• •					٠,					. 2					٠,					٠٧	
ဗို	•7					٠ ٢					. 0				_	. 7		_			. %	
2.1 gm/	• •	. 0	٠0	. 0	٠.		٠ -	. 0	. 0	٠٥		••	• •	• •	. 0		٠0	• 0	•	• • •		
2	٠0					.0					• 0					. 0					. 0	
	• •					٠.					• -					٠0					-0	
1	• 7					.0					. 0					• –					• 7	
	٠0					۰0					٠ 0					٠.					۰.	
\	۰۰	•0	۰۰	••	۰۰	••	۰۰	٠.	٠٥	۰۰		•0		٠٥	• 0	. 0	. 0	• •		.0	٠.	

22 Jgm/cc 22 Jgm/cc 1 1 8 8 9 -3 -2 -1 1 0 0 1 0 0 0 0 0 0 0 0 0 0 0 0 0 0	*	.0					••					·o					.0		STATION GRAVITY ERROR	(MGAL)X 10-8	0000 = 10000	OLYNOMIAL =5	FI GURE 10
21 gm/cc 2.1 gm/cc 2.1 gm/cc 2.2 Jm/cc 2.2 Jm/cc 2.2 Jm/cc 2.3 Jm/cc 3.4 Jm/cc 3.5 Jm/cc 3.6 Jm/cc 3.7 Jm/cc 3.8 Jm/cc 3.9 Jm/cc 3.0 Jm/cc 3		. 0	. 0	.0	• 0	· o	• •	• 0	• 0	. 0	• 0	.0	• 0	• 0	. 0	. 0		-	, V	3	₽,	M O	
21 gm/cc 2.1 gm/cc 2.1 gm/cc 2.2 Jm/cc 2.2 Jm/cc 2.2 Jm/cc 2.3 Jm/cc 3.4 Jm/cc 3.5 Jm/cc 3.6 Jm/cc 3.7 Jm/cc 3.8 Jm/cc 3.9 Jm/cc 3.0 Jm/cc 3		• •					. 0					• •							7.47		S	EGK	
21gm/cc		• •					• •					٠0					. 0		S		° 02 (۵	
21 gm/cc 22 cm/cc 23 cm/cc 24 cm/cc 25 cm/cc 26 cm/cc 27 cm/cc 28 cm/cc 29 cm/cc 20 cm/cc 20 cm/cc 20 cm/cc 20 cm/cc 21 cm/cc 22 cm/cc 23 cm/cc 24 cm/cc 25 cm/cc 26 cm/cc 27 cm/cc 28 cm/cc 28 cm/cc 29 cm/cc 20 cm/cc 20 cm/cc 20 cm/cc 20 cm/cc 21 cm/cc 22 cm/cc 23 cm/cc 24 cm/cc 25 cm/cc 26 cm/cc 27 cm/cc 27 cm/cc 28 cm/cc 28 cm/cc 29 cm/cc 20 cm/cc 20 cm/cc 20 cm/cc 20 cm/cc 20 cm/cc 21 cm/cc 22 cm/cc 23 cm/cc 24 cm/cc 25 cm/cc 26 cm/cc 27 cm/cc 27 cm/cc 28 cm/cc 29 cm/cc 20 cm/		• •					٠.					• •					• •	L					J
21g m/cc		• 0					• 0					• •					٠.						
2.1gm/cc 2.1gm/		•-	• •	• •	• -	• •	• •	۰۰	••	٠0	٠0	•0	٠0		٠ ،	- 7	• 7	٠-	• -	٠0	• -	•0	
2.1gm/cc 2.1gm/	/cc	• •					• -					• 7					٠ ٣					-0	7
2.1gm/cc 2.1gm/	Ę	.0					٠.					• 7					٠0					•	RIF
	-2.2	• -					۰۰					٠ %					• 0					۰۰	7 71
		• 0					٠0					• -					۰٥					••	101
		• •	٠.	••	• 0	• 0	٠0	٠-	-0		• •	• m	٠,	• -	•-	• -	• -	٠-	• -	٠-	• •	٠0	79
		• -					٠ %					٠ يم					·'n					٠,	'\NG
		• -					• 7					. ∞					۰ ،						,OLV
	ı	۰،					٠ ،					. မဂ္					٠ ،					٠•	1 %
	1	·					٠ ې					. ທຸ					. 17					٠٠,	730
	X	. •	. <u>m</u>	- 22	• 10	٠ ۍ	• •	• •	• •	••	٠ ،	· 10	• •	٠.0	٠ ٥	٠ ٥	• 10	٠.	. •		٠ ه	٠.	MO
2. 2. 3. 3. 3. 3. 3. 3. 3. 3. 3. 3. 3. 3. 3.	T	• •					٠.					• 10					. •						
2.		. 80					• •					. 10					. m					. •	
0.							. 10					· w					٠ ٨					٠ ٨	
0.	Ö	•-					. 10					. –										٠ ٨	
0.	È	•-	٠-	•-	• •	٠.	. 0	٠ %		٠.	. 0	٠.	۰.	٠.	٠.	• •	٠.	٠.	۰ ۰	٠.	٠_	٠ ٨	
	2.1.9	• •					• -					• •					. 0						
	1	•0					٠.					. 7										•0	
•• •• ••		٠ ~					٠.										. 7					٠ ٧	
		•0					٠,					٠.					٠.						
	*	• •	۰۰	۰.	••	••		۰.	٠٥	٠٥	••	٠0	۰۰	۰.	٠.	۰۰	٠.	• •	٠٥	•	٠.	.0	

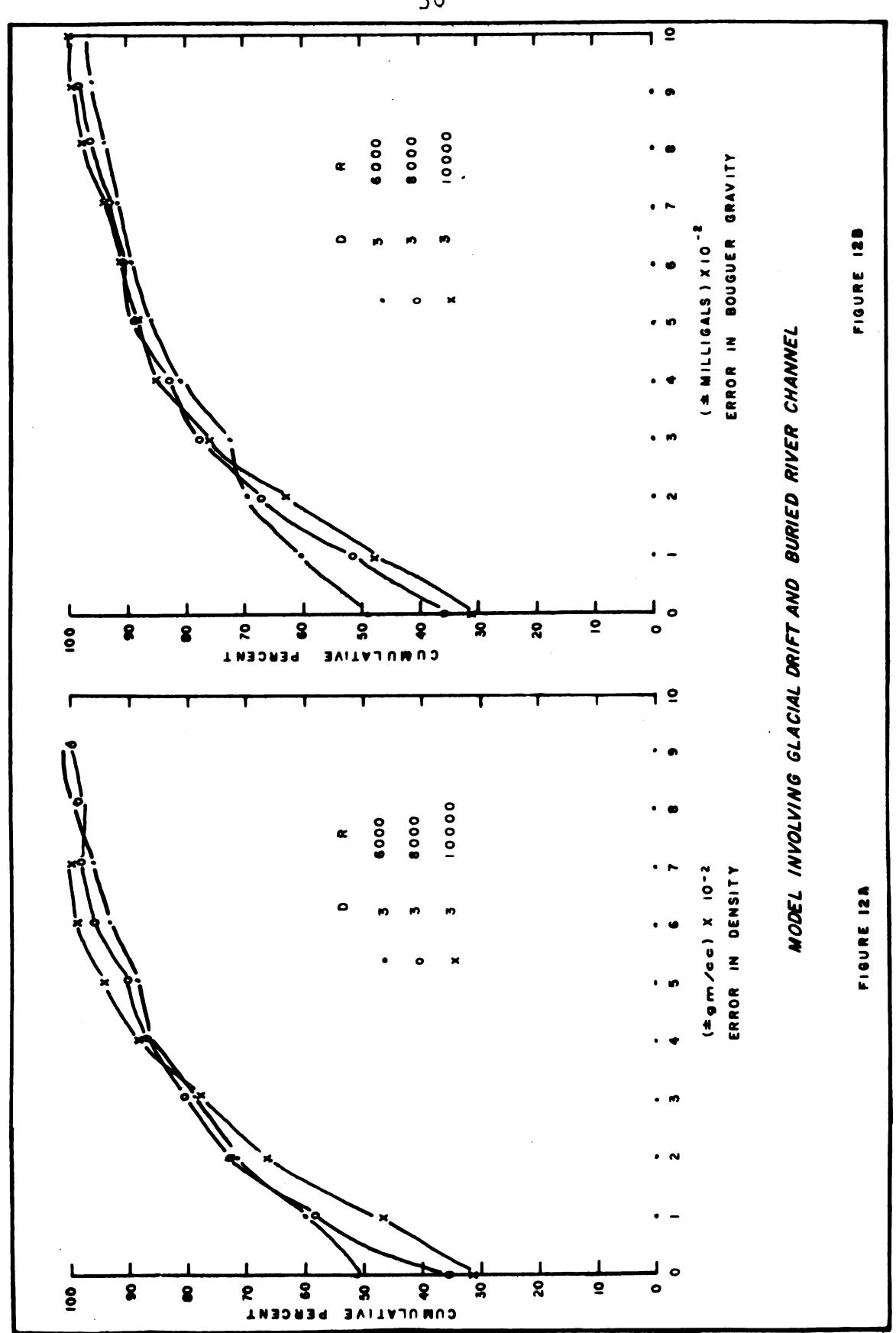


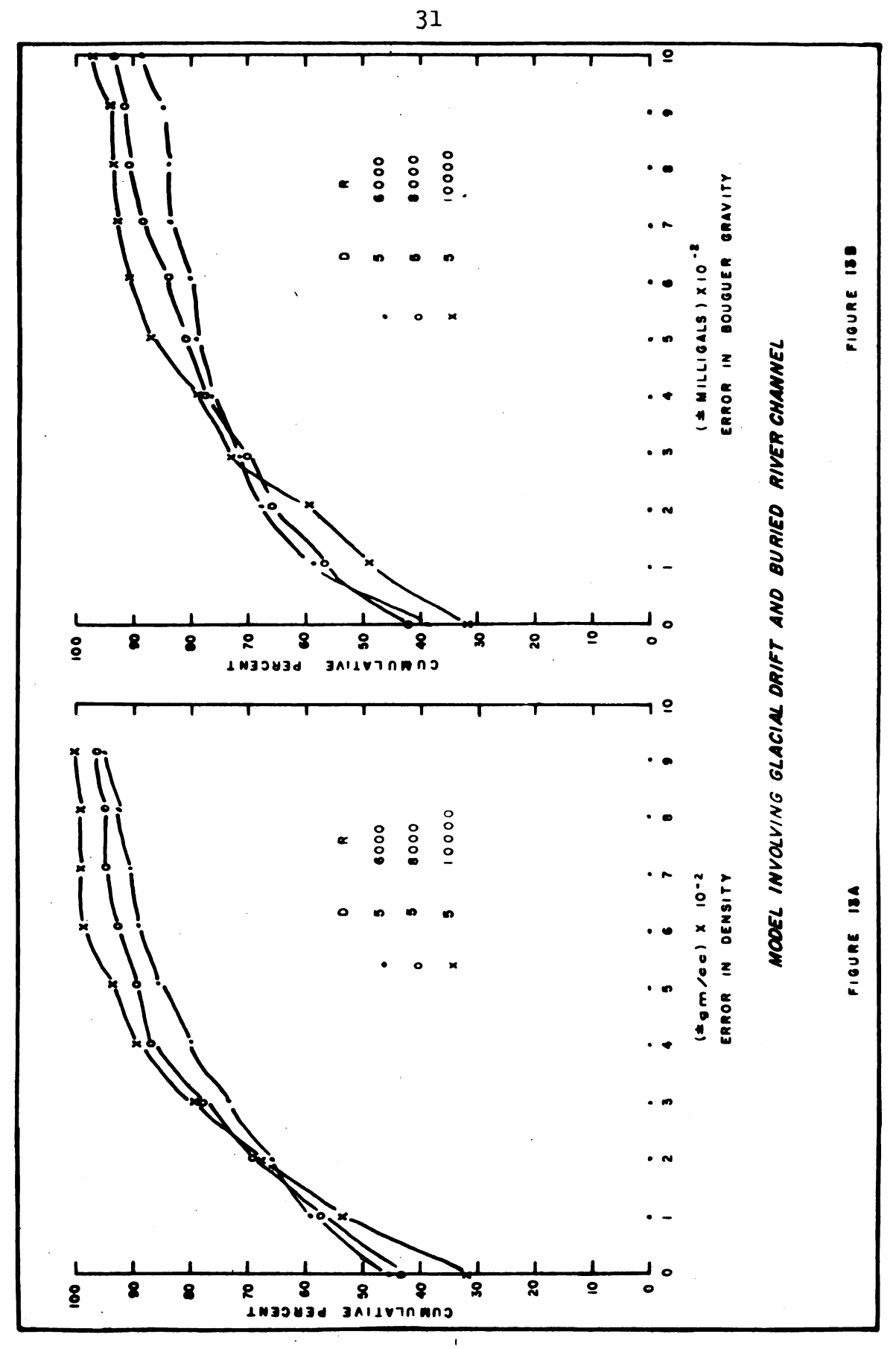
with a third and fifth degree polynomial. A radius of 6, 8, and 10 thousand feet was used for each degree polynomial. The difference between the known station density and the density obtained from the calculated elevation factor, along with the difference between the known and calculated station gravity are shown in graphic form in Figures 12-a and 12-b for a third degree polynomial. Similar values for the fifth degree polynomial are shown in Figures 13-a and 13-b. figures indicate that a 10,000 foot ring radius produces the most accurate results, and for that ring radius there is very little difference in accuracy between the third and fifth degree polynomial. The error in station density for a third and fifth degree polynomial and 10,000 foot ring radius is shown in Figures 14 and 15. associated errors in gravity are shown in Figures 16 and 17.

The graphs for both the third and fifth degree polynomial and various ring sizes show the 10,000 foot radius produces the most accurate results, with the third degree slightly more accurate than the fifth.

There is, however, a marked decrease in accuracy when compared to the model involving only density variations in the drift. The maps showing the error in the calculated station density and gravity for the fifth degree polynomial and ring size of 10,000 feet reveal that







,		رن ا	2.1 gm/cc	33/				¥					7	2 gT	22 gm/cc .						I	
• •	. 🕈	· 4	• •	, m	. •	. 4	. 7-	• •	• 10	. 10	, m	• •	•-		•-	٠.	۰.	.0	• •	۰0	.0	
ب.			٠ ۾				٠•					. 10				٠-				. 0		
. m			٠ %				. •					. m				. -				. 0		
٠ ۳			٠ ٢				٠.٣					. 10								. 0		
. en			٠ -				. 40					• 107				. –				۰۰		
- e		. -	·	٠ ،			'. "	• •	. •		. •	• •	٠, ٠	. •	. •		٠.				•	
				>				D	D	D	•		•	•	•	y . (-	-		· ·	•	
, .			·				• •					• .				n .				ο.		
· -							•					. 💠				m				7		
۰ ۰			· 0				. M					. •				۰ ،				٠-		
.0			۰0				. 10					. 🛊				. N				•-		
. 7	. 7	. 0	۰ ٥	۰ ٥	٠.		ج.	٠ 🕳	٠,	. •	. •	. 10	• 10	. 10	• 80	٠ %	٠ ~	, m	. 10	- 00	. 0	
- 10 1							. 17	,				. 10										
																·				٠. ٥	,	
,			٠.				? •					•								• .•		
•			0				7					•				~				7		_
۰.			٠ -				• 🕇					. •			•	٠ ٨				٠٦		
. 0	٠_	. 0		. m	, m	• 7	. 6	· b o	. 10	•	. •	. 4	•	. 10	. 100	٠ %	. ~		••	٠0	. 0	
			- 10				. 4					. 10				. ~						
(• •																STA	710N	STATION DENSITY ERROR	
.			y . (•									٠. ٠				/wo.	(0 m/c c) x 10 2	
•			7				•	_				٠.							ā	72	00001-	
·o			40				• •	_				•				•			DE:	SREE	DEGREE FCLYNOMIAL: 3	
· -	٠٥	. 7	۰ %	. 7	٠ ،	· ¶	• •	• •	. •	. •	. •	•		• -	• 7	٠ ٢				,	1900 2000 3000	
								(i		:				ļ			إ	١			

						••												STATION DENSITY ERROR	1 gm/c c) X 10-5	RACTUS = 10000 E PCLYNOMIAL= 5	500 2000 3000	
	• •	۰ ۰	۰.	• •	.0	. о	. 0	. 0	٠.	۰.	-	• 64	٠ ه	· 10	٠0			TION)	HING RACIUS DEGREE PCLY	o	
	. 0					. 0					. O					• 10	1	STA		F G		
	. 0					. –					. 10					• •						إ
	. 0					٠.					. 10					• -						NV
	۰ ٥	۰ ٥	٠0	۰0	· -	· -	٠ ٧	- m	. •	. •	• •	. 10	. ~	. ~	•-	٠ %	, w	٠ %	. 10	. ~	. 10	0
22 gm/cc	• 0					· -					.*					٠ ٨					• 10	DIVE
2 gm	. 0										•					. 10					· 7 · ?	6
7	••					. 0					· 10					. 10					. 0	JAND RIIDIED BIVER CHANNEI
	• -	. 0	٠.	. 0		.0		٠ ٨	. 4	٠.	. •	.4	. •	. •	. •			. 10	. •	• •	. ~	2
																• •						7
	. –					· N					. 10					. •					. •	100
	• •					٠ ٧٥					•					• 10					• •	181
¥	• 0					. 10					· 165					• •					• •	7
	•		. 7-	. 7	.1-	. 1	. 9	. •	•	•	. 5. -3.	. 🕈	. 4	. ~	. 17	-2 -2	. %	•7	• =	. 10	. m	THE CLACIAL DOIET
	. 4					. 17					۰۰,					٠,					. m	
						. 7					۰, ۲					٠, م					٠,	
ا ن	٠.					٠ ۲					٠,					• •					٠ ،	707
2.1 gm/cc _	. •	. .	٠.	. 10	٠ ٢	۰,4	. ທຸ	٠ ۾	٠ %	٠-	٠-,	• •	• 7	۰.	۰ ،	٠.	. –	٠.	٠-	•-	. 7	MODE!
. 2.1	٠ 🌳					۰.					• 7					٠0					. 0	3
	٠ ۴					ې. د					. 0					٠-					. 0	
	. .					٠٣.					. 1										• •	
\	. •	۰.		. -	. A		. ∾			. N	۰. ۲۹	. –	٠.	٠.	• •	. 0	. 0	. 0	٠ .	· · o	. 0	
-	· •	•	•	•	•	•	٠ ٢٠	7	•		• 7	•	-									

*	· • • • • • • •	· •	. 0	• •	. 0	. 0	• •			· -	-8 -5 -2 0	٠-,	. -	. –	. ~	. 0	STATION GRAVITY ERROR	8-01 % (18 9 %)		RING RADIUS = 10000 DEGREE POLYNOMIAL =3	0 ,000 2000 3000	
	· o					· T					. 4.					۰ ۲۰ ۲۰ ۰	<u> </u>					SWALL BYING CHANKE
	٠.	٠ -	. m	٠-	. ~	. 19	. u p	٠,	. •	. 🕈	٠.		- 10		٠•	٠•	٠•	. 10	- 107	۰.	. 10	3
ا ب	. 10		•	•	•	. 4					. 17			•		. e p					٠ ـ	7,50
Ę	·					. 4					. 🕈					. .					. 10	à
22 gm/cc	. 🕈					• -					۰ φ					. 7					٠.	7310
Ĩ						• 7					. ~					. প					٠ ٦	d
		. –					٠. ب	٠,	. ~	. m	• r ù	٠+	٠.	, IĄ	. 10	. 10	٠.	٠. ٢	٠,٠	٠-,		3
İ	. 7	•	•	•	•	, m	•	•	•	•	. 😛	·	•		•	. 🕶			·		. 10	000 57
	٠ ،					٠.					. <u>e</u>					. •					. 🕇	ò
	· w					, m					. •					. •					٠ ۴	3
	. .					• 🕈					٠٢					. 					٠ =	77.07.0
¥		·=	. <u>o</u>	. =	٠.	•	. 10	. •	- 10	. 10	. ~	. ~	. 10	. •	. ~	- 10	٠.	٠.	٠.	. 60	. 🕳	Ç
7	•		_			. 🕶					. 10										. m	1
	. 2					. m					. ~										. . .	
	. ~					. ~										٠ %					. 10	Š
, U											. 0					٠ ،					. •	
g m/cc		٠ ٨	. 10	. •	. ~	. ~	. №,		٠.		. 0	۰.	. 0	۰.	. –	. 10	. •	. ю	. 10	. 10	. 10	1000
-	. ~					. N				•	٠.					. 0					. m	9
7	. 10					. 10					٠.					٠.						
	. •					. 10					. –										. 7	
	• •					• 10					• 7			•							. 7	
¥	. 0	. –	· 10	٠ •	. •			· -	. 0				٠.	۰0	۰ ٥		. 0	۰۰	۰0	٠0		

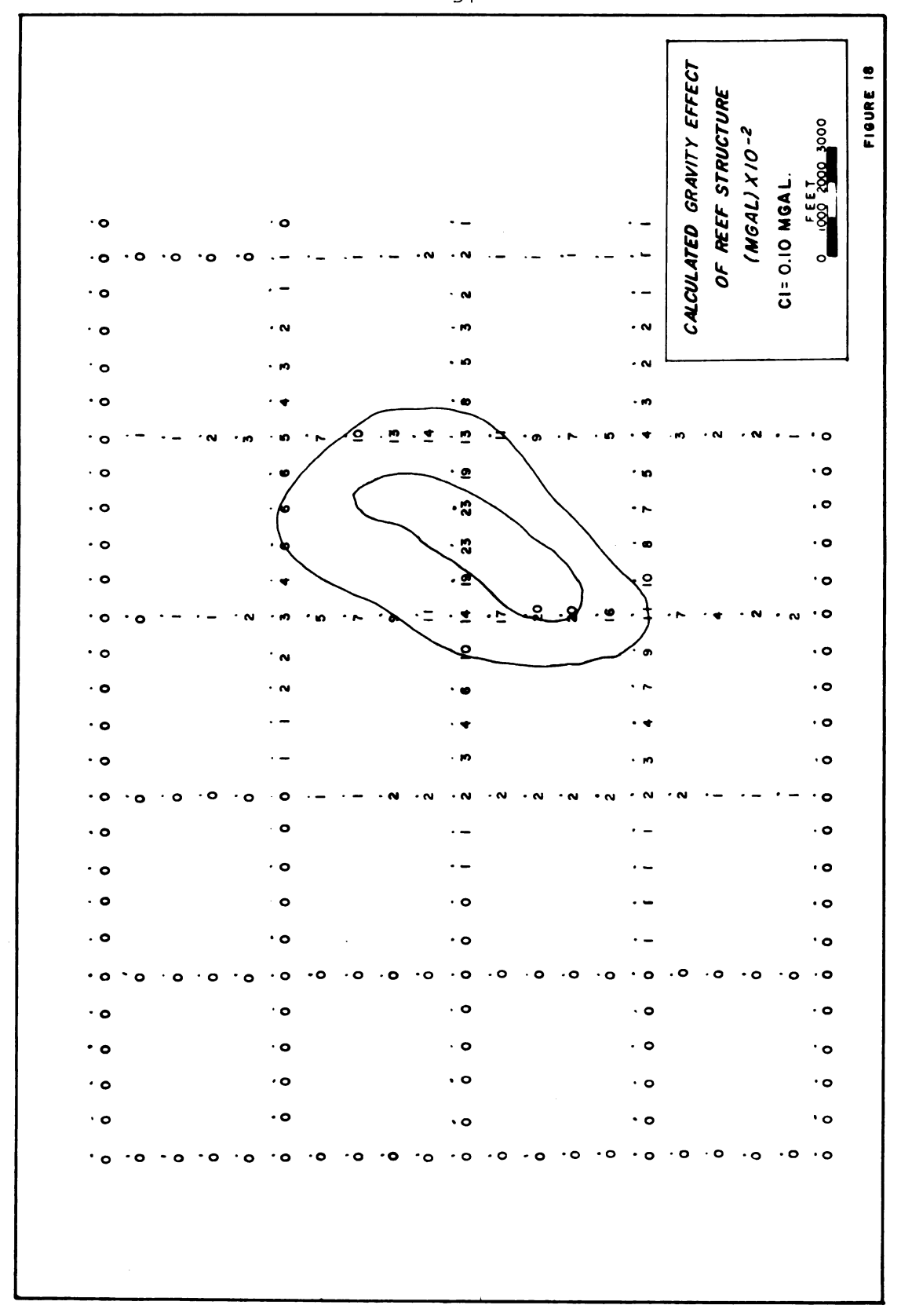
22,3m/cc 10 12 0 0 0 0 0 0 0 0 0	*		• 0	• (•	.0	••	•	0 0 0 0 1	••	•0	. 0	.0		· pū	• 147	. 10	• •			STATION GRAVITY ERROR	(MGAL) X10-2	RING RADIUS = 10000	0005 2000 0	EL FIGURE 17
									7					. ~						•					NNE
M			. 0		_	. 0	- 84	•	_	. •	- 10	. •		. 4	. 10	.≠	. 10				. 10	. 10	. 10	.=	CHA
				•	-	-	7		í	1	7	- 1	ĩ	. 10	1	•	7	- 4		- 47	7	i	7		Ę
	۲ /c																								RIV
	2.							•						. •										.0	150
	7	•												•											Z Z
		. 0	. 0		0		. 0			. 0		• 04	. •		. 10	, m	. ~	• 100		· 10	٠ ۵۱		• -		9 9
		. 0			_	•			_		7	- 17	•		•	'	•	4		1	7	•	,		A A
									_					_											616
																									70 7
	١								_															.=	Z/Z
	¥		. 🛨	. 9	N	. <u>m</u>	. ø	. •	9	. 10	. 9	• 4	. •	. 10	٠ ،	.4	. 4		. ~	. ~	٠ ٧	. –	. 10	. 0	હે
	7								~					• W					• ~						THE
		•=							•					. ທ					• -					. •	9
		. 🖻							•					. •					٠ ۵					. m	11/7/
	o'	٠.							•					. –					. –					- 01	№
0 .0 .0 .0 .0 .0 .0 .0 .0 .0 .0 .0 .0 .0	Ε	. •	. •	• (10	٠.	. •		•		. m	. •	• 00		۰.			. ~	. 0	• ÷	٠ ٥	. ~	. –	٠,	
0 · · · · · · · · · · · · · · · · · · ·	-	. ~						•						. ~					• •	•					MODEL
•• •• •• •• •• •• •• •• •• •• •• •• ••	Ī								10					••					• 7					.0	~
		٠.							ю					•-										٠,	
o. o		•							~					• 10					.0					•0	
	\	. 10		- 1	0	• -	٠.		~	. m		- 0	• M)	•-	•-	۰.	٠0	۰۰	.0	.0	٠.	.0	• •	۰۰	

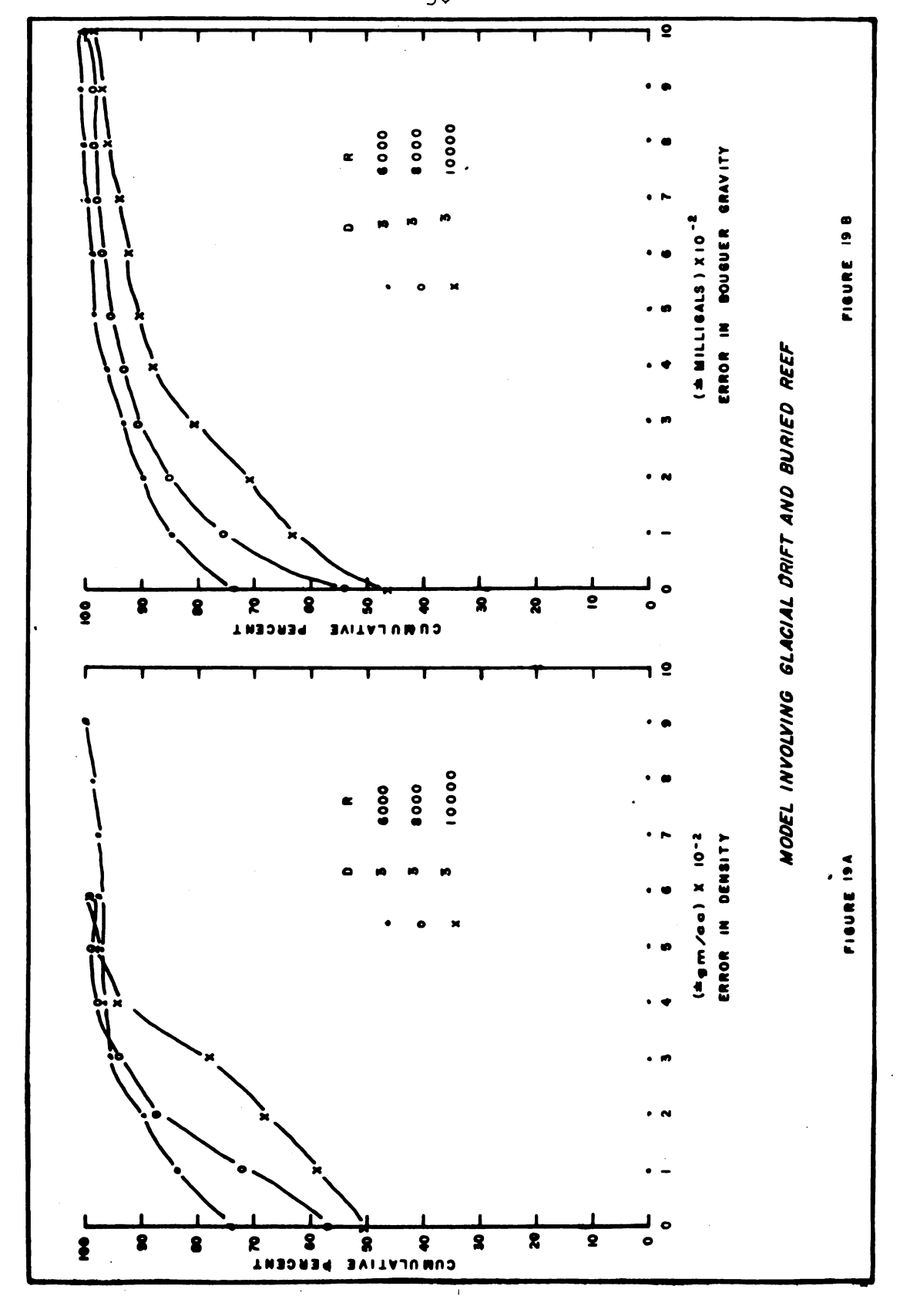
these errors are associated with both the river channel and the density contrast zone in the drift.

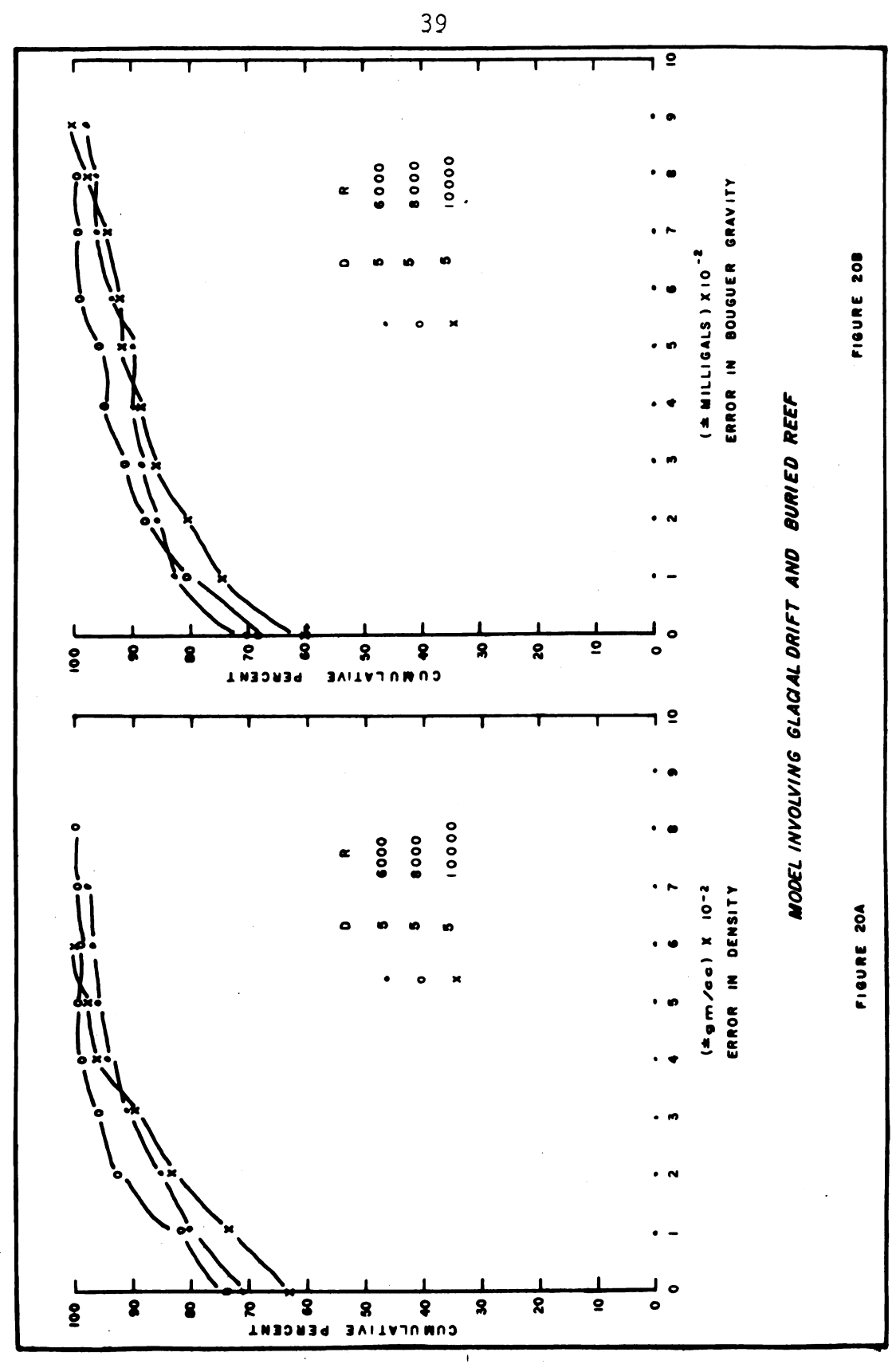
Structure. -- The reef structure was buried 2,500 feet beneath the glacial drift and assigned a positive density contrast of 0.45 gm/cc. The gravity effect of this structure was calculated at the surface elevations by the same method used for calculating the effect of the river channel. The associated anomaly is shown in Figure 18 and closely approximates the magnitude and shape of the observed anomaly (Servos, 1965).

The combined observed gravity values for the river channel and reef were studied with third and fifth degree polynomials for ring sizes 6, 8, and 10 thousand feet. Figures 19-a and 19-b are graphs of the error in density and gravity for the third degree polynomial and various ring sizes. Figures 20-a and 20-b are similar graphs for the fifth degree polynomial. Figures 21 and 22 are maps showing station density and gravity errors for the third degree polynomial with 10,000 foot ring radius. Similar maps for the fifth degree are shown in Figures 23 and 24.

The graphs for this model are almost duplicates of the graphs for the glacial drift model, revealing that deep sources with their broader anomalies exert little influence of the accuracy of the calculated







2.1 gm/cc 2.1 gm/cc 2.2 gm/cc 2.2 gm/cc 2.3 gm/cc 2.4 gm/cc 2.5 gm/cc 2.6 gm/cc 2.7 gm/cc 2.8 gm/cc 2.8 gm/cc 2.9 gm/cc 2.9 gm/cc 2.0 gm/cc 2.1 gm/cc 2.2 gm/cc 2.2 gm/cc 2.2 gm/cc 2.3 gm/cc 2.4 gm/cc 2.5 gm/cc 2.6 gm/cc 2.7 gm/cc 2.7 gm/cc 2.8 gm/cc 2.8 gm/cc 2.9 gm/cc 2.0 gm/cc 2.1 gm/cc 2.1 gm/cc 2.2 gm/cc 2.2 gm/cc 2.3 gm/cc 2.4 gm/cc 2.5 gm/cc 2.6 gm/cc 2.7 gm/cc
2.1 gm/cc
2.1 gm/cc 1.0 0 0 1 0 -6 -6 -6 -6 -7 -7 -7 -7 -7 -7 -7 -7 -7 -7 -7 -7 -7
·- ·- ·-
<u></u>

																				Q:				FIGURE 22	
	• 7						••						.7					••		STATION GRAVITY ERROR	(MGAL) X10-8	RING RADIUS = 10000		F1 61	
•	• •	٠.		_	. 0	٠0	٠.	• 0	, .			. ,	0	. 0	. 0	. 0	. 0			₹	3	AD	og S	ļ	
	. 0			•			٠-			•	•		٠.					.7		A 7.10		2	SEE.		
	٠.						• -													27		N.	DEG		
	. 0						• -						. 7					••	L						
	٠.						• 7						. 7					.7							ĺ
	٠.	. 0	•	0		•т	• -	٠-,			. 7	. 7	• • -	٠.	0	۰۰	٠.	٠.		. 0		٠ ٨	• 00	EEF	ĺ
)	. 0						٠.						٠٨					٠,) R	
22 /	. 0						. •?						. 17					. •					٠4	RIEI	
•	. 0						٠,						, ທຸ					٠,					۰.	BU	
	. 0						٠,						٠, ٨					۰.					• •	GLACIAL DRIFT AND BURIED REEF	١
	• 7	٠,	•	-		•-	• 7	٠٩		ې.	٠.	. 107	•	, m	, m	٠.	· m	'n,	- 10	٠ ،	۰ ،	•-	٠,	L	l
	. 7						. "						٠.					۰ ب					· m	DRII	ŀ
	. ?						٠ ٦						٠,					, s n					۰۴	741	l
	. 10						٠,						. ທຸ					٠,					. 🕶	LAC	l
•	• ф						. 10						. "					• •					٩.		l
	. ~	•=	•	<u>.</u>	. º	٠.	• •	• 14		. 9	- ເ	. 10	. 10	٠.	• 0	٠ 9	• 0	• 10	• 🛭	۰ م	• თ	۰۰	٠.	ODEL INVOLVING	l
	• •						٠.						•10					• •						170/	Į
	• •						. 4						• 10					• 10					• •	§	
	• •						• -						• 4	•				• •					• 10	DEL	
)	• •						۰ ۵						•-					. 10					• •	¥	
	• 7	• -	•	۰ .	-	• m	٠ ٨	• 10		~	· m	• -	•-	٠-		• –	• -	• 10	• •	· w	• •	. 10	. 10		ĺ
	• •						٠,						۰.					• 7					• 10		į
	• •						۰۰						• -					• 7					•-		
	• 7						• 7						• 7					٠ ٢					• 7		
	• 7						• -						• 7					• 7					• 7		
!	• •	٠0	•	۰ ۰	• •	٠0	٠.	٠٠		0	۰ ٥	.6	••	•0	•0	٠.	٠.	• •	• 0	••	•	•0	••		

1	. 0	. 0	.0	. 0	٠,	. 0	• •	. 0	.0	.0		٠0	• 0	. 0	.0	. 0		STATION DENSITY ERROR	(9m/cc) x10-8	RING RADIUS : 10000 DEGREE POLYNOMIAL:5	0 1000 5000 3000	
	. 0					. 0					. 0					٠0	L	_				
	. 0					۰ ۰					٠.					.7						
	. 0	.7	. 7	٠,	.0	٠,	. 0	٠-	. 0	. 0	۰ ۰	۰.		٠.	٠.	۰.	٠.	٠,	.7	.,		
000	. 0					۰.					• ~											
22 gm/cc	. 0					٠.					- 2					٠ 0					٠,	
22	.0										· N					• -					· 7	
	. 0					٠-					. ~					٠ م					٠ ۰	
	. 0		٠-	٠ ٥	. 0		- N	. N	. 10	. 10	. 10				٠ %	. 10	. 10	. 10	. 10	٠.	• -	
	. ~					٠ %					٠.					٠ %					. 10	
	. ~					. 10					·.un					. 0					. 10	
	. 2					. 10					. 10					. 10					. 4	
V	- 10					• •					. 10					• •					. w	
Ā	. 1	. 1	٠ •	-1	٠,	٠ ۴	• 🕇	• 1	·	• 🕇	4	. 10	٠ ۴	• •	۰ ۴	٠ ۲	• •	. 1	*	*	٠ ب	
	٠ ۴					. 4					. 2					٠.۳					٠.	-
	. 🕶					. 7					. 7					. "?					. 4	
	. 1					. 7					. 7					. ?					. ?	
22/0	. 7					. %					. 0					• т					٠ ،	
2.1 gm/cc -	. 0	. 0	. 0	. 0	. 0	.0	. 4	. 0	. 0	.0	. 0	٠0	٠0	. 0	. 0	. 0	٠ ٥	٠.	`7	7	. 1	
- 2	. 0					.0					. 0					. 0					. 0	
	. 0					.0															. 0	
	. 7					.0					. 0										٠,	
1	. 0										. 0					.0					. 0	
•	. 0	.0	. 0	. 0	. 0	. 0	. 0	. 0	. 0	.0	. 0	- 0	. 0	.0	. 0	. 0	. 0	. 0	.0	.0	. 0	

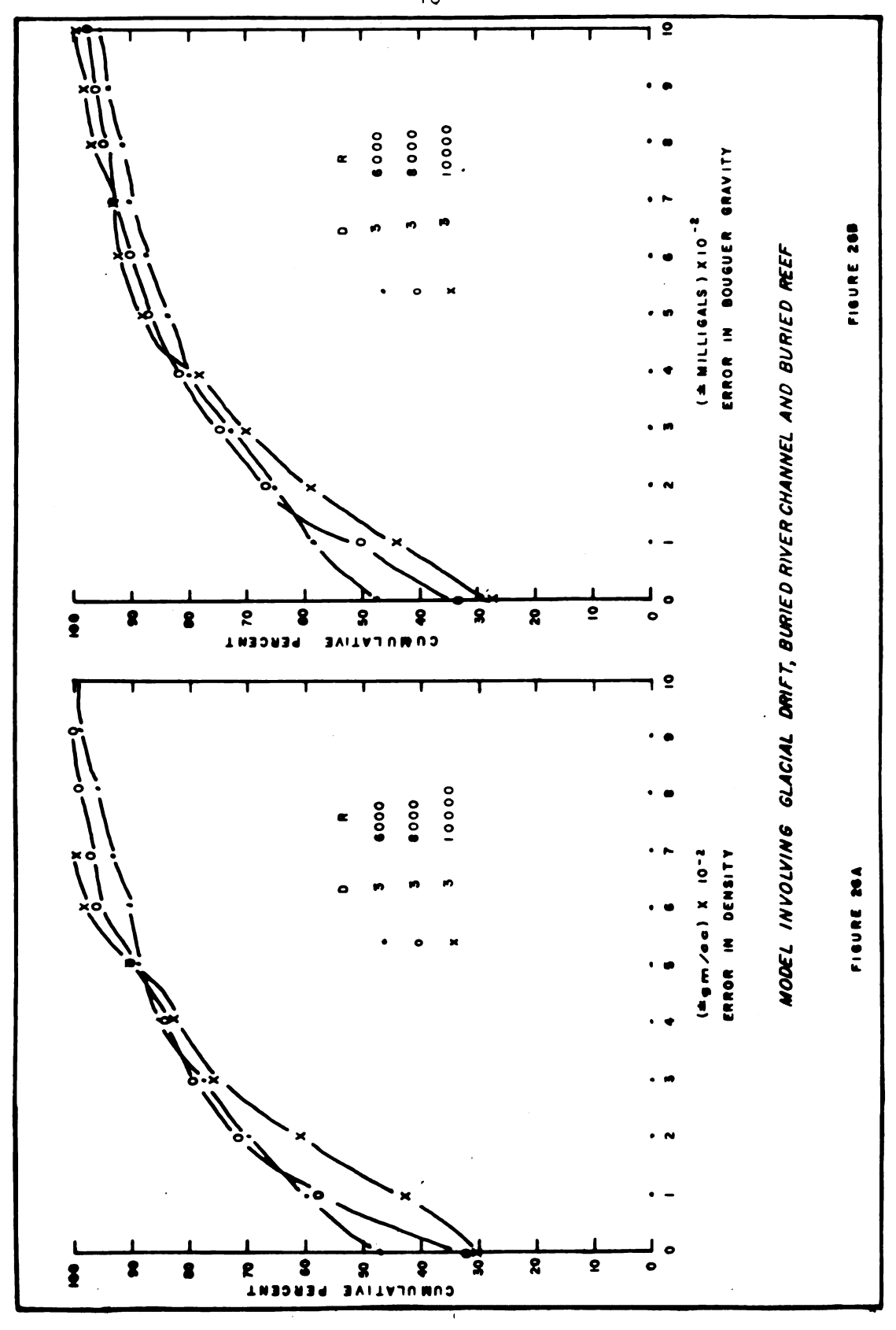
*	. 0		• •	. 0	• •	.0	• 0	• •	• •	• 0		• •	••	• •		. 0		STATION GRAVITY ERROR	(MGAL) X10-2	RING RADIUS = 10000	0 000 2000 3000	FIGURE 24
	. 0					۰۰										٠.						
	٠.					. –					۰.					. –						ķ.
		. –	۰ ∾		. 7		۰ ۰	٠,	٠ ٦	٠-,	٠.	۰0		۰ م	٠-,	. 0	۰.	· -	. N		٠.	REEF
- 55	. 0					. 7					٠ ۲					٠ ،					٠ ۵	
22 gm/cc	. 0					. 0					·					٠.					. –	781
2	• -					٠.					, m					٠.					٠0	9 0
Ì	• •					۰.					٠,					. 7					٠.	DRIFT AND BURIED
	٠0	٠.	۰۰	• •	٠,	••	٠ ٦	٠,	• 7	٠,	·m	٠4	٠,	٠,	٠,	٠.	٠ ٩	• 7	.7	٠ ٥	۰ ۰	FT
Ì	• 7					٠ ٢					· ຫຼ					• 🕆					٠,	DR1
	• 7					٠-					우.					٠ ۳					. 17	
	٠ %					٠ ،					٠ ٣					. ທຸ					• •	MODEL INVOLVING GLACIAL
1	. 10					• 🔊					. "					• 🕈					٠,	6
¥	• •	• ≈	•=	. 2	• 10	• •	• m	• •	- 10	. 10	• 10	• •	• 🙃	٠ م	٠ ٥	• •	٠ •	. •	. •	٠ ٢	· =	<i>``</i> ₩
	• •					• 10					٠.					. 10					• •	170/
	• •					• 10					٠ ٨					٠ ٨					• •	<u> </u>
-	• •					٠ %					٠ %					. –					· 10	DEL
υγ	• -					. w					٠.										- ~	8
E	• 0	• 7	• 7	٠ ٥	• •	• -	•	• -	٠0	• •	٠0	.0	• •	• •	• •	. 0	٠0	. 0	•-	· -	. ~	
2.1	••					• -					••					• 7					· -	
	• •					• -					• 7					• 7					• •	
	. ~					• •					••					• 7					. N	
	••					• •					• •					• 7					• •	
Y	• •	۰.	. 0	٠.	٠0	٠0	. •	. 0	• •	••	٠0	٠0	٠0	٠0	۰۰	••	• •	٠0	•0	٠.	• •	
*			-		-				_			_			-					•		

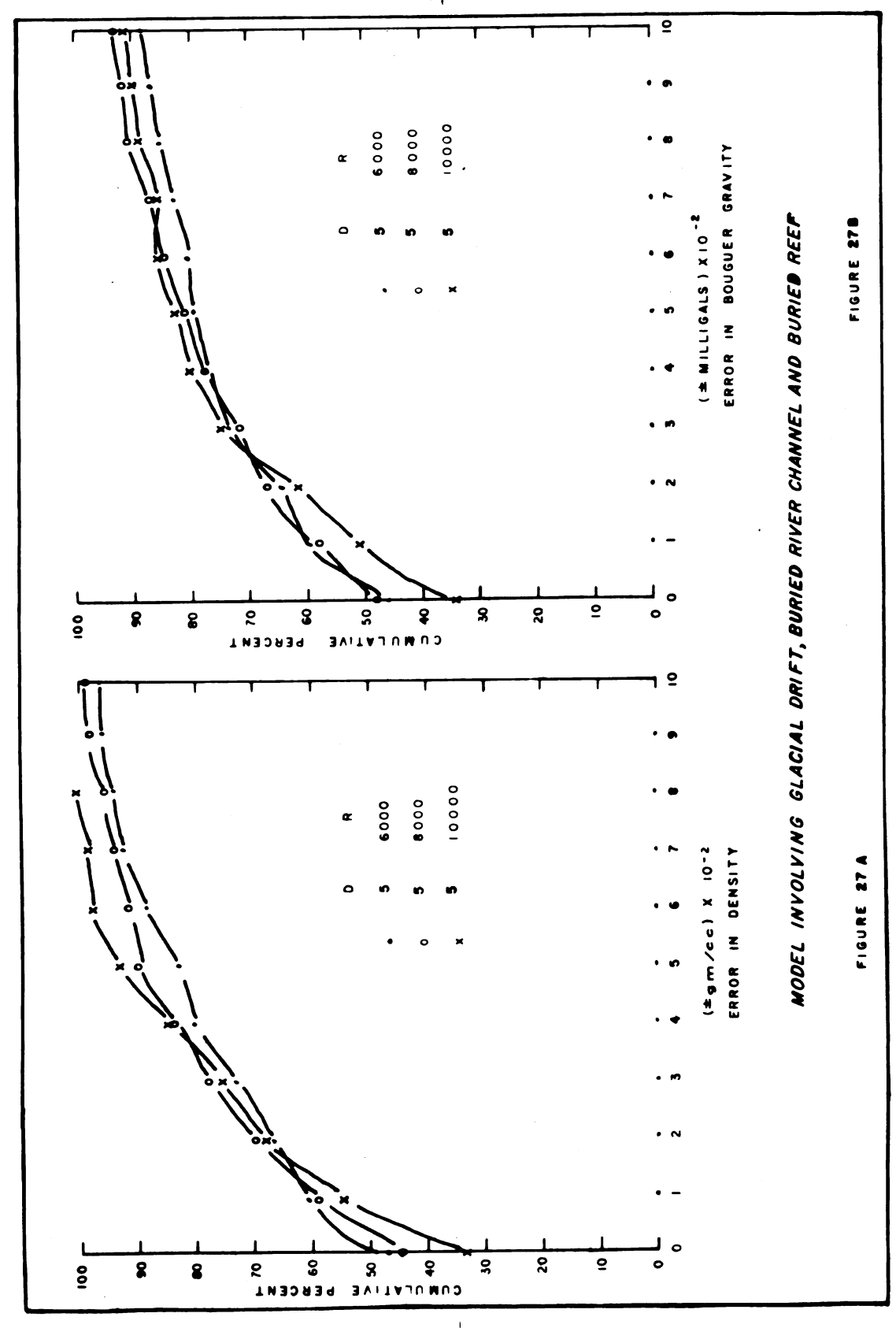
elevation factor. This is further emphasized when the error in station density values shown in Figure 23 is compared with the glacial drift model values in Figure 9. This comparison reveals that station for station, the magnitude of the error is the same and these errors are associated with the density contrast zone within the drift.

Gravity Model of All the Sources.—The combined gravity effects of the buried channel and the reef structure are shown in Figure 25. These values were added to the observed gravity values associated with the glacial drift and the model restudied. The graphs of the error in density and gravity for the third degree polynomial are shown in Figures 26-a and 26-b. Similar graphs for the fifth degree polynomial are shown in Figures 27-a and 27-b. The errors in station density and gravity for the third and fifth degree polynomials are shown in Figures 28 through 31. The graphs and maps for this model are near duplicates of equivalent graphs and maps for the model of the bedrock channel.

The high degree of similarity in the results for these two models indicates that near surface sources exert more influence than do the deeper sources. A comparison of the error in density and gravity for all models is provided in Figures 32-a and 32-b. The results for all models that include the effect of the

3000 3001 3000	30.01	3000	30.01	30.03 30.02 30.01 30.04	3001	30.01	30.01	3001	90.05 30.03 30.02 30.01 30.01	3001	30,01	30.01	30.01	10.05 10.05 1000 3000 3000 30.01	COMPINED GRAVITY FFFECT		OF BURIED SOURCES	CI = 0.10 MGAL.	0 000 2000 3000
3001	3001	30.02	3003	3006 3006 3005 30,04 3	30,07	3010	30.13	3043	3022,501930.13,5008 3	- Jak	3008	2000	2		29.82	8800	0000	30.00	
3001	3001	30.02	3002	300 3001 3001 3002 3002 3002 3004 3006 3005 3005 30.04 30.03 30.02 30.01 30.01	3000	30.06	3006	3009	3000 3000 3000 3000 3000 3000 3000 300	, desc	1000	Soil	/ sios	30.00 3000 3000 3000 3000 3000 3001 3001	30.06	3004	30.02	30.01	
30.00	3000	3000	3000	9500	6682	862	29.80	29.98	3000 30.01 30.01 30.00 20.07	3002	3002	30.02	30.02	30.01 30.02 30.03 30.04	3001	3001	300	3001	TOTAL
29.98	/ The state of the		200	30,00 3000 3000 2898 28.98 28.98 29.96 28.74 28	86.98	3000	30,00	3000	30.00 30.00 30.00 30.00	30.00	3000	3000	30.00	3000 3000 3000 3000 3000	3000	30.00	3000	30.00	OUT OUT ITUE ITUE ITUE POE POE POE POE POE POE POE POE POE PO
2894	2897	29.98	28.03	30,00 30,00 30,00	3000	3000	30.00	39,00	3000 3000 3000	3005	3000	3000	30,00	30,00 3000 30,00	30.00	30.00	3000	30.00	



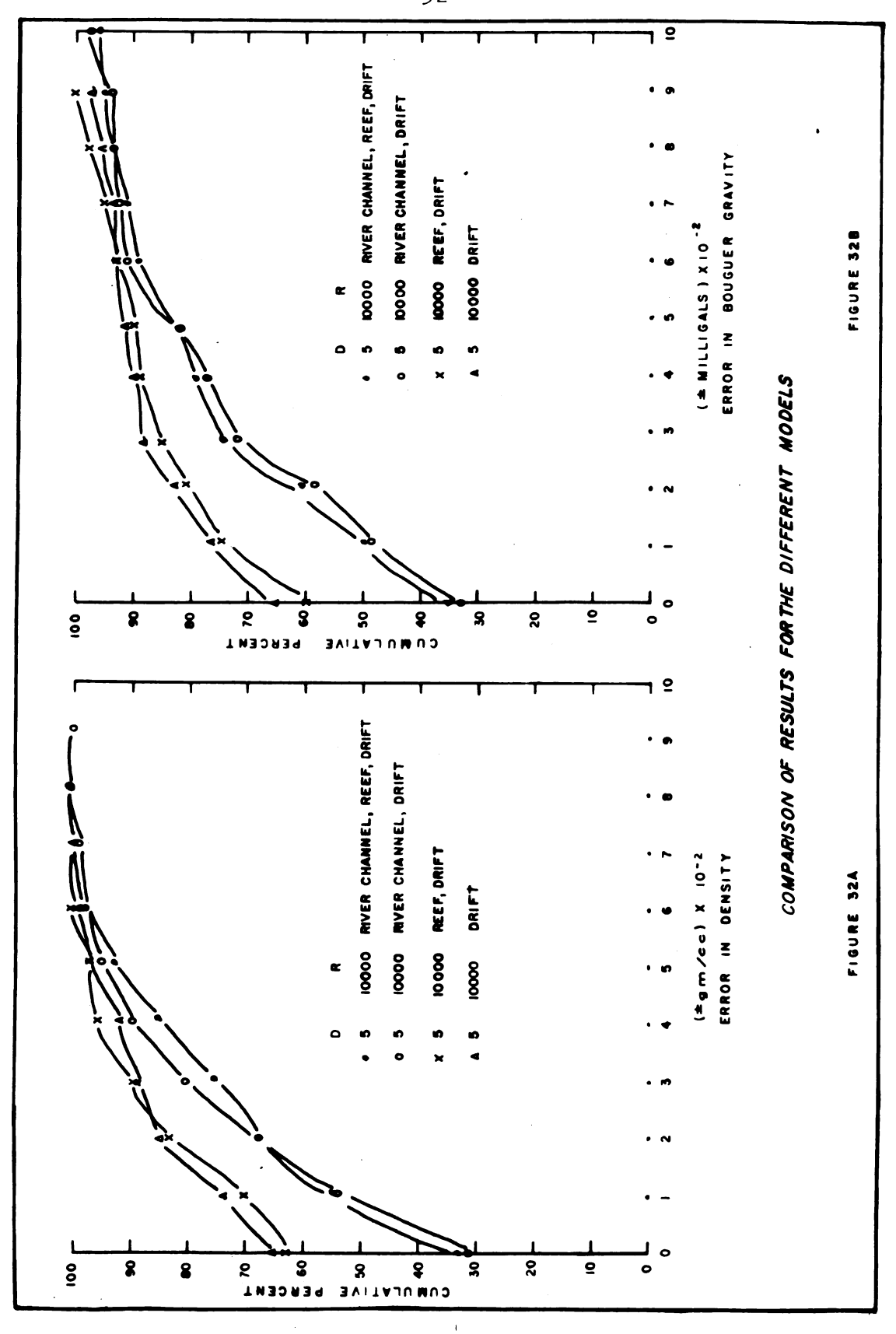


*			· o	·	· - · - · -	•	. 0	. •	· N	· 0 N · N		.0	. •	٠-٦			STATION DENSITY ERROR	(gm/cc)X10-2	MING RACIUS : 10000 DEGREE PCLY40MALL: 3	0 170C 2440 3000	D DEFE
ļ	. 0				. ~					. 10					• 10						1
		• . <u> </u>			ю. •	•	. •	, m	. 10	· m	. ~	. ~	. ~	- 10	. 10	. 10	٠ ~	٠ ،	. 0	٠,	à
ا ي					ın.					. 10					. •					٠.	CHANG ONF ISHNEND ASKID CIBIBLE BIRED ON INCOLUNIONI
2.2 gm/cc					, m					- m										٠.	Ų
2.2 (,	· ~					. •										•	444
	• ••				. •										. •					••	3
		0 - 10		• •	٠٠ .	•	. m	. 10		. •	. ب	٠ ٠	٠.	٠.	٠,	٠,	. •	. •	. •	•	NEB
	•				· 10					٠,					٠.					.0	9
	• m				. 🛭					• •					• •					··o	7101
	. 10				. 🕈					٠.					, •					••	7 8
¥	• •				• 🕏					. •					. 🖝					••	BIE
A	•	• •	٠ 🌳	• 🛊 •	•	n ·	•	٠ ٢	. M	- 10	. 10	. 2	. 19	. 17	٠ ۴	. •	• •	, 10	. 17	•	2
	٠,				. rņ					· 🕶					• •					٠•	7/36
	• 4				٠ ٦					۰ ۴					. 0					٠•	3
	٠ ۴				• 7					٠,					, 17					۾.	٠ ٧
- ၁၁/w ɓ	. 4	u		•	. 0				_	. 0			_		. 10	•		_		. F.	2
2.1 9 1	. ? . ?	7 .7		7	` -	7	• =	. 0	. 0	. 0	• •	٠٥	. 0	٠ -		• •	. "	. 1	• 7		<u> </u>
7	. Y				· T . ~					. 0					. 0					-7	7
	. T				. ~ . ~					· •										٦٠ ص	MODEL
	, e				· 7 · 70																•
\blacksquare	· T	v . pp	. 10	_	· 7	_	· -		۰.	. ~	- 10	. 🕶	٠.			. 0	. 0	. 0		۰.	
		7	. 17	•	•	7	•	•		•	•	•									

7		· -	· -,	. 0	· -	·;	. 0	.0	. 0	• -	. 0 8-	·=	•	. –		.0		SIMILON GRAVILY ERROR	0/ X (7 X)	RING RADIUS = 10000	0 1005 2000 3000	
ļ	٠.					• 7					٠ ٩					٠-	3	3		e c	2	
1	• 0					• 7					. •					٠٠?	<u> </u>					J
	. 0					· m					٠•					٠•						
١	٠.	• •	٠٩	٠ ٣	٠ ښ	. •	٠ چ	. •	. ເ	. m	. m	٠.	.#7 1	٠ ۾	. જ	- ຜຸ	٠ ۴	•	٠ ۴	۰.	~ N	
Ü	. ?					٠ ۴					٠+										•	
E	٠,					. 7					. •					. φ					•	
22 gm/cc -	. 17					. 7					٠,					. 7					٠.	
Ĭ	. 0					. 7					, m					۰.						
	. 0	٠-				. 7	٠ ،	٠. ٨	٠.	. 🛊	٠.	. u n	٠.	.4	, φ	. 🕈	٠,	٠.	٠ ې	. 7	ې.	
		·	·	•	•	• 4				·	. •					٠٠					٠.	
	٠ ،					٠ ٦					. •					٠.					۰,	
	. ••					. •					. •					٠.					·Ŧ	
	. .					. 4					٠,					۰.					. 🕇	
¥	. •	. =		. º	. 49	• •	٠ ~	. •	• •	. •	. ~	. m	••0		. 10	٠ ٨	. •	. •	٠.	. •	. •	
7	•					, 10					. +										٠.	
	٠ 0					۰, م					. 10					. 0						
1	. ~										• ~					. 10					. 10	
0						٠.										. m					- 💠	
3/cc	. س	• •				. ~	. 🖍			٠.	••	۰.	۰.	۰.		. 10	• •	. •	. •	. 4	. 10	
E 0	, es				- 14	٠ ٨					٠.					٠.		•			· 10	
- 21											••					••						
	•					. 10										٠,					. 7	
	• •					. (*)																
	••					. 10					• 7			_	_	• •	. ~					
T	• 0	• •	107	• •	•	• 🖻	٠ ٧		٠-	- 0	- 143	-0	• 4	.0	.0	•0	. 0	•0	. 0	• 0	. 0	

*		. •	٠.	· •			. 0	. 0	• •	- 0		• 10	. ~	٠,	. CI			STATION DENSITY ERROR	3-0/X(20/wb)	RING RACIUS : 10000 DEGREE POLYNOMIAL: 5	0 1000 2000 3000	REEF FIGURE 30
	•					. –					٠ %					• 4	L					
	. •					۰۰					. 10					. •						ME
	٠.					. 0		•	• •	٠ •	. •	. 10	. ~	٠ ~			٠ %	. –	۰ م	٠ ٨	•	96
ပ္ပ	• •										•10					٠ %					• 00	ANC
Ę	. •					٠ ~					• 10					٠ ~					٠,	73
22 gm/cc	. •					, ~					• •					. 🗢					٠.	GLACIAL DRIFT, BURIED RIVER CHANNEL AND BURNED
-											. m					. 60					•-	CH
		. 0	٠.		٠.	.0		. m		٠ ن٥	. •	.*	. •		• •	٠.	٠ •	. •	. •		. 10	VER
											. •					• •			•		. •	E C
-						· N					. •	•										WED
						. :					۰ ۳					. •						108
	. –					٠.					. •					٠,					• •	FT,
X	•	٠,	٠,	•	. •	٠ ا	. 🚓	· ĸņ	· iņ	. 10	·m	. 🛊	٠ ۾		. 17	٠ -	. 0	٠,		٠. ٣	, ep	DRI
	•	·	•	•	•	٠,٣		•	•	•					·	• -					· m	74/
	. 7					٠.					٠-					٠-					٠•	LAC
	٠,										۰،					٠-					۰.	
9	٠•					. 🕶					٠-					٠-					٠.	///
2.1 gm/cc	. •		. 😝		٠ ۾	, m	. 📪	٠ ٨	· -	٠-	. 7	••	٠ -	٠٠	٠ ،	٠ ٥		٠.	٠-			701
2.1	٠.	·	•	·					·		٠-					٠.					.0	×
l	٠ ٣					٠.					۰ ٥					. –					۰.	MODEL INVOLVING
•	٠ 🕶					٠.					٠-					٠.					٠٠	\$
	· •					.,					۰ې					٠.					۰0	
\blacksquare	•	•#	• -	• -	٠ م	٠,	٠ ~		٠-	· N	• -		٠ .	٠.	٠.	. 0		٠ ٥	۰۰	,	۰.	
		•	•	•	•	•	•	•	•	•												

-	• •							.8.							STATION GRAVITY ERROR	(MGAL) X 10-8	RING RADIUS = 10000	006 2000 3000	FIGURE SI
7		.0 .0	• •	·_ ·	ò . o	. 0	. 0		. 10	. 10	, m	. 19	. 7		>	Ž	Ap	ភ្នំ ្	
	• 6		_	٠0					•	•	•	•	• 7	'	7.0		22 ر دی:	ָ ה ה	4
	• •		٠	٠0				. 10						İ	57.4		N. C	2 2	REEF
	• •			. –				. •						L					BURIED
	• •			`				. 🛊					• 7						URI
	•-•-	· - · N	• -		٠.	. •	. •	• •	. 19	٠.	. 10	. ~	• •	.10	. (4	. •	. •	.=	
1	• •		•	. m		•	• •		•	•	,	• •	. pa	ī	7	i	7	.4	GLACIAL DRIFT, BURIED RIVER CHANNEL AND
22 gm/cc	• 6			. m . m				. e p					· 17					• •	VEL
29				• 7				٠,										-0	NY.
7	-			· c				ا .											ž
	.0			•0	-	. ~	. •		. 🕶	. 10	, eu	. +	. %	. 10	. ~		. –	• •	/ER
			- 0		7	- "	- 7	• •	١	•	77	٠,	``i	•	- 17	. 4	••	` ī	Š
	. —			· -				· P					. 9					. •	IEO
	•			, n				· 1					. 7					· i	708
				- I				• •					.1.					-12 -7	7, 6
*	* T	. 0 . 0		. m	•		_	• 7	. 🚗				• •					. "	RIF
1		•- •-	•	• 60	•	• (4)	• •	• 14	. ,,,	•		• 60	-	.0	• 1	• 7	• #1	. •	07
	. 9		,					- ~					•-					•	7/3
	· = .		,	. =				. ~										. •	6LA
1	_		,										•-					. 10	
2.1 g m/cc	• •	_	_	• •	_	_		•-	_				••		_			- ~	MODEL INVOLVING
0			• •	• • • (. w	. •	• 0	•-	.0	•-	•-	• ~	.0	• •	.0	• -	•	. ~	* 70
رن ا	• •			• 10				• 00					• •					• -	7.
	. ~			. m				••					• •					• •	ODE
	• •			• 10				•-			•		٠ %					• -	*
	• •			• ••				• 10					••					• •	
T	• m ·-	• •• • ••	• 60	- 04 - 1	0	- 60	• 10	•-		••	. 0	••	••	••	••	• 0	••	• •	

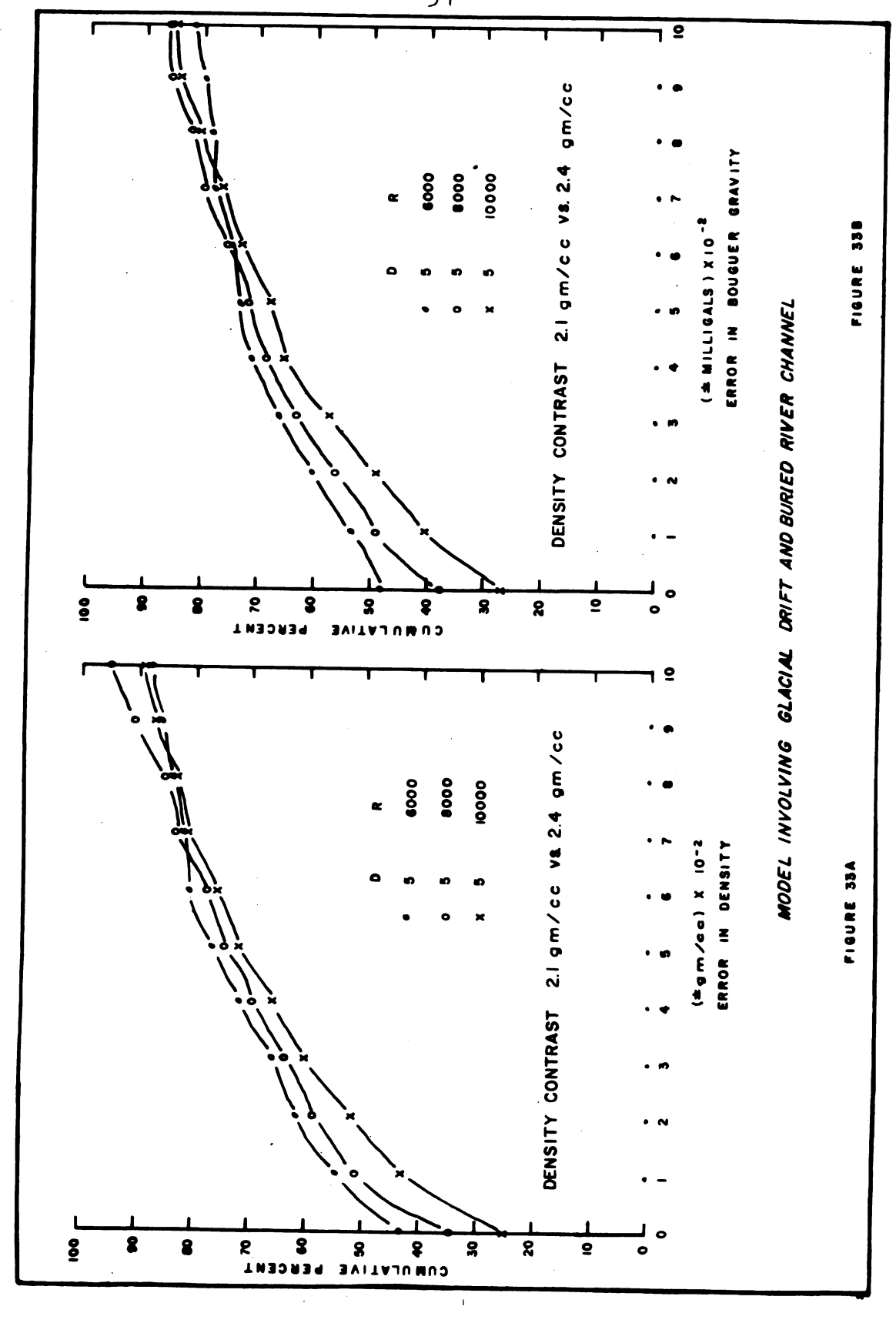


bedrock channel are closely associated and distinctly less accurate than the results for the models which involve the glacial drift and reef.

Increasing the Density Contrast Within the Drift.—
The previous discussion shows that the errors in the calculated elevation factor are directly associated with near surface density contrasts. This source of error was further investigated by reprocessing the glacial drift and bedrock channel model with a fifth degree polynomial after increasing the density contrast within the drift from 0.1 gm/cc to 0.3 gm/cc.

The error in density values for a 6, 8, and 10 thousand foot radius is shown in Figure 33-a, with the corresponding error in gravity shown in Figure 33-b. Although the density contrast was increased threefold, a ring radius of 8,000 feet or greater, results in 87 per cent of the density values and 84 per cent of the gravity values having errors less than 0.1 gm/cc and 0.1 mgal. The areal distribution of the station density and gravity errors for the 10,000 foot ring radius are shown in Figures 34 and 35.

Decreasing the Station Spacing. -- There are a definite number of data points required to satisfy any given degree polynomial, and thus the station spacing will dictate the minimum ring radius required to insure these data points. For example, a first degree equation requires only 4 data points whereas a fifth degree requires 22 data points.



2.1 gm/cc 3. 7. 18. 18. 18. 18. 18. 18. 18. 18. 18. 18	o i i i z z z z z z z z z z y z z z z y z z z y z	9 m / C) X/0 2 5 R L DIUS = 10000 18 EE FEET 10000	70 4411012
2.1 gm/cc 3. 7. 16. 17. 18. 17. 18. 17. 18. 17. 18. 17. 18. 17. 18. 17. 18. 17. 18. 17. 18. 17. 18. 17. 18. 17. 18. 17. 18. 17. 18. 17. 18. 18. 18. 18. 18. 18. 18. 18. 18. 18	9 8	6 19 2 2 E	
2.1 gm/cc 2.1 gm/cc 2.2 gm/cc 2.3 gm/cc 2.4 gm/cc 2.5 gm/cc 2.6 gm/cc 2.7 gm/cc 2.8 gm/cc 2.9 gm/cc 2.0 gm/cc	· · · · · · · · · · · · · · · · · · ·	9 8 8 8 8 9 9 9 9 9 9 9 9 9 9 9 9 9 9 9	İ
2.1 gm/cc 4. 7. 18. 17. 18. 17. 18. 18. 18. 18. 18. 18. 18. 18. 18. 18	.0	N N N N N N N N N N N N N N N N N N N	l
2.1 gm/cc 2.1 gm/cc 3. 7	٠٠ ٠٠ ٧		
2.1 gan/cc 2.1 gan/cc 3. 7. 16. 17. 19. 19. 6. 6. 6. 6. 6. 17. 19. 19. 6. 6. 6. 6. 6. 6. 17. 19. 19. 6. 6. 6. 6. 6. 6. 17. 19. 19. 6. 6. 6. 6. 6. 6. 6. 6. 6. 6. 6. 6. 6.	· • • • • • • • • • • • • • • • • • • •]]
2.1 gan/cc	·m		N/N
2. gan/cc 3. 7 - 6 - 6 - 7 - 7 - 15 - 17 - 20 - 20 - 6 - 6 - 6 - 6 - 6 - 10 - 20 - 3 - 7 - 6 - 6 - 7 - 7 - 15 - 17 - 20 - 20 - 3 - 7 - 6 - 7 - 7 - 15 - 17 - 20 - 20 - 1 - 1 - 1 - 12 - 1 - 1 - 12 - 1 - 1 - 12 - 1 - 1 - 12 - 1 - 1 - 12 - 1 - 12 - 1 - 12 - 13 - 14 - 15 - 15 - 16 - 17 - 18 - 18 - 19 - 10 -	- M - 4 - 4 - 4 - 4 - M - 4 - 4 - M - M	מוי מוי מ	CHANNEI
2.1 gm/Cc 3. 7 - 5 - 6 - 7 - 7 - 16 - 17 - 20 - 24 - 6 - 6 - 6 - 15 - 2 - 1 - 20 - 2. 3 - 2 - 5 - 6 - 6 - 16 - 20 - 1 - 2 - 3 - 2 - 5 - 6 - 6 - 16 - 20 - 1 - 2 - 3 - 2 - 5 - 6 - 6 - 16 - 10 - 1 - 2 - 1 - 1 - 12 - 1 - 2 - 1 - 13 - 13 - 13 - 13 - 14 - 1 - 2 - 2 - 1 - 16 - 13 - 13 - 13 - 14 - 1 - 2 - 2 - 1 - 16 - 13 - 13 - 15 - 15 - 1 - 2 - 2 - 1 - 16 - 13 - 13 - 15 - 1 - 2 - 2 - 1 - 16 - 17 - 1 - 2 - 2 - 1 - 16 - 17 - 1 - 2 - 2 - 1 - 16 - 17 - 1 - 3 - 3 - 3 - 3 - 3 - 3 - 3 - 3 - 1 - 3 - 3 - 3 - 3 - 3 - 3 - 1 - 3 - 3 - 3 - 3 - 3 - 3 - 1 - 3 - 3 - 3 - 3 - 3 - 3 - 1 - 3 - 3 - 3 - 3 - 3 - 1 - 3 - 3 - 3 - 3 - 3 - 1 - 3 - 3 - 3 - 3 - 3 - 1 - 3 - 3 - 3 - 3 - 1 - 3 - 3 - 3 - 3 - 1 - 3 - 3 - 3 - 3 - 1 - 3 - 3 - 3 - 3 - 1 - 3 - 3 - 3 - 3 - 1 - 3 - 3 - 3 - 3 - 1 - 3 - 3 - 3 - 3 - 1 - 3 - 3 - 3 - 3 - 1 - 3 - 3 - 3 - 3 - 1 - 3 - 3 - 3 - 3 - 1 - 3 - 3 - 3 - 1 - 3 - 3 - 3 - 1 - 3 - 3 - 3 - 1 - 3 - 3 - 3 - 1 - 3 - 3 - 3 - 1 - 3 - 3 - 3 - 1 - 3 - 3 - 3 - 1 - 3 - 3 - 3 - 1 - 3 - 3 - 3 - 3 - 3 - 3 - 3 - 3 - 4 - 5 - 5 - 6 - 6 - 7 - 7 - 6 - 7 - 8 - 7 - 8 - 7 - 8 - 7 - 8 - 7 - 8 - 7 - 9 - 9 - 13 - 13 - 10 - 10 - 10 - 10 - 10 - 10 - 10 - 10	• 6 0 · 6 0	••	20
2.1 gm/Cc 3. 7 - 5 - 6 - 7 - 7 - 16 - 17 - 20 - 24 - 6 - 6 - 6 - 15 - 2 - 1 - 20 - 2. 3 - 2 - 5 - 6 - 6 - 16 - 20 - 1 - 2 - 3 - 2 - 5 - 6 - 6 - 16 - 20 - 1 - 2 - 3 - 2 - 5 - 6 - 6 - 16 - 10 - 1 - 2 - 1 - 1 - 12 - 1 - 2 - 1 - 13 - 13 - 13 - 13 - 14 - 1 - 2 - 2 - 1 - 16 - 13 - 13 - 13 - 14 - 1 - 2 - 2 - 1 - 16 - 13 - 13 - 15 - 15 - 1 - 2 - 2 - 1 - 16 - 13 - 13 - 15 - 1 - 2 - 2 - 1 - 16 - 17 - 1 - 2 - 2 - 1 - 16 - 17 - 1 - 2 - 2 - 1 - 16 - 17 - 1 - 3 - 3 - 3 - 3 - 3 - 3 - 3 - 3 - 1 - 3 - 3 - 3 - 3 - 3 - 3 - 1 - 3 - 3 - 3 - 3 - 3 - 3 - 1 - 3 - 3 - 3 - 3 - 3 - 3 - 1 - 3 - 3 - 3 - 3 - 3 - 1 - 3 - 3 - 3 - 3 - 3 - 1 - 3 - 3 - 3 - 3 - 3 - 1 - 3 - 3 - 3 - 3 - 1 - 3 - 3 - 3 - 3 - 1 - 3 - 3 - 3 - 3 - 1 - 3 - 3 - 3 - 3 - 1 - 3 - 3 - 3 - 3 - 1 - 3 - 3 - 3 - 3 - 1 - 3 - 3 - 3 - 3 - 1 - 3 - 3 - 3 - 3 - 1 - 3 - 3 - 3 - 3 - 1 - 3 - 3 - 3 - 3 - 1 - 3 - 3 - 3 - 1 - 3 - 3 - 3 - 1 - 3 - 3 - 3 - 1 - 3 - 3 - 3 - 1 - 3 - 3 - 3 - 1 - 3 - 3 - 3 - 1 - 3 - 3 - 3 - 1 - 3 - 3 - 3 - 1 - 3 - 3 - 3 - 3 - 3 - 3 - 3 - 3 - 4 - 5 - 5 - 6 - 6 - 7 - 7 - 6 - 7 - 8 - 7 - 8 - 7 - 8 - 7 - 8 - 7 - 8 - 7 - 9 - 9 - 13 - 13 - 10 - 10 - 10 - 10 - 10 - 10 - 10 - 10	•n · N	•=	INVOLVING GLACIAL DRIFT AND BURIED BIVER
2.1 gm/Cc 37 - 5 - 6 - 7 - 7 - 15 - 17 - 20 - 20 - 6 - 6 - 6 - 6 - 22 - 1 - 22 - 22 - 22	• 🗷	- 10	20
2.1 gm/cc 3. 7. 18 47 79 28 6 8 6 8 6 8 7 6 7 7 1 18 12 13 18 12 1 18 12 1 1 18 12 1 1 18 12 1 1 18 12 1 1 18 12 1 1 18 12 1 1 18 12 1 1 18 12 1 1 18 12 1 1 18 12 1 1 18 12 1 1 1 1	• 🕫	••	1811
2.1 gm/cc 3. 7. 8. 4. 7. 7. 15. 4.7 150 1.8 8 8 8 8 8 8 8 8 8 8 8 8 8 8 8 8 8 8	-m -4 -8 -8 -0 -18 -1 -1 -1 -18 -18 -18 -1	0 · ~ · ~ · · · · · · · · · ·	8
2.1 gm/CC 3. 7 7 7 16 17 100 24 6 8 8 8 8 8 8 8 8 8 8 8 8 8 8 8 8 8 8	· <u>n</u>	٠.0	4
2.1 gm/cc 37 -5 -6 -7 -7 -15 -17 -20 -24 -6 -3 -5 -5 -5 -6 -6 -16 -20 -9 -15 -5 -5 -6 -6 -16 -20 -9 -15 -5 -5 -6 -6 -16 -20 -9 -15 -7 -5 -7 -12 -12 -15 -7 -6 -7 -12 -13 -15 -7 -6 -7 -12 -13 -15 -7 -6 -7 -12 -13 -15 -7 -6 -7 -12 -13 -15 -7 -6 -7 -12 -13 -15 -7 -6 -7 -12 -13 -15 -7 -6 -7 -12 -13 -15 -7 -6 -7 -12 -13 -15 -7 -6 -7 -12 -13 -15 -7 -6 -7 -12 -13 -15 -7 -6 -7 -12 -13 -17 -7 -12 -13 -1 -7 -7 -12 -13 -1 -7 -7 -12 -13 -1 -7 -7 -12 -13 -1 -7 -7 -12 -13 -1 -7 -7 -7 -12 -13 -1 -7 -7 -7 -7 -7 -7 -7 -7 -7 -7 -7 -7 -7	٠.	•2	157
2.1 gm/cc 4. 7. 7. 7. 7. 15. 17. 19. 29. 5. 8. 15. 12. 12. 6. 10. 12. 12. 1. 10. 12. 12.	. <u>n</u>	••	80
	. <u>N</u>	•=	14/
	· · · · · · · · · · · · · · · · · · ·	i	140
		•	9
	_	. 9	NN.
			1701
	۰. م		_
			MODEL
		7	NO
· · · · · · · · · · · · · · · · ·		•	
-7	· o · N	٠,	
.	· -	• •	
A		•• •• ••	

*	•••	•	• •	. 0	-0		• •	• •	• •	. 0	· 7 · 7		, m	. pg	· •	• • • •		STATION GRAVITY ERROR	(MGAL) XIO-	R.NS RADIUS = 10000	C .000 2000 3000	1 1 1 1 1 1 1 1 1 1 1 1 1 1 1 1 1 1 1
Ì	٠.				-	٠.					٠٠					٠,		57	,	ָ מַבְּי	3	
	٠ ٥					. 7					٠,					٠,	L					J
	٠.					٠.					٠.					٠٠						141
	. 10	• -	٠.	٠-	٠ %		. 10	• •	٠ •	٠ پ	•	·w	٠٢.	. 약	٠•	. 10	. 60	· ທຸ	· 10	. 10	٥.	144
ا ن	• -					٠,					. .					· e p					۰.	CLACIAL DRIET AND BIDIED BIVED CHANNEL
24 Jm/cc	٠,					٠٩					۰ م					. m					-10	וועצו
24	. 0					٠,					. ტ					• -					-0	8 6
-	• 0					•					, m					۰.					۰.	jan
	• •	٠,	٠.	۰۰	۰۰	••	٠-	٠,	•	•	•6	٠,	• 10	•	٠ φ	٠.	. 10	• H)	· 10	٠-		q
	٠ ،					٠,					-28 -16					٠=					٠٠	86
	• 🕇					٠ ،					-28					. 우					·=	(3/0
	• 4					. ທຸ					٠					٠٩					i4 - i	
	٠,					٠,					. 10					· 10					5 .	
X	· 8	· g	36	• 8	. 22	- 88	• <u>m</u>	• <u>-</u>	• 6	• ѿ	• ō	. ∾	*	. 8	٠ %	· 10	. 💇	٠ ق	. ₫	. 22	-\$	3
	. 92 20					•=					۰.					٠.					· 0	
	· 12					•=					٠.					٠.					· 50	7
	· 8					• •					٠ ق					. 0					• 60	
۷٥/	٠2					•=					٠,					٠.					۰ پ	ì
Ę	••	• 10	· 10	٠.	• 10	. 10	• ത	. 10	· w	• 0	۰0	۰0	· -	•-	٠,	• 7	٠٩	۰ ٥	. 10	٠ ٨	. 10	707
2.1.						• •					•-					• 7					٠0	4
	٠.					• •					·					٠ %					•0	
	•=					. 10					•-					٠ ۴					, ଜ୍ୱ	
	• IO					۰0					• 10					• 7					٠0	
*	• 10	· -	· 0	•-	٠ %	. 4	. W		٠ ه	•10	•-	•	٠0	٠٥	۰0	• •	••	-0	•0	٠٥	• 0	

If the data set encompasses a complex gravity field, then a higher degree polynomial will be required to satisfactorily fit the data. Increasing the number of data points per unit area will permit the use of a smaller ring size and decrease the complexity of the gravity field in the data set. The result of this combined effect is demonstrated in the following study.

The model involving the glacial drift and buried river channel was processed after calculating the data on a 1,000 foot grid spacing. The calculated density values shown in Figure 36 were obtained from using a first degree polynomial and 1,200 foot ring radius. The excellent results were obtained even though the density values in the glacial drift changed from 2.2 gm/cc to 2.6 gm/cc.

Altering the Elevation Datum. -- Vajk (1956) has shown that the variable datum to which the observed gravity values are reduced through the use of a local representative elevation factor should be subject to geological considerations. A study was undertaken to find what effect the elevation datum had on the calculated elevation factor.

The observed gravity values for the model involving all of the sources were calculated at the station ele-vations. The elevation datum was raised 100 feet, producing both positive and negative values as shown in

280 2.80 2.80 2.80

CALCULATED DENSITY VALUES DEGREE POLYNOMIAL= 1

GLACIAL DRIFT AND BURIED RIVER CHANNEL MODEL INVOLVING

 2.80 2.80

2.60 gm/cc_

2.20 gm/cc

Figure 37. These values along with the previously calculated observed gravity values were used in calculating the station elevation factor. The results, along with the results obtained when the elevation datum was lowered from the original by 100 feet, matched exactly the values obtained from the original complete model study. This study shows the calculated elevation factor is a function of the elevation differences, and not a function of the absolute station elevation.

Summary of the Model Studies

An individual elevation factor can be obtained at each station in the survey through the use of the proposed least squares process. The use of the observed gravity and elevation values of the surrounding stations negates the need for making preliminary data reductions. Evaluation of the assets and limitations of the method through the model studies indicate the following:

- 1. Rapid variations in the surface topography do not affect the calculated elevation factor when the topographic expression is not associated with a near surface density change. This eliminates the possibility of creating anomalies which are topographically associated.
- 2. An intermediate density value is obtained in the immediate vicinity of a sharp near surface density change.

-11 -18 -17					-32					-22					. -		ELEVATION VALUES AFTER RAISING DATUM	100 FEET		1000 2000 3000	
	• •	<u>.</u> 5	-2,		-5-	· #	-27	-33	- &	٠.	•	۰.	. <u>m</u>	. <u>10</u>	٠,٠		4 9	į		٥	l
-	•	•	•	` '		·	•	•	•	· 5					- 8	i	77				١
• 👱					. 6					-8					-1		¥	t			١
٠.					-20 -35					٠.=					.0						1
٠9					. 10					٠,					5.						
. \$. e	- 2	. 2	. 55	٠ ۾	٠ ۾	- 88	. 4	- 2	- 1	•	. 14	• 66	. 2	. 99	· 👼	٠.	• 4	. 6	. 2	
					. 10					***					٠,					. 10	
. 10					. ถึ					•=					- <u>m</u>					. 9	
• ≘					. 6					. 0					- 8					-90	8
-87 118										-62					-69					39 -13 -45 -69 -62 -90	
•=	. 73	-7.7	. 2	-1.	17- 47- 11- 87-	. 99	. 89	-62	-8.	٠ ۾	-35	. 9	-57	• \$	٠ ق	. 26	-70	. 7.	• 4	. 6	
-2	•	•	•	·	•					· 10					. 00						
• 👨					. P					• 20					۰ 0					• 📆	
-37 -51 -76 - 81					• 4					٠ ٥					•=						i
• m					, 38 ·					• ‡					٠ ڳ					,£	
• •	. 4 0	. 66	٠.	- 0	٠,	. 86-	· •	-23	٠ ٥	• ¹⁰	-36	• 4	. 69	• 4	· \$. 2	27	. 10	• 4	٠4	
• ~					. ማ					• •					.35 -19					-18	
. \$					• •					•=										٠.	
• 4					٠ <u>٠</u>					. 5					- 32					٠.0	
. 13					. 8					• •					•					•=	
٠8	- 7	32	• 😇	· E		-8	•₹	. w	. 9	• 4	- 23	٠5-	-38	. 8	٠,	. 10	•	• •	.8		
• 4					52					٠ ٨					٠,					. 9	
• •					. 8					• •					٠,					٠й	
25.					, <u></u>					23					37					•80	
-23					• 10)					2,			•		••					14	
-59	. 8	- M	• 4	· nò	-5.		-36	- 2-	- 2	- 0	-42	• ⊙	-27	. 4	•=	. 80	. 12	. ~	<u>.</u>	· <u>-</u> -	

		1
		1

- 3. Steep gravity gradients caused by near surface sources have a negative effect on the accuracy.
- 4. The magnitude and lateral extent of the negative effect caused by sharp density changes and steep gravity gradients related to near surface sources is greatly reduced by decreasing the station spacing.
- 5. The calculated elevation factor, being a function of the station elevation differences within the data set, permits the reduction of the data to some geologically significant non-horizontal datum with the calculated elevation factor, and then to a horizontal datum with a pre-selected elevation factor.

Elevation and Mass Correction for the Field Data

An elevation factor was calculated for each station in the survey by using a fifth degree polynomial equation and a ring radius of 10,000 feet. A third degree polynomial was used on the elevation values shown in Figure 38 to provide the residual values shown in Figure 39. These residual values were then combined with the observed gravity values in the least squares process and an elevation factor calculated for each station. The calculated station density values are shown in contour form in Figure 40.

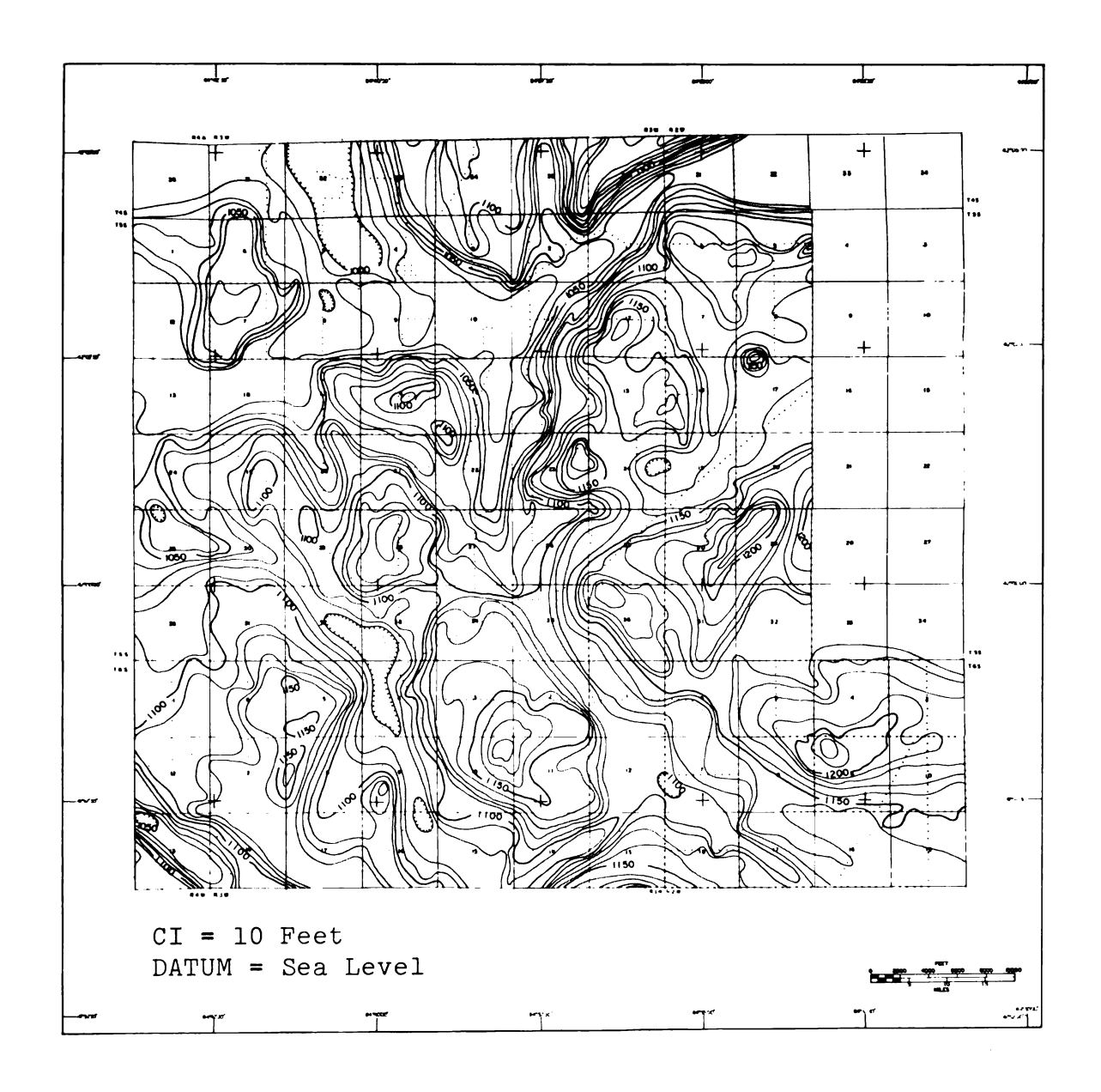


FIGURE 38.--Contour map of the survey elevations.

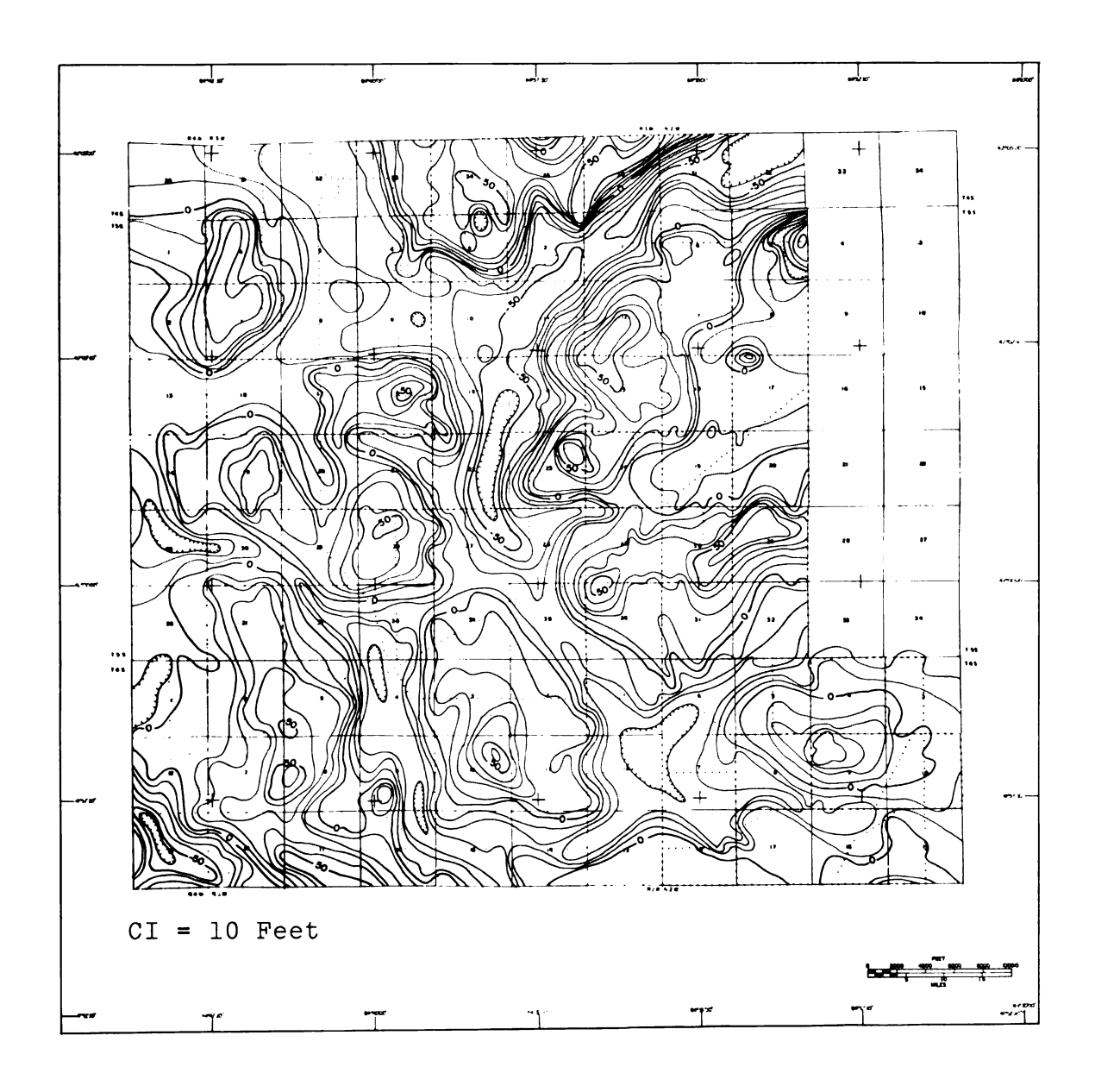


FIGURE 39.--Contour map of the residual elevations from a third order polynomial approximation to the elevation surface.

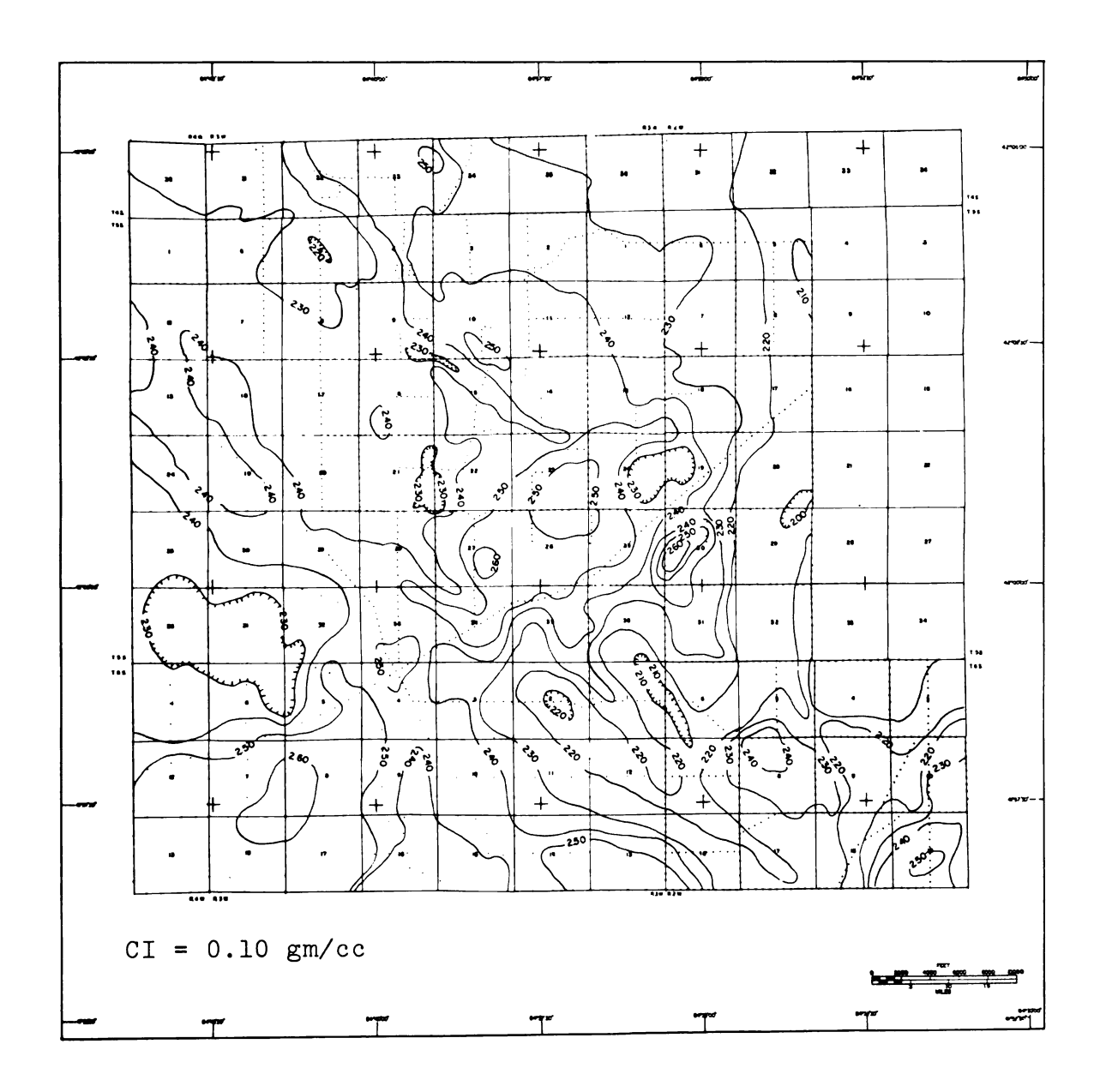
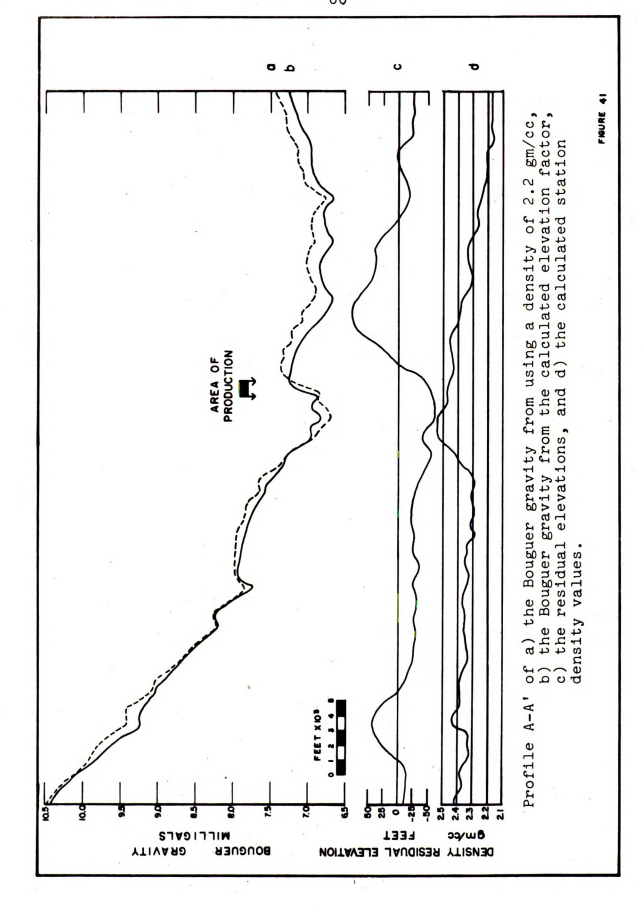


FIGURE 40.--Variable density map from the least squares method using a fifth degree polynomial and a 10,000 foot ring radius.

The calculated station elevation factor was used to correct the station observed gravity value to the third degree polynomial elevation datum. A constant elevation factor equivalent to a density value of 2.30 gm/cc was employed to correct from the polynomial datum to a horizontal datum equal to the lowest station elevation in the survey. This density was selected as representative of the surface density on the basis of the values shown in Figure 40.

Profile A-A' in Figure 41 illustrates the relation-ship between the calculated density values, the residual elevations, the Bouguer gravity using a constant density of 2.2 gm/cc, and the Bouguer gravity using the calculated elevation factor. Figure 42 is the Bouguer gravity map after employing the variable elevation factor.



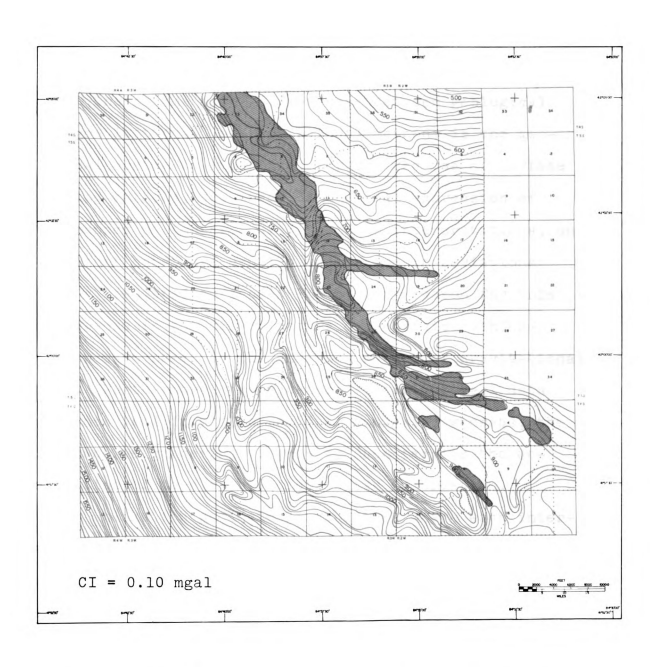


FIGURE 42.--Bouguer gravity map after employing the variable elevation factor.

METHODS OF DATA ANALYSIS

One of the major differences between geological and gravitational interpretational methods is the geological desire to recapture, through the use of surface fitting methods, the three dimensional expression of the mapped parameter. Gravitational interpretations, on the other hand, are usually manifested in deviations from a predicted surface. The primary reason for this difference is the direct nature of geological information as opposed to the indirect nature of gravitational data. Furthermore, the clustered nature of well data does not lend itself to residual analysis, whereas, the inexpensive gathering of gravity data permits the acquisition of more evenly distributed information.

Unlike the geological situation, where each interval or formation conveys specific information and is a measurable entity, the Bouguer gravity map contains information from or caused by geological conditions extending from the surface down to and including the basement complex. Since the mapped parameter is a composite, it becomes necessary to extract and display those signals which may be caused by or related to some known or hypothesized geological situation.

The extraction or isolation of selected information from the Bouguer gravity map may be accomplished by several different methods. The methods used in this study include polynomial analysis, double Fourier series analysis, and linear filtering methods. The latter two methods were selected for their ability to quantify the type of information to be extracted from the total map. Furthermore, the parameters of the desired information can be ascertained from geological and geophysical model studies. Polynomial analysis has been widely used as an interpretational technique in the State of Michigan and is included as a standard of comparison.

Polynomial Approximations to the Bouguer Surface

Polynomial approximations to the Bouguer gravity surface using the least squares criterion are generally used for the removal of the long wavelength regional component. The degree of the approximation polynomial which will satisfactorily represent the regional is subject to personal interpretation and is influenced by the distribution and spacing of the data points, the complexity of the regional, and the size of the map area.

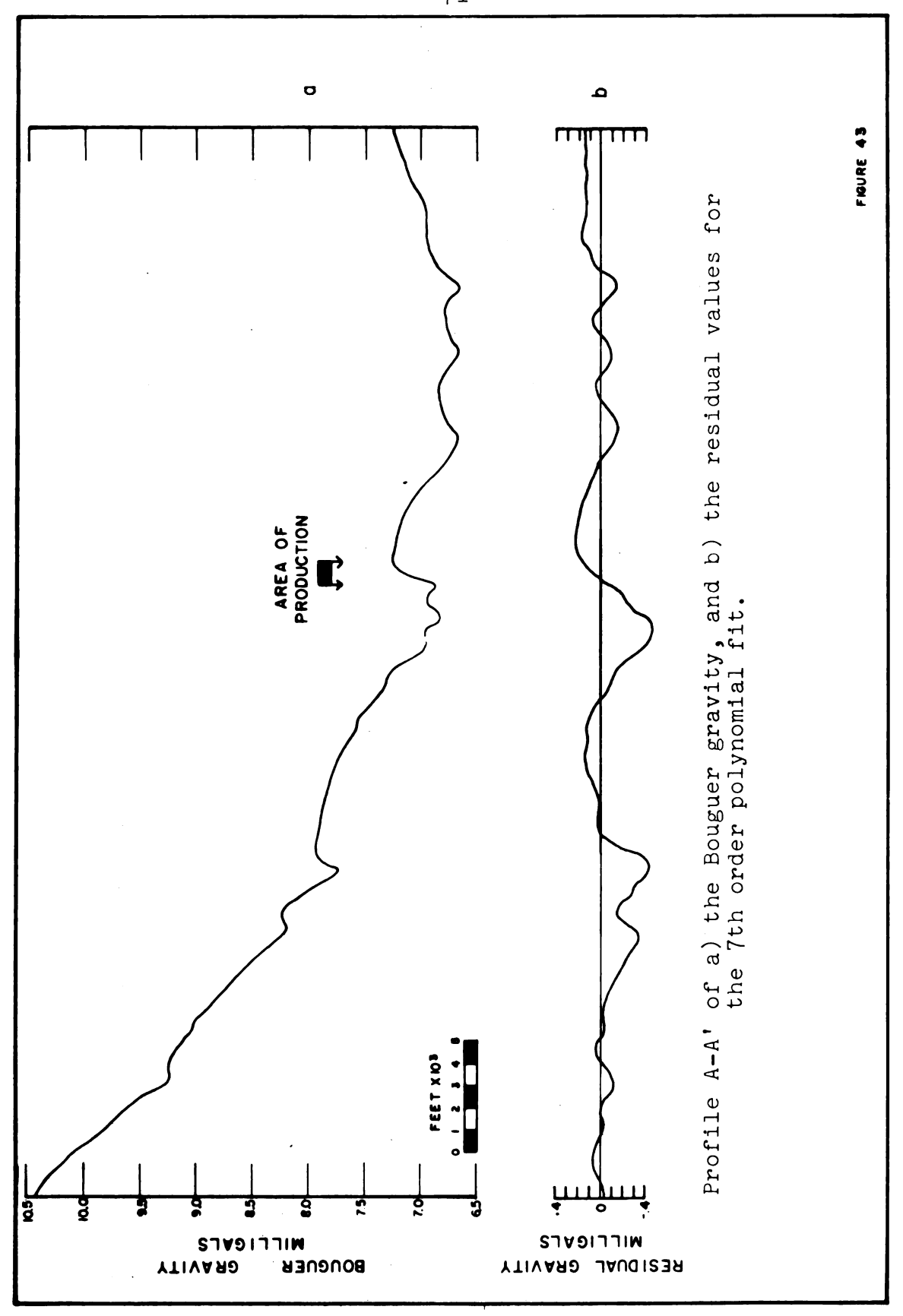
The major limitation of the polynomial approach is the inability to specify the range of wavelengths to be isolated. Signal extraction thus takes the form of

increasing the degree of the polynomial until the residual values display either known local geological situations, or hypothesized conditions. If an anomaly can be associated with a specific known geological entity, then predictions concerning the occurrence of similar features in the map area can be made on a comparison basis. The other approach is to compare the residual anomalies with an expected anomaly, where the magnitude and configuration of the expected anomaly is obtained through model studies employing theoretical bodies.

The seventh degree polynomial representation of the regional resulted in the residual values for profile A-A' shown in Figure 43 and for the map area shown in Figure 44.

Double Fourier Series Analysis

The recent use of the double Fourier series for surface fitting of irregularly spaced geological data has been described by James (1966). In the present instance, the purpose is to represent the Bouguer gravity (Gba) as a function of the two coordinates x and y. This function may be considered to be oscillatory in these two mutually perpendicular directions and representable by the equation



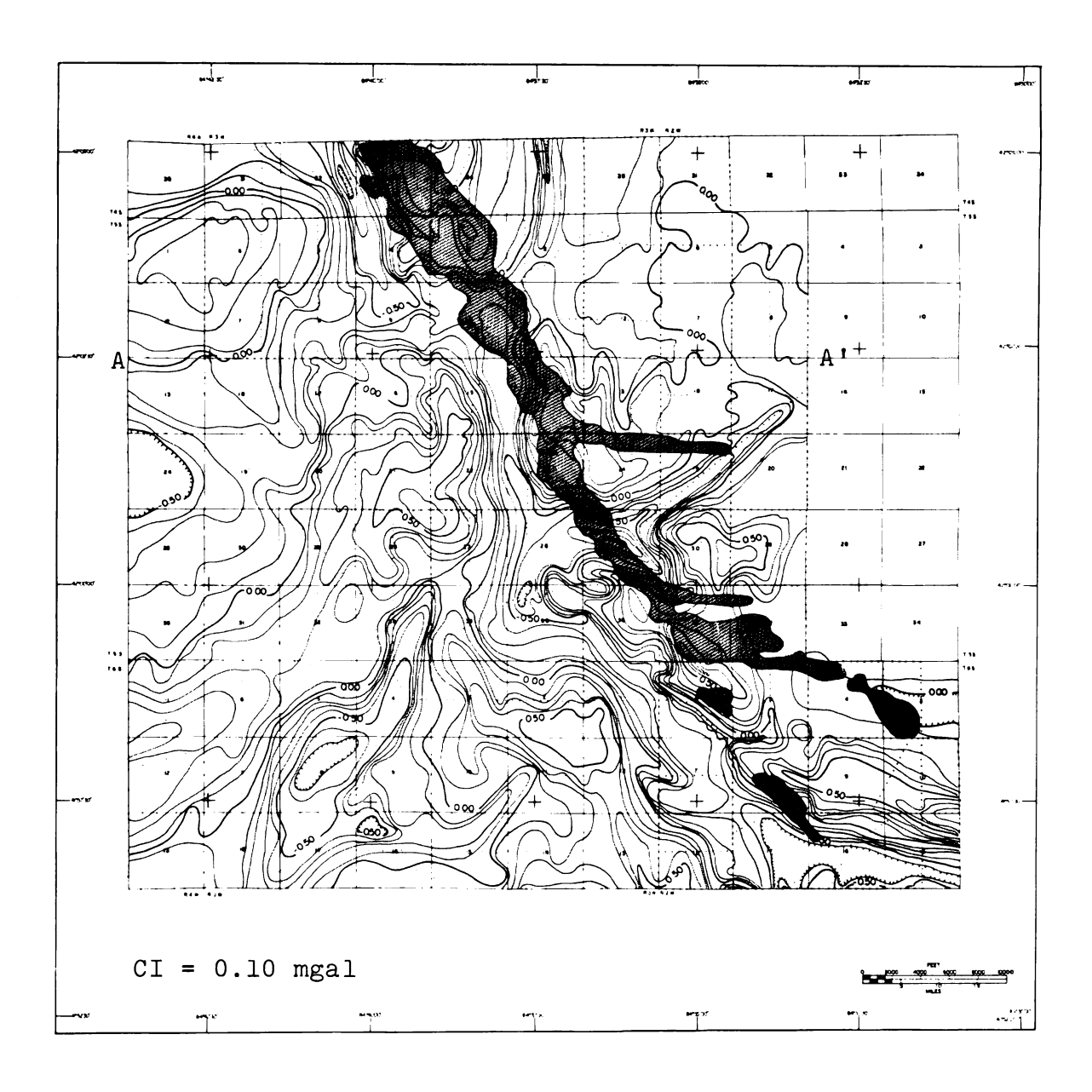


FIGURE 44.--Map of the residual values from the 7th degree polynomial approximation to the Bouguer surface.

If the function is considered to have a fundamental wavelength of 2_L along the x direction and 2_H along the y direction, then the double Fourier series is:

Gba
$$\stackrel{\sim}{=}$$
 $\stackrel{m}{\sum}$ $\stackrel{n}{\sum}$ $\stackrel{n}{\sum}$ $\stackrel{n}{\sum}$ $\stackrel{n}{\sum}$ $\stackrel{mmx}{\sum}$ $\stackrel{mny}{\sum}$ $\stackrel{mny}{\sum}$ + bm,n Sin $\frac{\pi mx}{L}$ Cos $\frac{\pi ny}{H}$ (11) + cm,n Cos $\frac{\pi mx}{L}$ Sin $\frac{\pi ny}{H}$

where

$$\zeta m, n = 1/4$$
 $m = n = 0$
 $\zeta m, n = 1/2$ $m = 0, n > 0, or m > 0, n = 0$
 $\zeta m, n = 1$ $m > 0, n > 0$

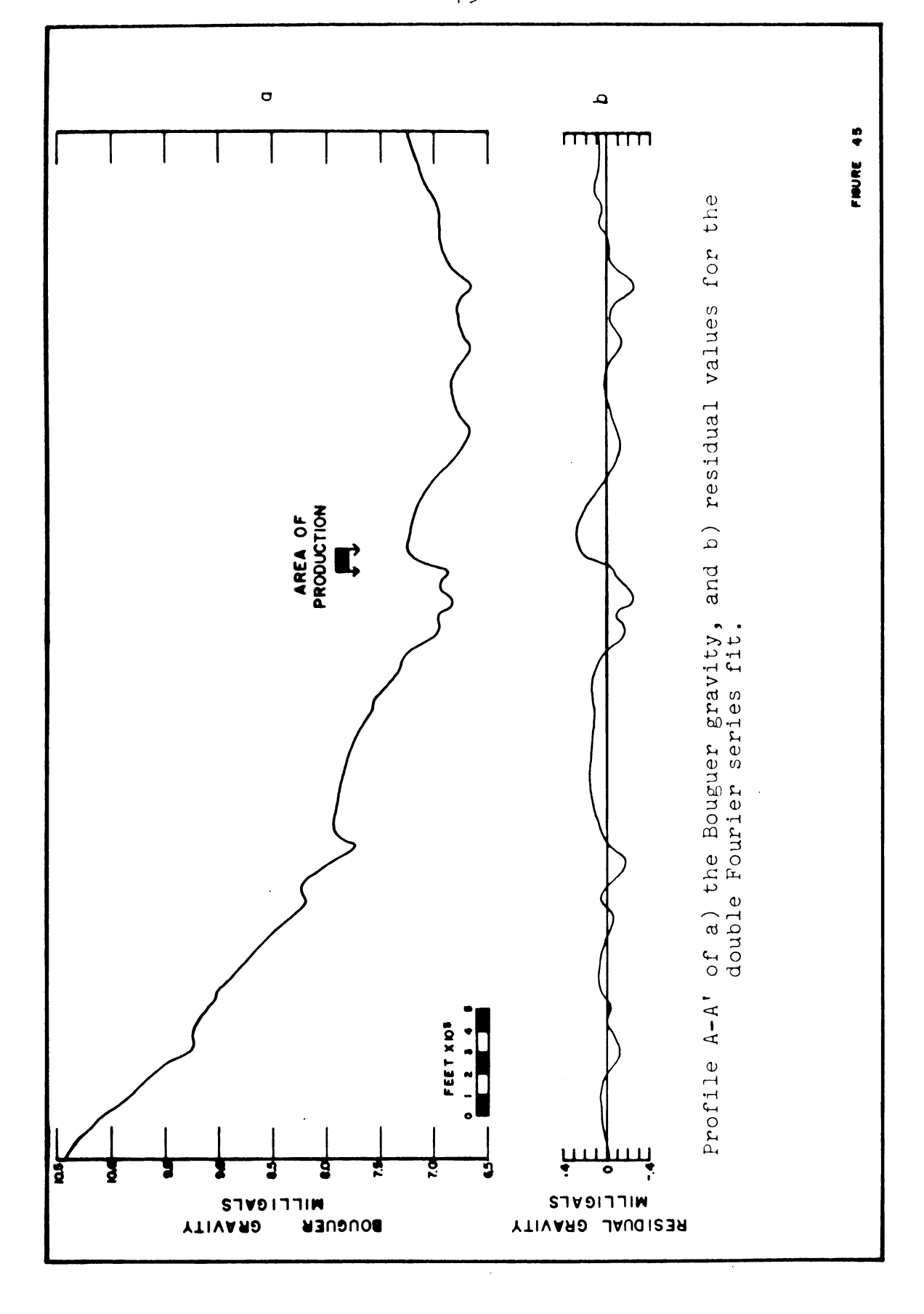
The series is linear with respect to its coefficients and thus the least squares method may be used to calculate these coefficients in a manner similar to that used in calculating the coefficients for the polynomial functions. The A matrix is now composed of the sums of squares and cross-products of the Fourier series terms, the B matrix is the column vector of coefficients, and the C matrix is a column vector of sums of products of observed values and individual Fourier series terms.

The double Fourier series has an advantage over polynomial analysis in that specific wavelengths may be included in the regional values. A present limitation is the large computer memory requirements which prevent calculating coefficients for other than the fundamental wavelengths, and the first five harmonics in both directions. These limitations prevented the calculation in the regional expression of wavelengths less than 20,000 feet in the x direction and 24,000 feet in the y direction.

The residual values shown in profile A-A' of Figure 45 were obtained by removing from the Bouguer gravity map a fundamental wavelength in both directions of 120,000 feet, along with the first five harmonics in the x direction and the first four harmonics in the y direction. Figure 46 is a map of the residual values.

Linear Filtering Methods

Digital filtering of space oriented data has become a powerful tool for interpreting gravity data. This study makes use of the approach presented by Fraser, Fuller, and Ward (1966) which employs various filters on profile data to either enhance or eliminate anomalies of specified characteristics. The theory underlying the filtering methods used in this report is presented in the following section.



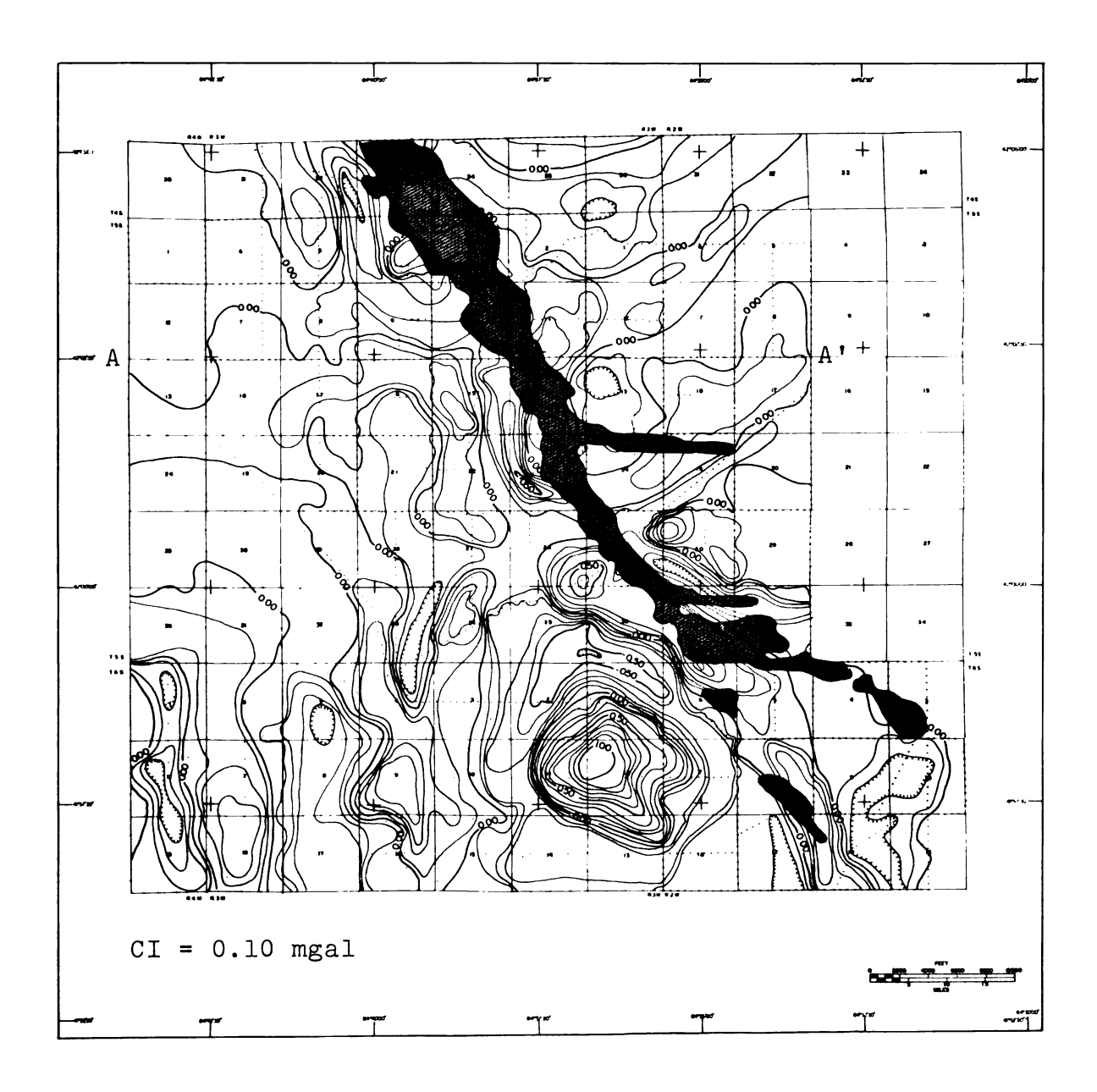


FIGURE 46.--Map of the residual values from the double Fourier series approximation to the Bouguer surface.

Theory

The input to a linear filter $\phi(x)$ is related to the output $\phi'(x)$ by the convolution of the filter with the data

$$\phi'(x) = \int_{-\infty}^{\infty} \phi(x - \tau) W(\tau) d\tau$$
 (12)

where the weighting function $W(\tau)$ is the response of the filter to an impulse.

Dean (1958) has shown that a digital representation of a continuous time domain filter, expressed here as a distance domain filter, can be represented by the equation

$$\phi(x) \stackrel{\simeq}{=} \sum_{k} W(k\Delta x) \phi(x - k\Delta x) \Delta x \qquad (13)$$

where the smooth variable τ has been replaced by the discrete variable $k\Delta x$, with Δx representing the data increment.

The problem of building a filter with the desired frequency response is accomplished through the use of Fourier transforms. The Fourier integral representation of a general filtering function can be expressed in the form

$$g(x) = \int_{-\infty}^{\infty} F(\sigma) e^{2\pi i \sigma x} d\sigma$$
 (14)

where

$$F(\sigma) = \int_{-\infty}^{\infty} g(x) e^{-2\pi i \sigma x} dx . \qquad (15)$$

 $F(\sigma)$ is the density function which describes the amount of the frequency that is present in the function g(x) and is called the transform of g(x). The Fourier integral thus decomposes the distance domain function g(x) into frequencies of intensity $F(\sigma)$.

When the desired frequency response of a filter is specified, the filtering function g(x) may be obtained from the inverse transform of $F(\sigma)$. For example, the ideal rectangular filter will pass frequencies in the band (Fo - ΔF) $\leq F \leq$ (Fo + ΔF)) without distortion, and reject all frequencies outside of this band.

The inverse transform of $F(\sigma)$ is g(x) and may be expressed as

$$g(x) = \int_{-\infty}^{\infty} F(\sigma) \cos 2\pi \sigma x d\sigma + i \int_{-\infty}^{\infty} F(\sigma) \sin 2\pi \sigma x d\sigma.$$
 (16)

By specifying $F(\sigma)$ as a real, even function, g(x) is constrained to be real and even, thus avoiding a space phase shift. These constraints cause the second integral to drop out, resulting in

$$g(x) = \int_{F_0 - \Delta F} \cos 2\pi \sigma x d\sigma$$

$$F_0 - \Delta F$$

$$= \frac{1}{\pi x} [\sin 2\pi (F_0 + \Delta F) \times - \sin 2\pi (F_0 - \Delta f) \times].$$
(17)

After applying the addition and subtraction formulas to the sine function, the filtering function takes the form

$$g(x) = \frac{2}{\pi x} \cos 2\pi Fox \sin 2\pi \Delta fx.$$
 (18)

This infinite length filter is shortened to a finite length by applying the hanning function (Blackman and Tukey, 1958),

$$S(x) = \begin{cases} 1/2(1 + \cos \frac{\pi x}{T}) & |x| < T \\ 0 & |x| \ge T \end{cases}$$
 (19)

where 2 T is the desired filter length in units of distance. In practice, it was found necessary to include the Lancos sigma factor to compensate for the Gibbs phenomenon (Hamming, 1962). The weighting function used in this study now becomes

$$W(k) = g(k\Delta x) S(k\Delta x) sigma(k\Delta x)\Delta x$$
 (20)

where the Lancos sigma factor is expressed as

Sigma (k) =
$$\left[\sin \frac{k\pi}{T} \right] / \frac{k\pi}{T}$$
 (21)

The frequency response of this modified filter is calculated from the Fourier transform of the weighting function:

$$F(\sigma) \cong \int_{-T}^{T} g(x) s(x) Lancos (x)e^{-2\pi i \sigma x} dx, \qquad (22)$$

which may be expressed in summation form as

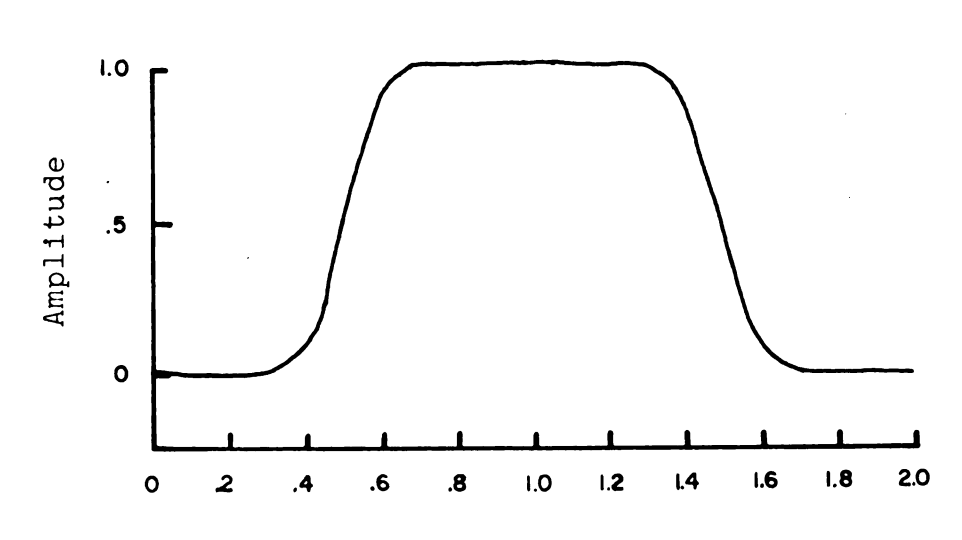
$$F(\sigma) \cong 2 \sum_{k=0}^{T} W(k) \cos 2\pi\sigma k \Delta x.$$
 (23)

The above presentation follows that of Fraser,
Fuller, and Ward (1966) with the exception of the Lancos
sigma factor. The response of both low pass and band
pass filters used in the study are shown in Figure 47.

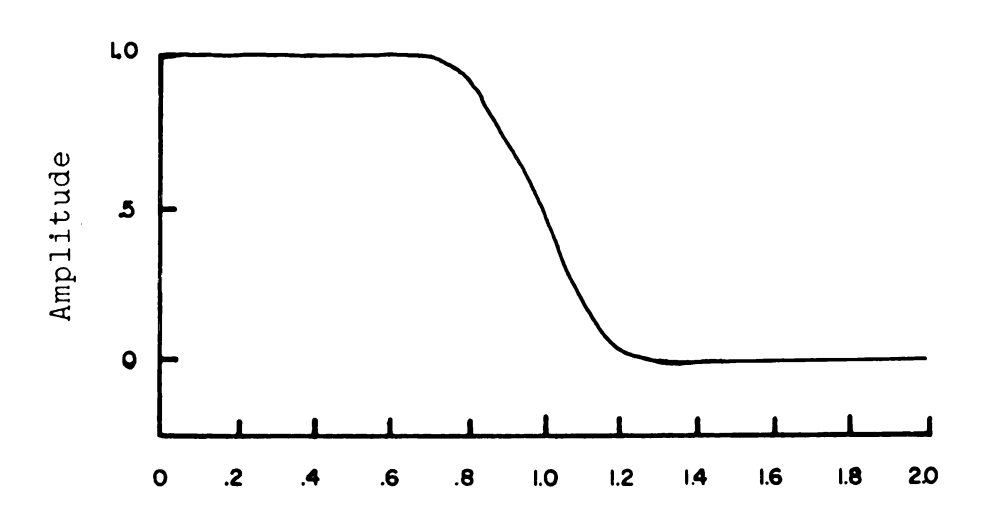
The requirement of using evenly spaced data was met by contouring the Bouguer gravity and interpolating onto a 500 foot spacing in the x direction for lines 1,000 feet apart in the y direction. The program extended the ends of the lines the necessary number of data points so that the number of filtered stations equaled the number of input points. The extended values were projected through the use of the mean slope of the end ten stations.

Band Pass Filtering

The ideal band pass filter will pass without amplitude or phase distortion all information which has a frequency within a specified range, and reject all other information. For example, the filter with a center frequency equivalent to a 5,000 foot half wavelength



Frequency/Center Frequency



Frequency/Cut Off Frequency

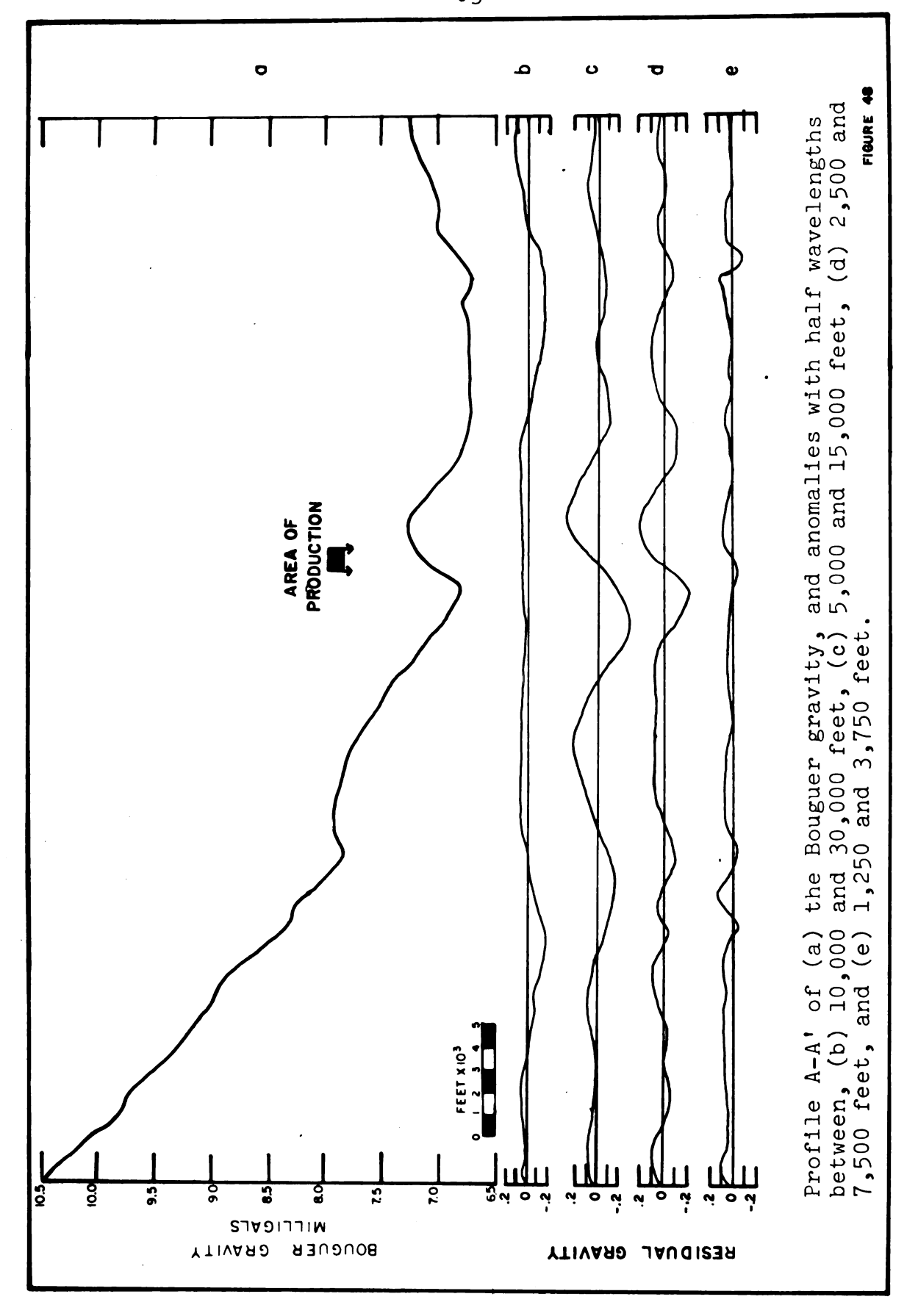
Frequency response of the band pass and low pass filters.

and a band pass of half the center frequency will pass all information with half wavelengths between 2,500 and 7,500 feet.

Each data line was processed with band pass filters having center frequencies equivalent to half wavelengths of 20,000, 10,000, and 5,000 feet with band widths of half the center frequency. Profile A-A' in Figure 48 presents: (a) the Bouguer gravity, and the associated anomalies with half wavelengths between, (b) 10,000 and 30,000 feet, (c) 5,000 and 15,000 feet, (d) 2,500 and 7,500 feet, and (e) 1,250 and 3,750 feet. The maps associated with the first three filters are shown in Figures 49 through 51. The anomalies associated with the fourth filter are too small in magnitude and random in shape to be geologically significant.

Low Pass Filters That Include the Regional

Low pass filters were used in the analysis to emphasize the longer wavelength information. This was accomplished by passing all information with half wavelengths from infinity to 20,000 feet, 10,000 feet, 5,000 feet, and 2,500 feet. The effect of including the progressively shorter wavelength anomalies in the regional is shown in profile A-A' of Figure 52, and in map form in Figures 53 through 56.



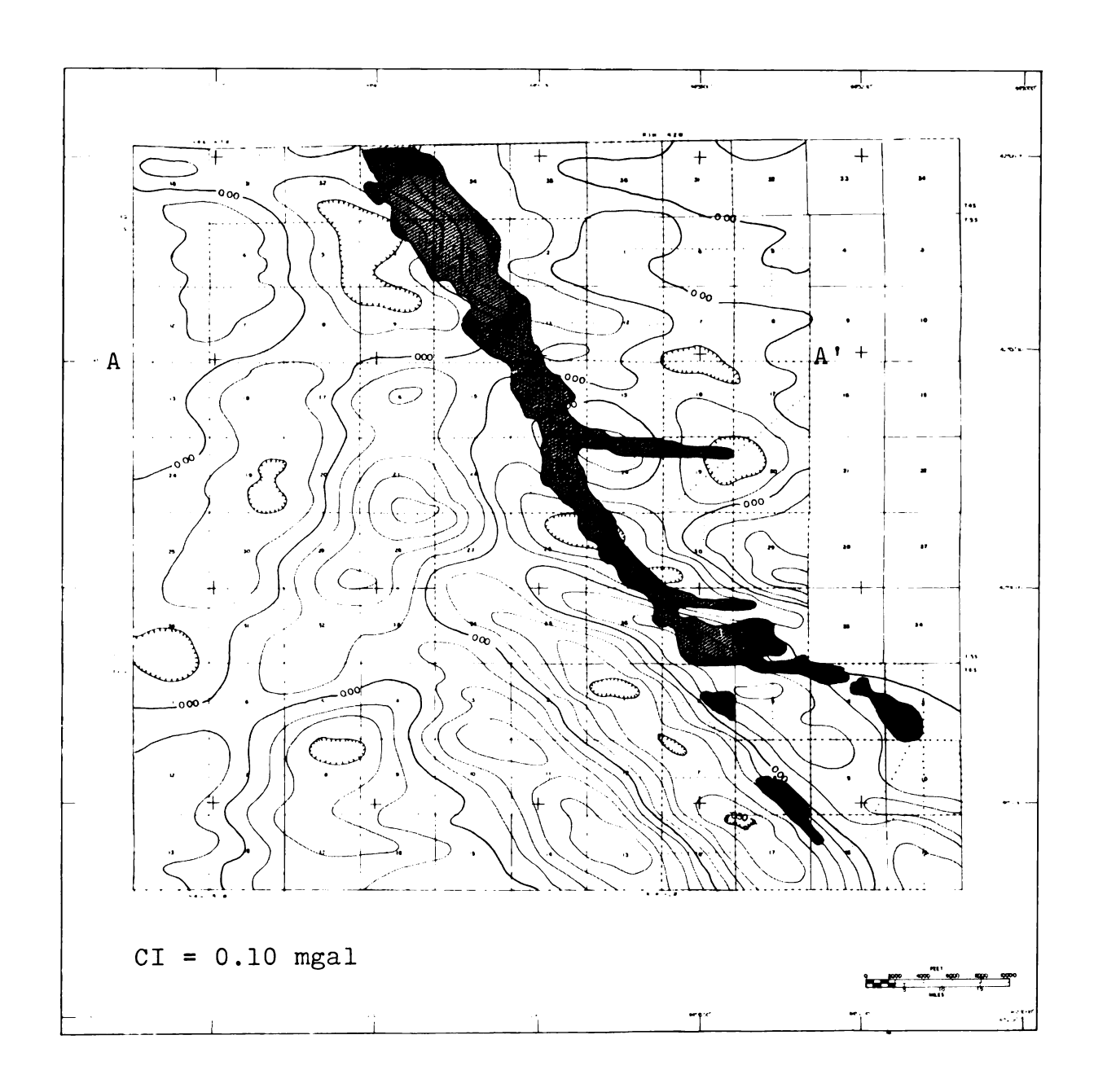


FIGURE 49.--Residual map of half wavelengths from 10,000 to 30,000 feet.

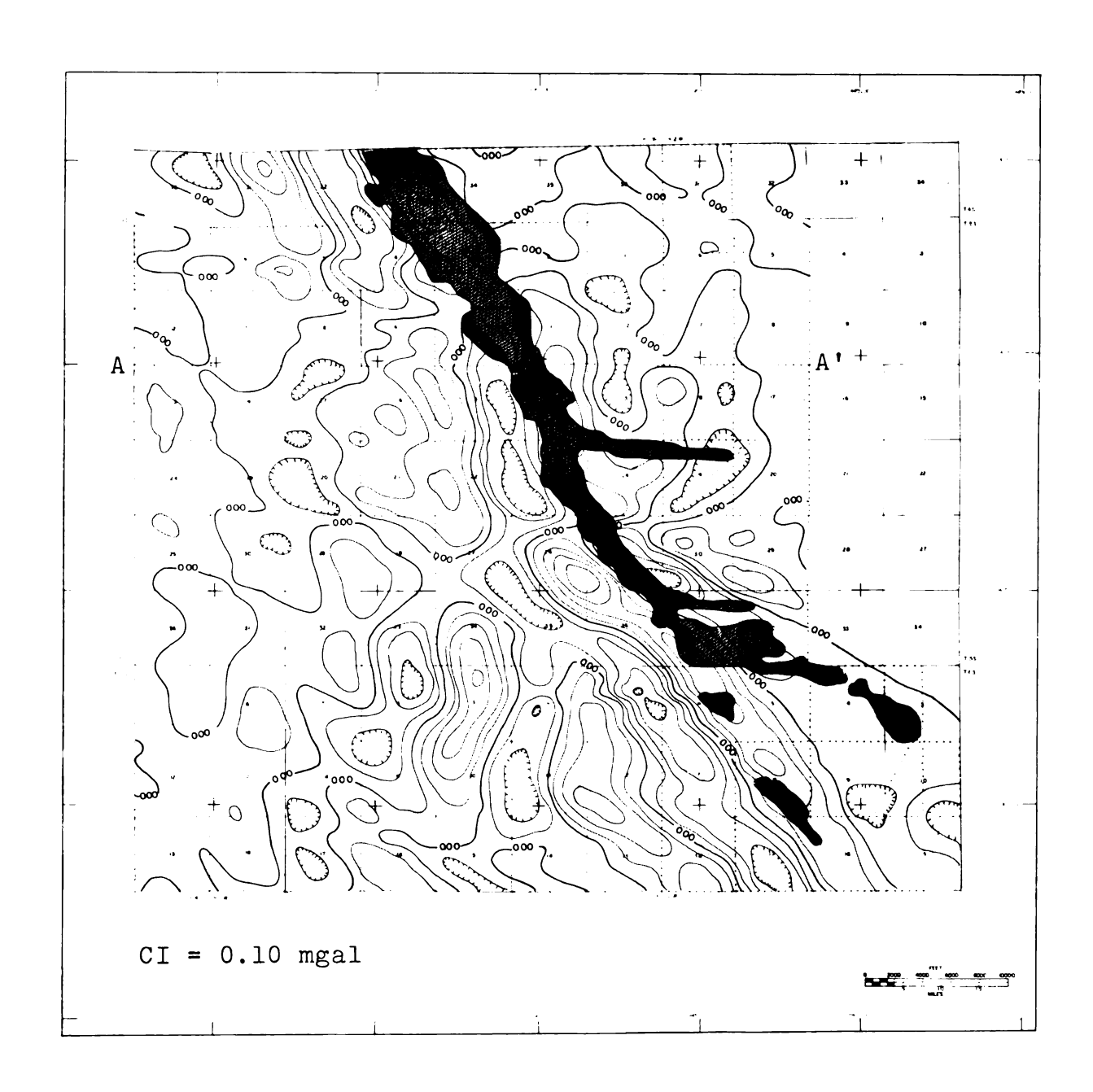


FIGURE 50.--Residual map of half wavelengths from 5,000 to 15,000 feet.

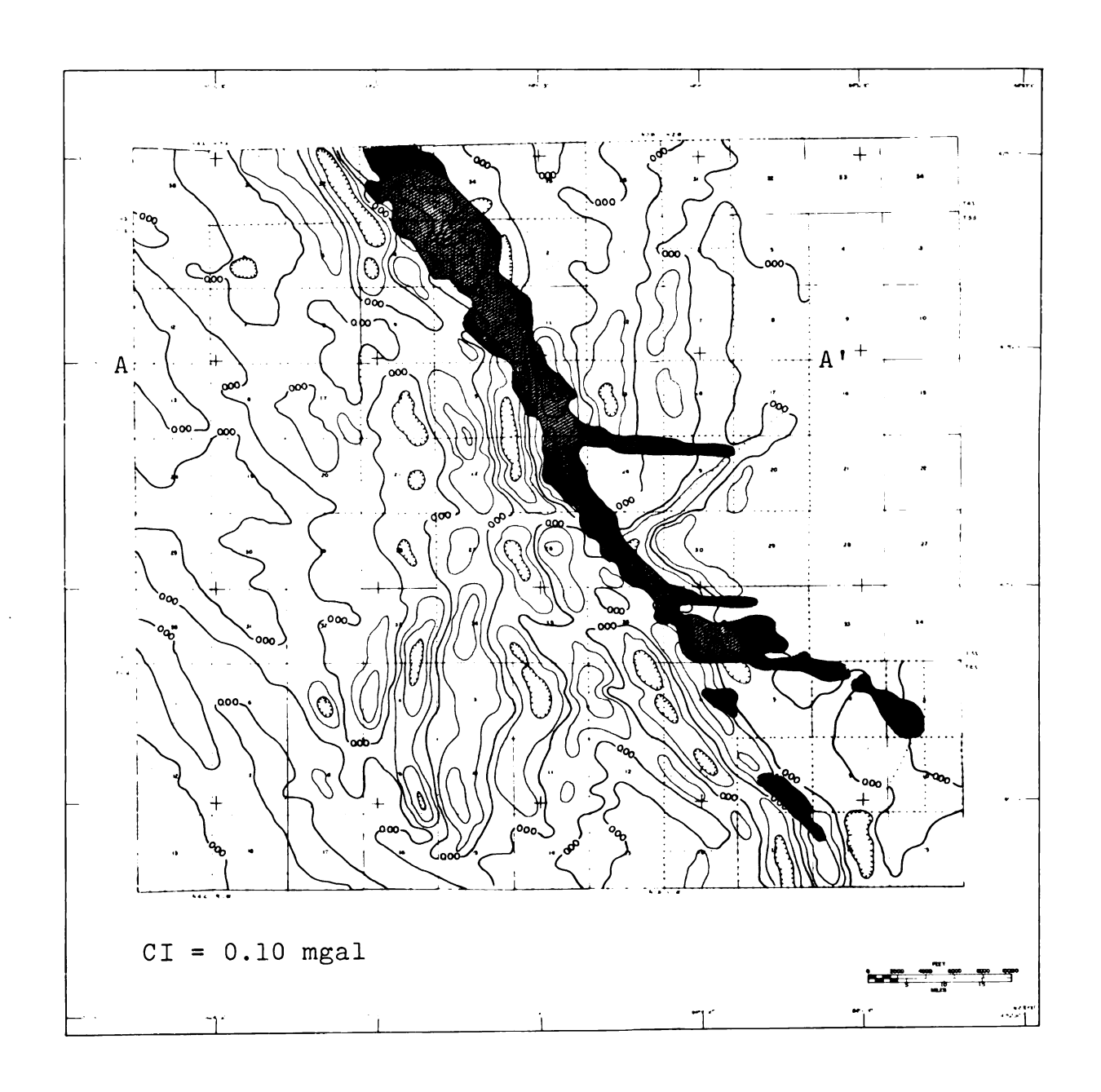
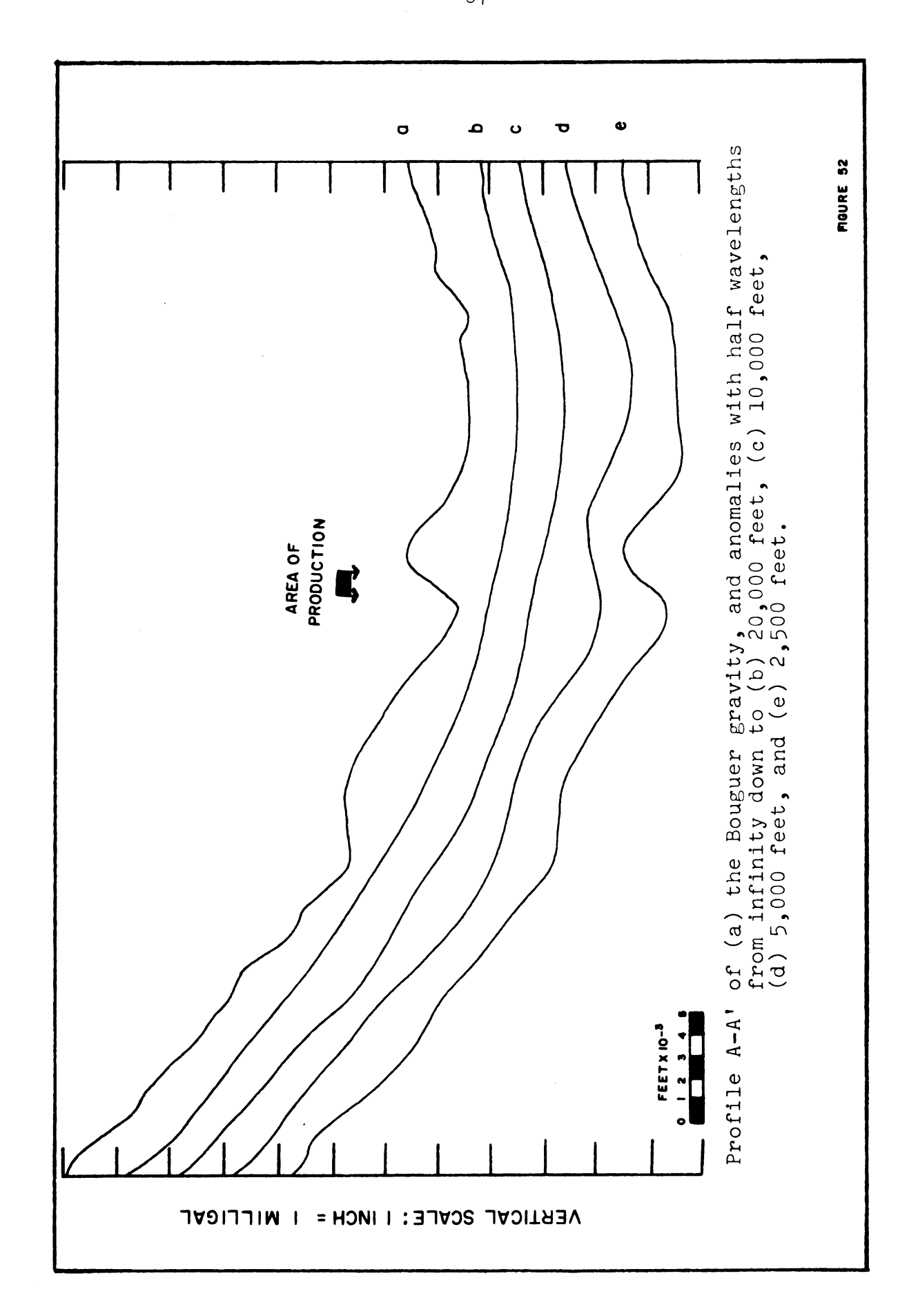


FIGURE 51.--Residual map of half wavelengths from 2,500 to 7,500 feet.



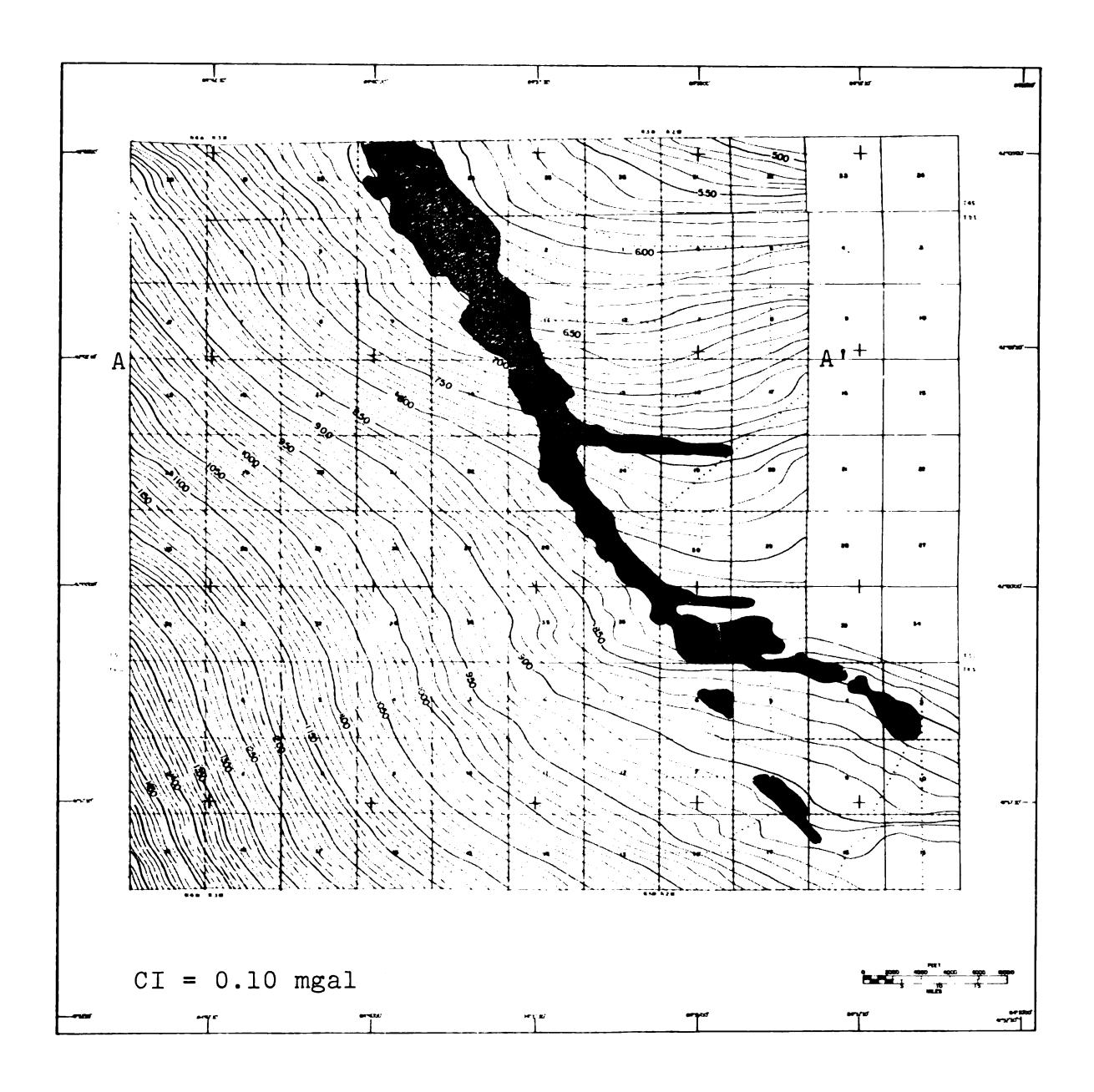


FIGURE 53.--Residual map of half wavelengths from infinity to 20,000 feet.

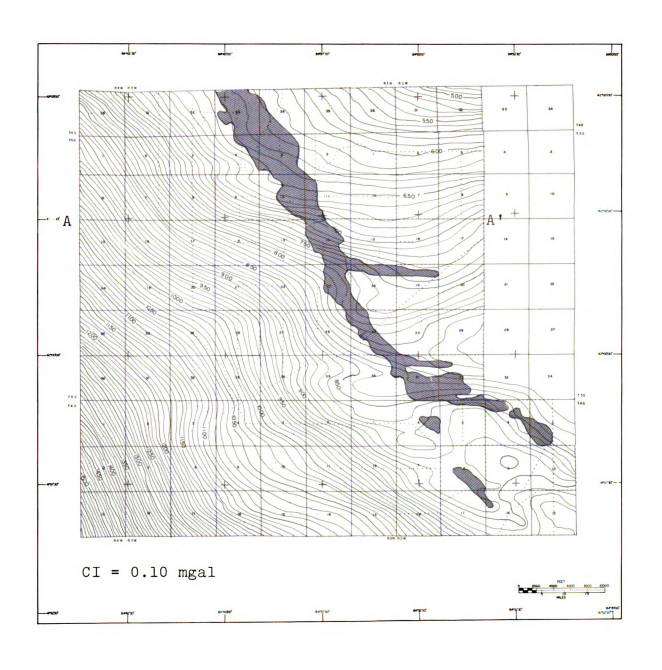


FIGURE 54.--Residual map of half wavelengths from infinity to 10,000 feet.

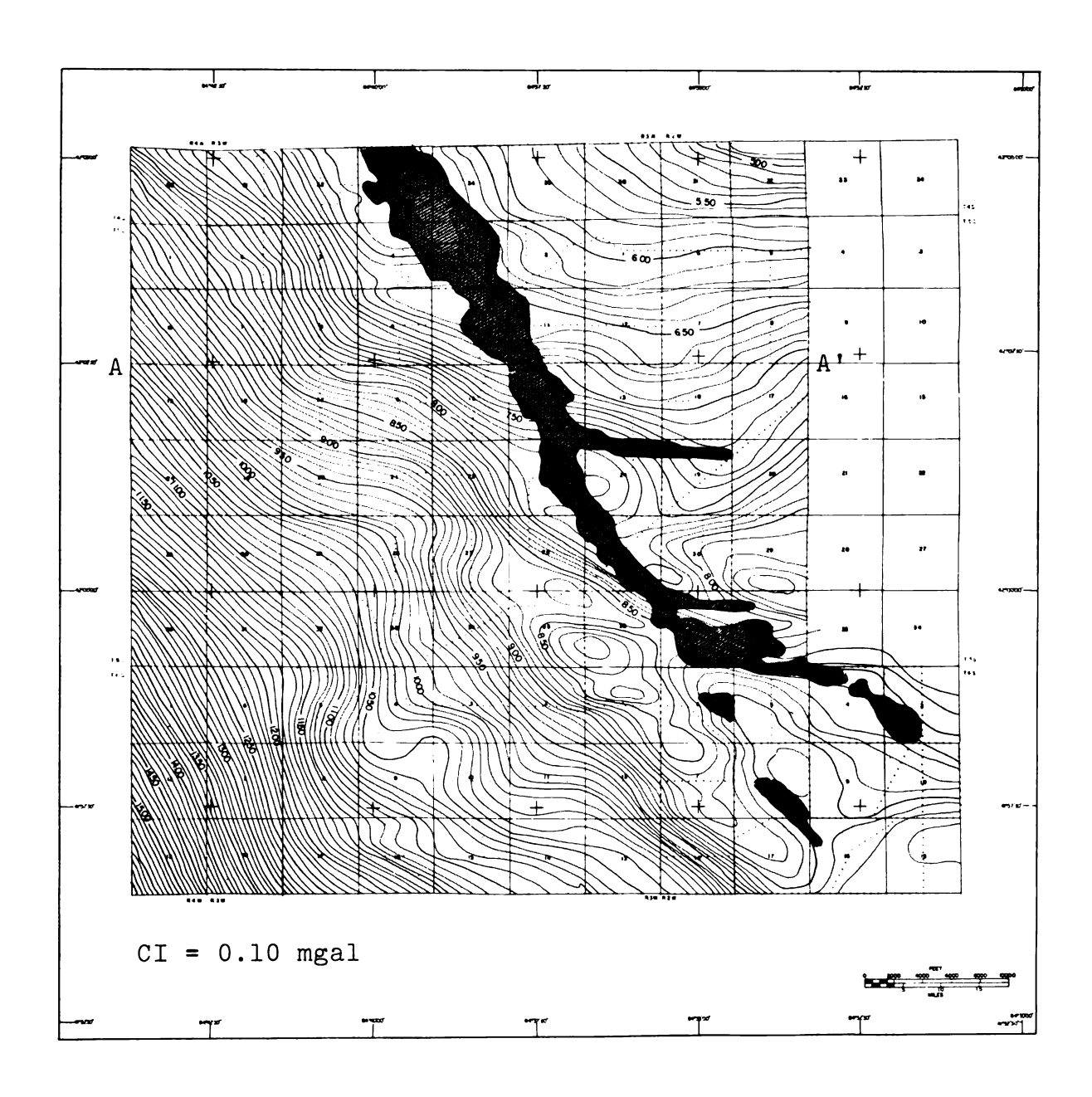


FIGURE 55.--Residual map of half wavelengths from infinity to 5,000 feet.

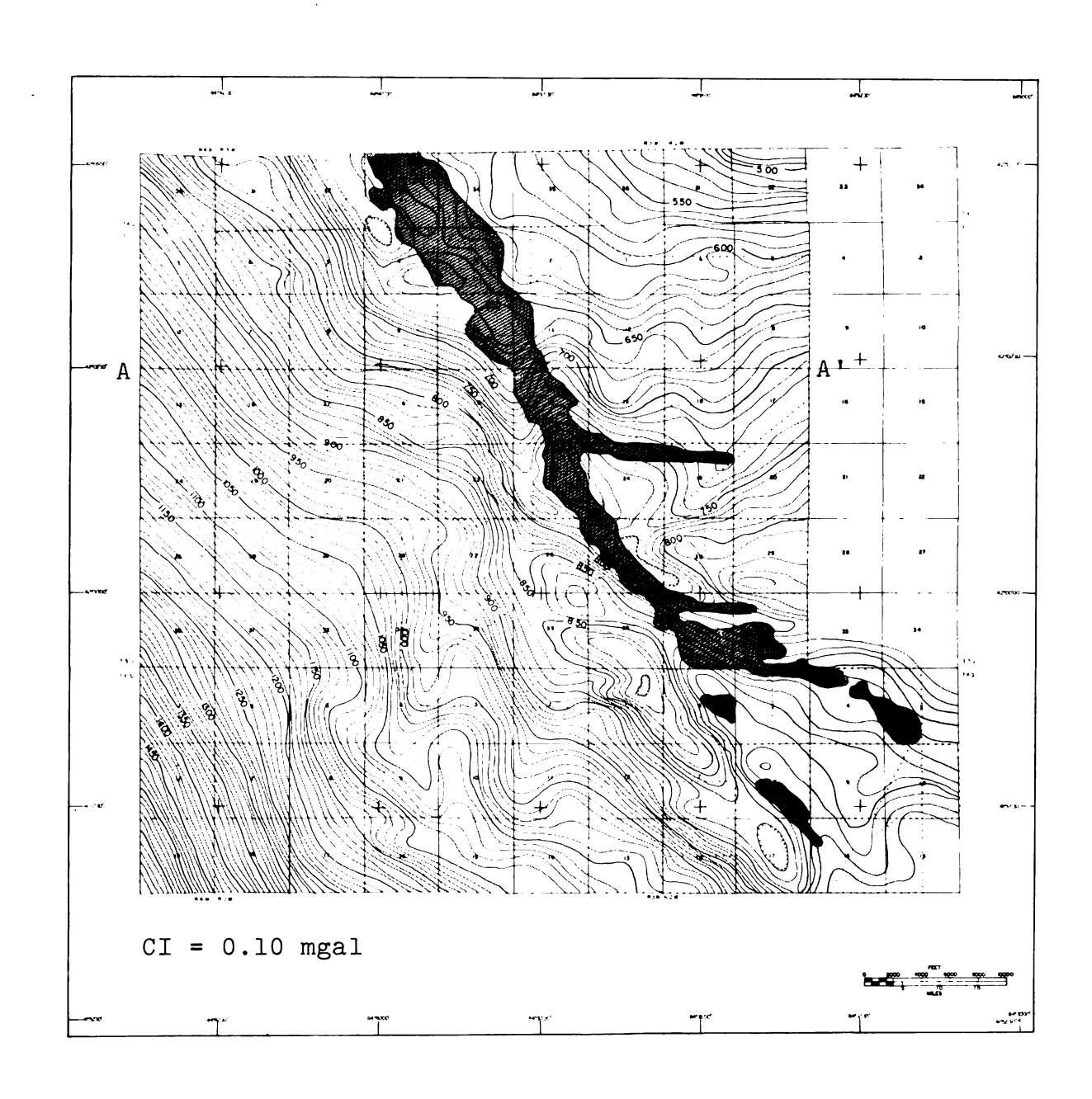


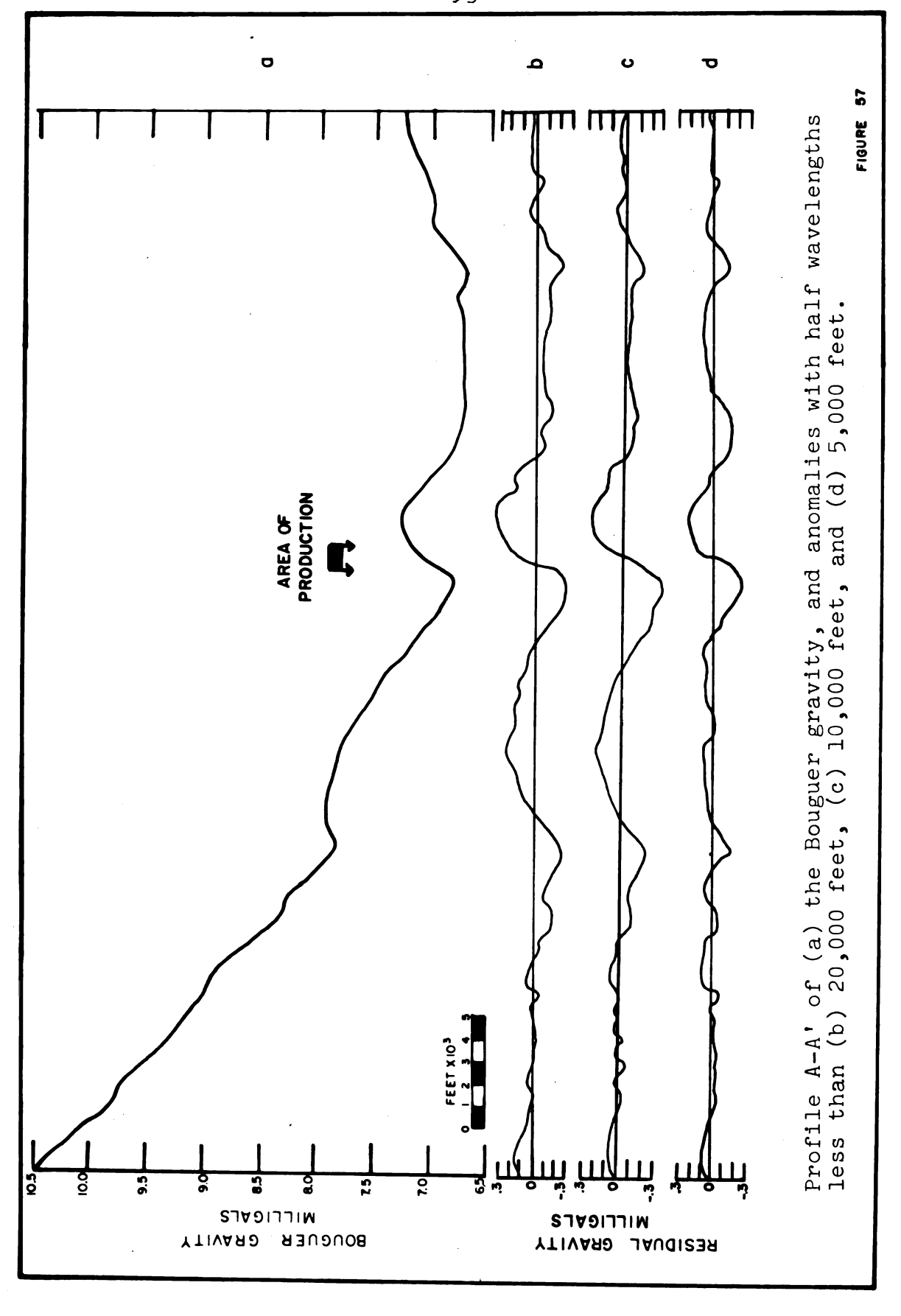
FIGURE 56.--Residual map of half wavelengths from infinity to 2,500 feet.

High Pass Filters That Exclude the Regional

High pass filters may be used to display the shorter wavelength anomalies in the same way as low pass filters are used to bring forth the long wavelengths. The high regional gradients that predominate in the results of the low pass filter are now effectively removed by convolving the data with filters that eliminate anomalies with half wavelengths greater than 20,000 feet, 10,000 feet, and 5,000 feet. These results are shown in profile form in Figure 57, and in map form in Figures 58 through 60.

Combining High and Low Pass Filters

A selective combination of high and low pass filters will result in a band pass representation. This process of data evaluation was accomplished by using a low pass filter to remove all half wavelengths greater than 20,000 feet and then re-evaluating the residuals with filters that removed half wavelengths less than 10,000 feet, 5,000 feet, and 2,500 feet. The anomalies shown in profile A-A' of Figure 61 represent half wavelengths between (a) 10,000 and 20,000 feet, (b) 5,000 and 20,000 feet, and (c) 2,500 and 20,000 feet. The residual maps from using these filters are shown in Figures 62 through 64.



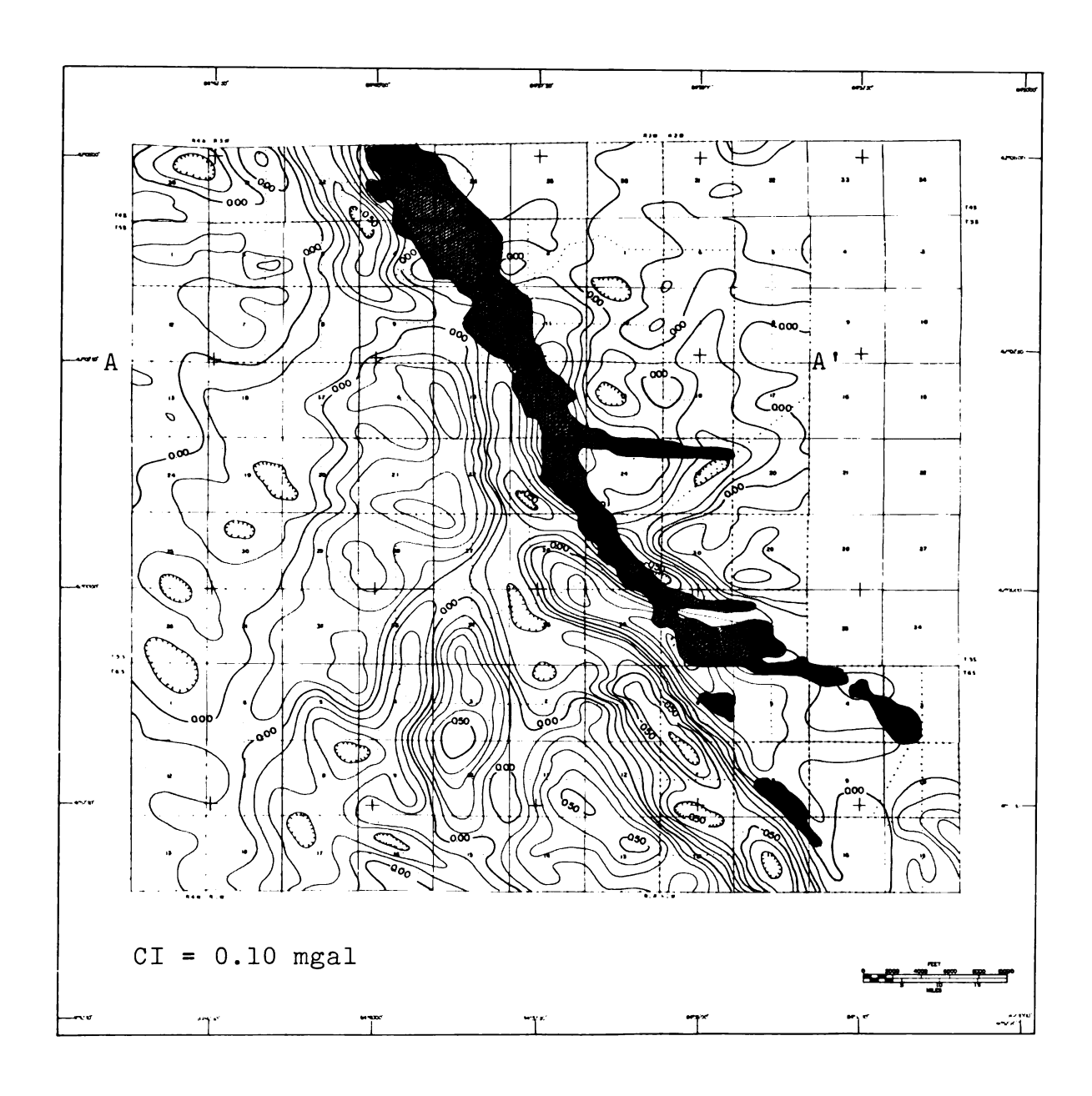


FIGURE 58.--Residual map of half wavelengths less than 20,000 feet.

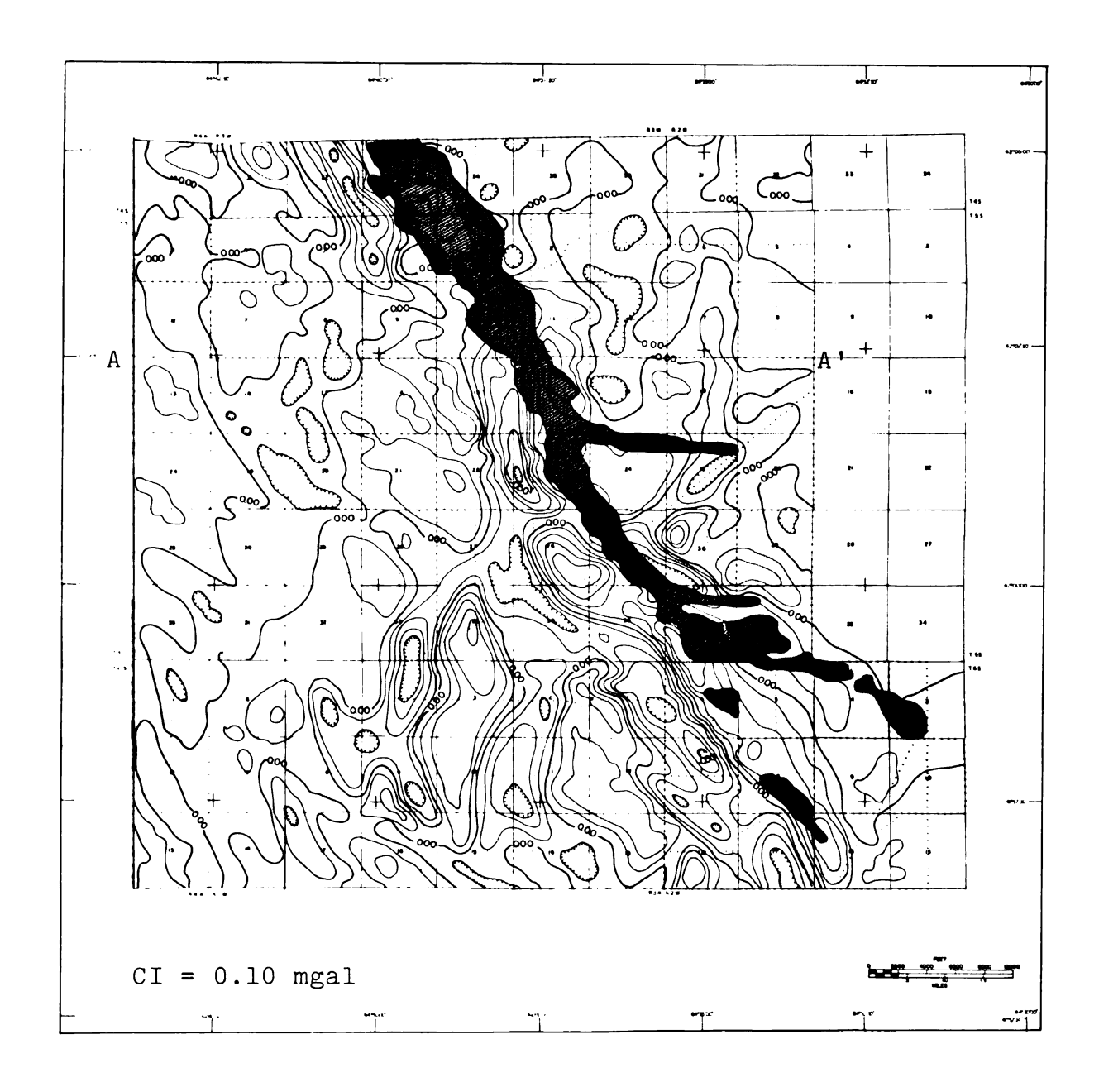


FIGURE 59.--Residual map of half wavelengths less than 10,000 feet.

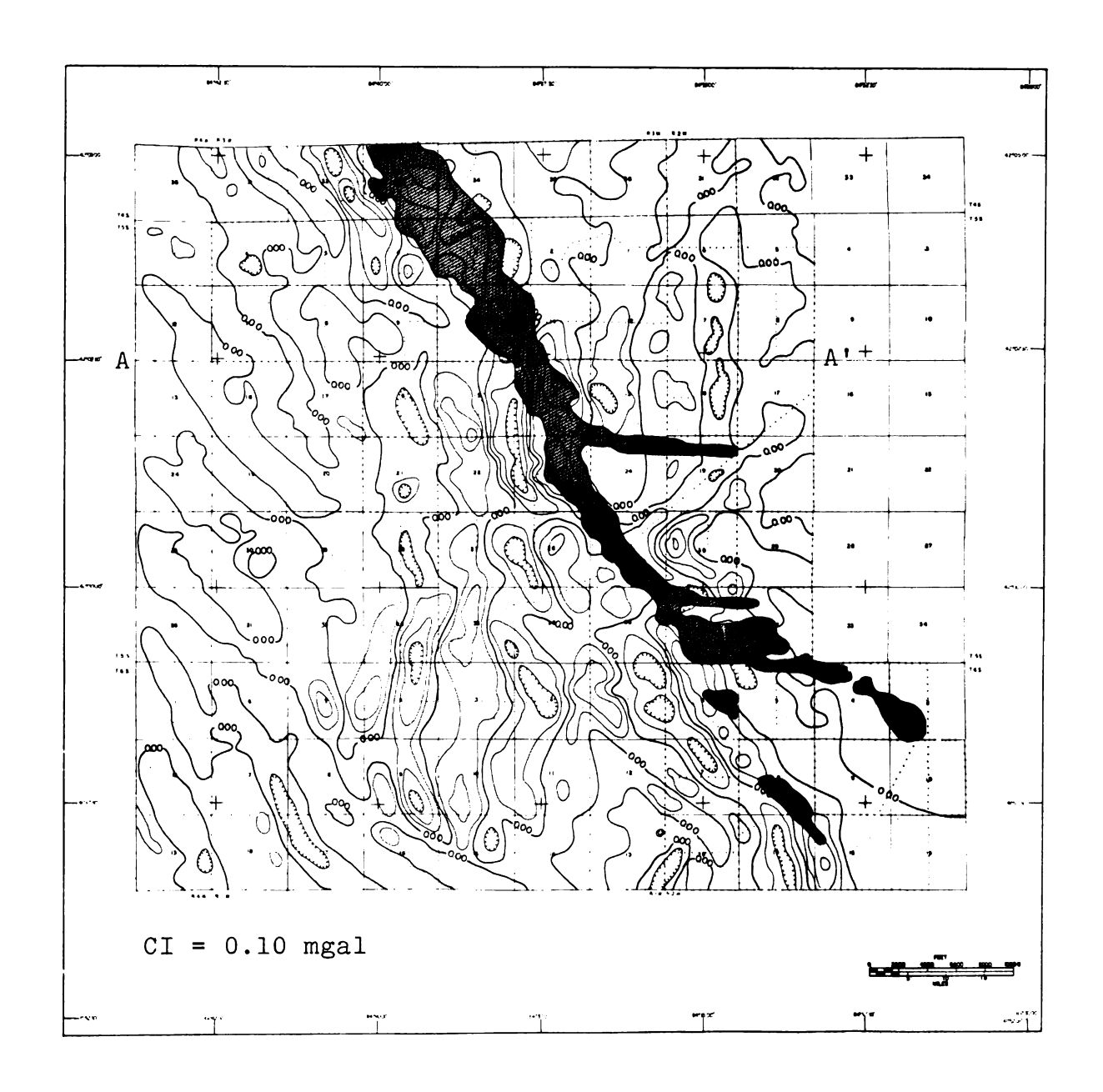
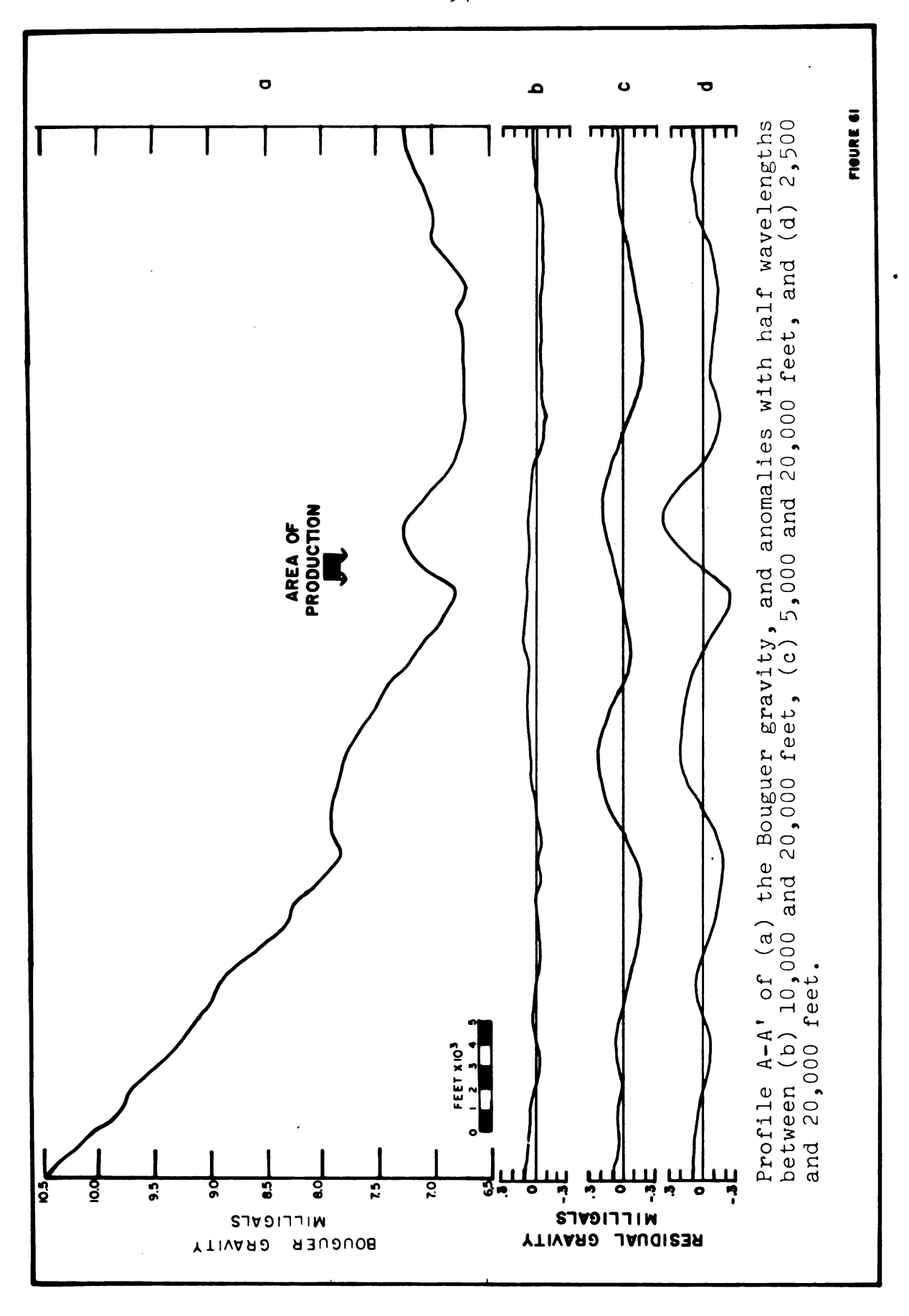


FIGURE 60.--Residual map of half wavelenghts less than 5,000 feet.



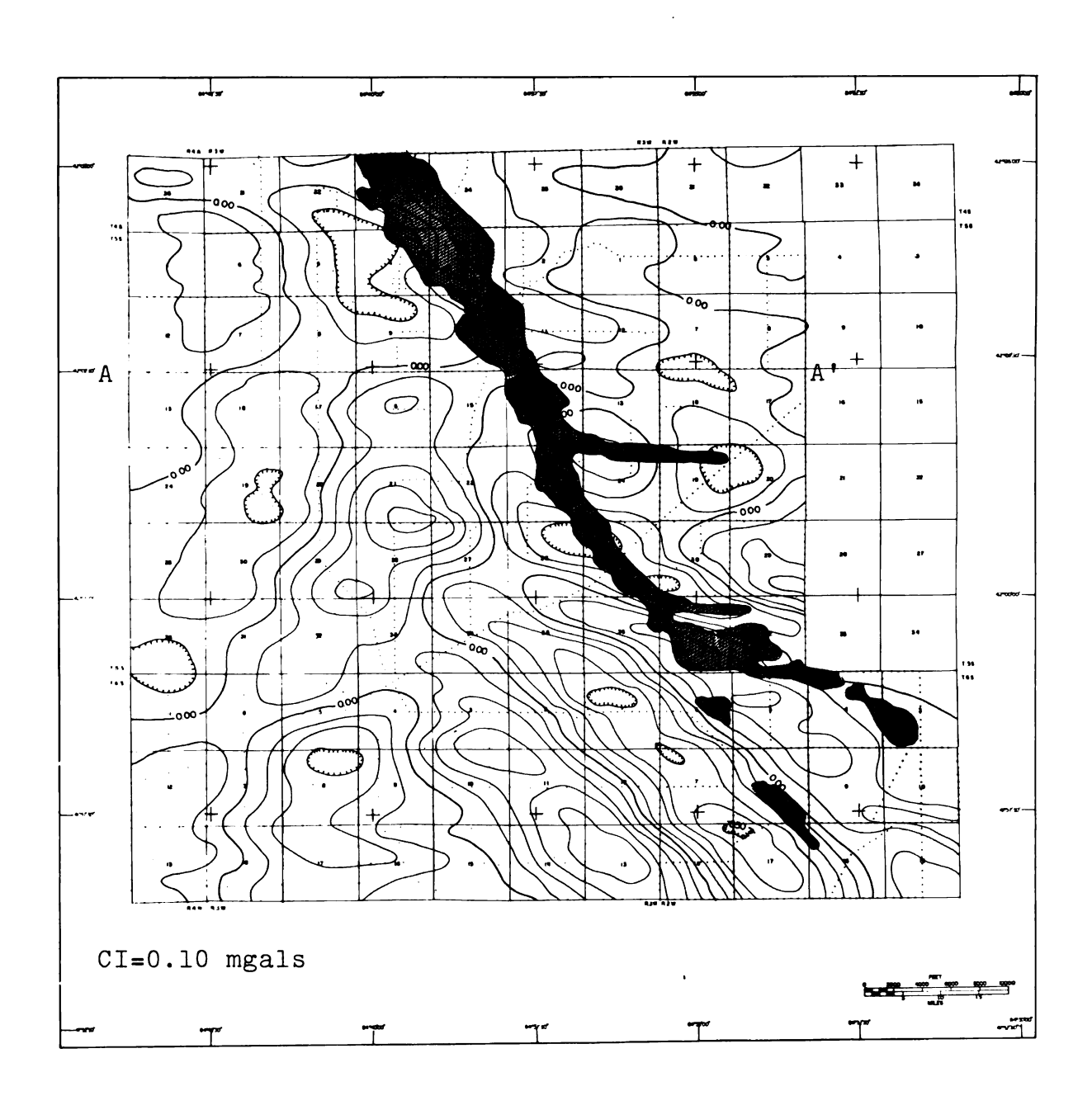


FIGURE 62.—Residual map of half wavelengths from 10,000 to 20,000 feet.

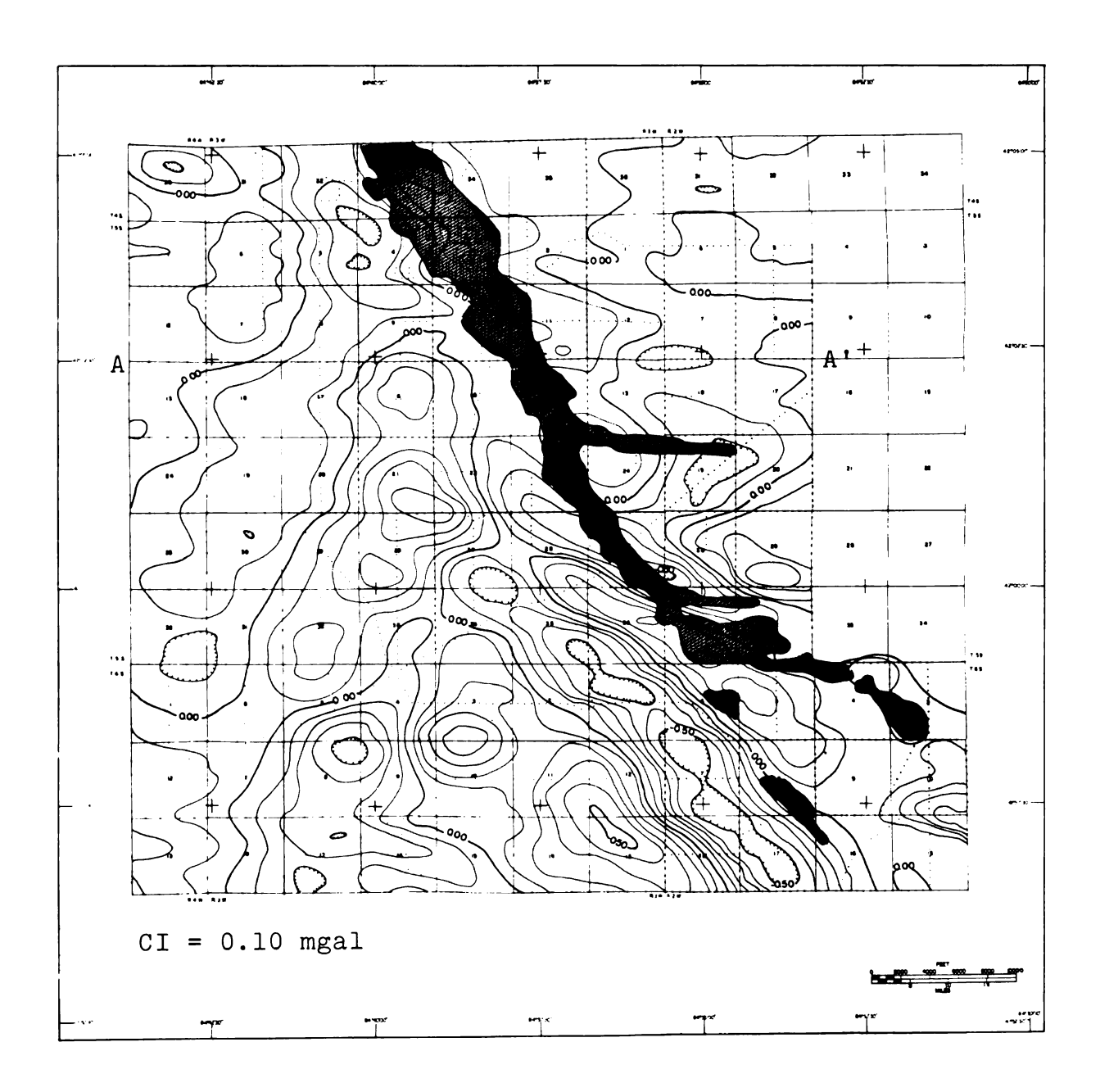


FIGURE 63.--Residual map of half wavelengths from 5,000 to 20,000 feet.

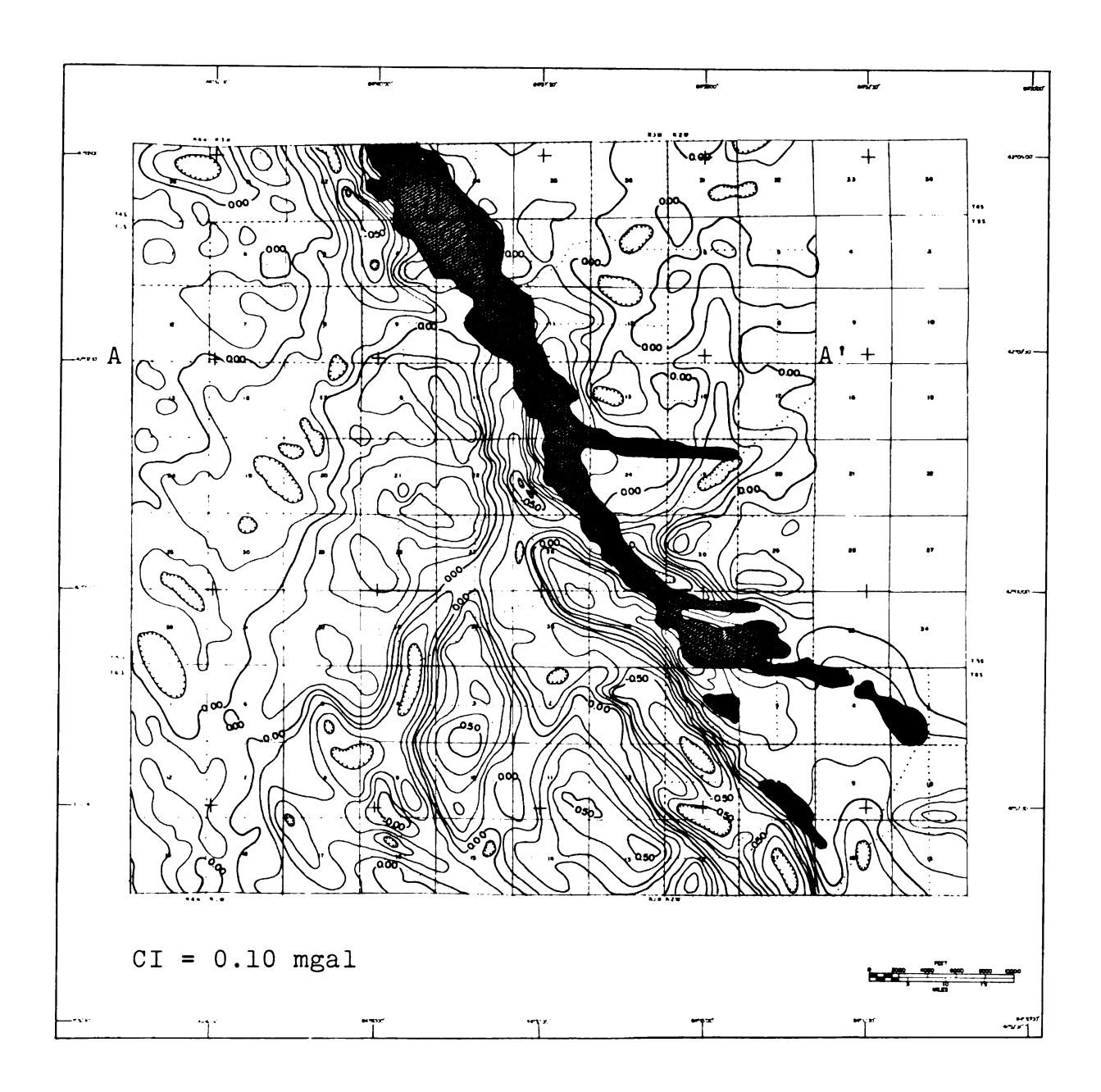


FIGURE 64.--Residual map of half wavelengths from 2,500 to 20,000 feet.

INTERPRETATION

Detectable gravity anomalies which may be associated with the Scipio Oil Field have two possible origins. The first source is the density contrast between the producing dolomite and the non-producing dolomitic limestone. The other is lithologic or structural changes within the basement complex. The magnitude and shape of the anomalies which could be expected from the density contrast directly associated with the producing body were delineated by model studies.

Model Study of the Scipio Oil Field

The geometrical form for the model was obtained by spotting all wells in the survey area and outlining the limits of production. A 610 foot thick three dimensional body was constructed, with vertical sides conforming to the irregular shape of the outlined production.

The density contrast between the producing and non-producing lithologies is governed by their contrasting composition and porosities. Core analysis from wells in the Scipio Field provided by the McClure Oil Company indicate a 1 per cent porosity for the dolomitic

limestone, and a 4 per cent average value for the dolomite. These porosity values were associated with density values through the use of a graph presented by Roth (1965). This graph, which gives the relationship between the density and porosity of water saturated dolomite and limestone, produced density values of 2.73 gm/cc for the dolomitic limestone and 2.79 gm/cc for the dolomite.

The body was given a northwest plunge equivalent to the regional dip of the Trenton Formation and the gravity effect was calculated at the surface elevations. The magnitude and configuration of the anomaly, calculated through the method described by Talwani and Ewing (1960), is shown in Figure 65.

Geological Factors Which Will Distort the Anomaly

Geological factors in the Trenton-Black River sequence and higher in the section in the Niagaran sequence will cause distortions in the gravity anomaly now shown by the model study.

The 4 per cent porosity value associated with the Scipio Field is an average value and may not represent local conditions. Table 1 shows the porosity values obtained from core analysis for six different wells in the field. These values range from 6.4 per cent down to 1.5 per cent, and would produce density values from

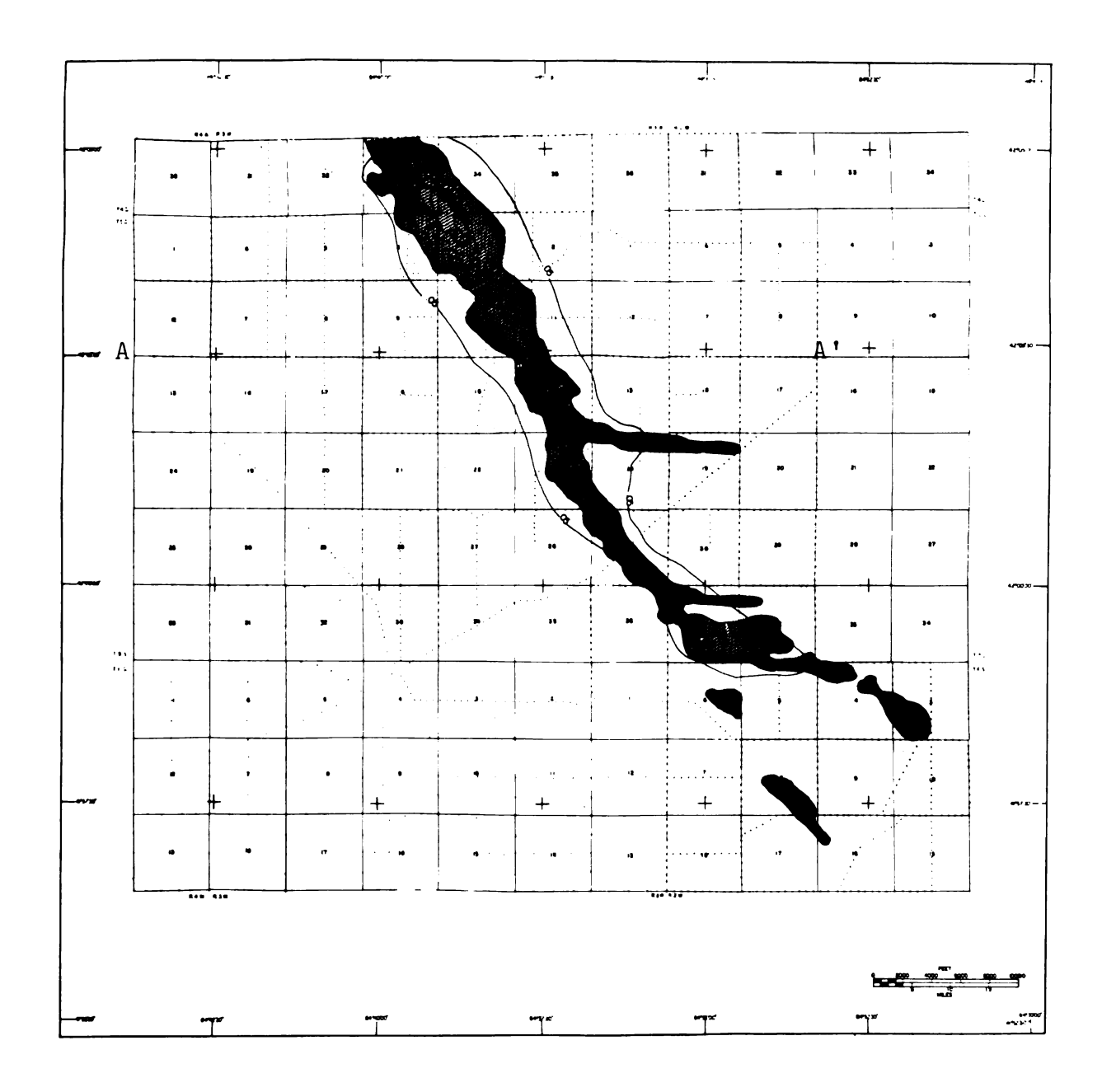


FIGURE 65.--Calculated gravity anomaly of the Scipio Oil Field for a density contrast of 0.05 gm/cc between the dolomite and dolomitic limestone.

WELL NAME		LOCATION	z	FORMATION	FOOTAGE	AVERAGE POROSITY
	SEC.	TWP	RNG.			%
BUEHRER # 1	=	S S	æ	TRENTON TRENTON BLACK RIVER	3610 — 3840 3840 — 3901 3902 — 4000	4.1 6.1 4.7
H.T. MANN#6	53	S S	×ε	BLACK RIVER	3936 – 3946 4015 – 4047 4047 – 4083	3.3 1.9 2.2
W.ROWE A-2	ю	S S	æ	TRENTON TRENTON BLACK RIVER	3727-3828 3828-3983 3983-4030	- N N 10 80 80
V.W. SKINNER#1	83	ည	¥ε	TRENTON - BLACK RIVER BLACK RIVER BLACK RIVER	3875 – 3890 3898 – 3950 3950 – 4000	5.5 1.6 2.5
BRAINARD#4	59	4	3₩	TRENTON TRENTON TRENTON	3862-3922 3922-3980 3982-4009	6.4 6.6 7.8
JORDAN#1	25	58	3W	TRENTON	3870 – 4000	5.2

2.75 gm/cc to 2.85 gm/cc. This density range would result in density contrasts between the dolomite and the host rock from the low value of 0.02 gm/cc up to 0.12 gm/cc, with associated non-measurable anomalies up to anomalies with magnitudes in excess of 0.2 mgals. For example, an average density contrast of 0.125 gm/cc would result in the anomaly shown in Figure 66.

A further complicating factor is that all producing wells do not contain a complete dolomite section. Ells (1962) points out that ". . . the amount of dolomitization of Trenton-Black River rocks along the Trend varies vertically and laterally within the section, and is by no means consistent throughout."

Reefing conditions in the Niagaran rocks will cause further distortions in the observed anomaly when the reefal development is directly associated with the geographical location of the production. Ells believes the ". . . association of the reefs with the folds is probably entirely coincidence since reefs and reef like masses are found throughout the Niagaran complex of this region." He does, however, say that ". . . the orientation, shape, and size of the reefs may be directly related to the lineation and deformational patterns of the Trend." Ferris proposes that the Trend is a direct result of the reefs, but the studies by Ells and Bishop fail to reveal any reefal pattern consistent with the Trenton-Black River production.

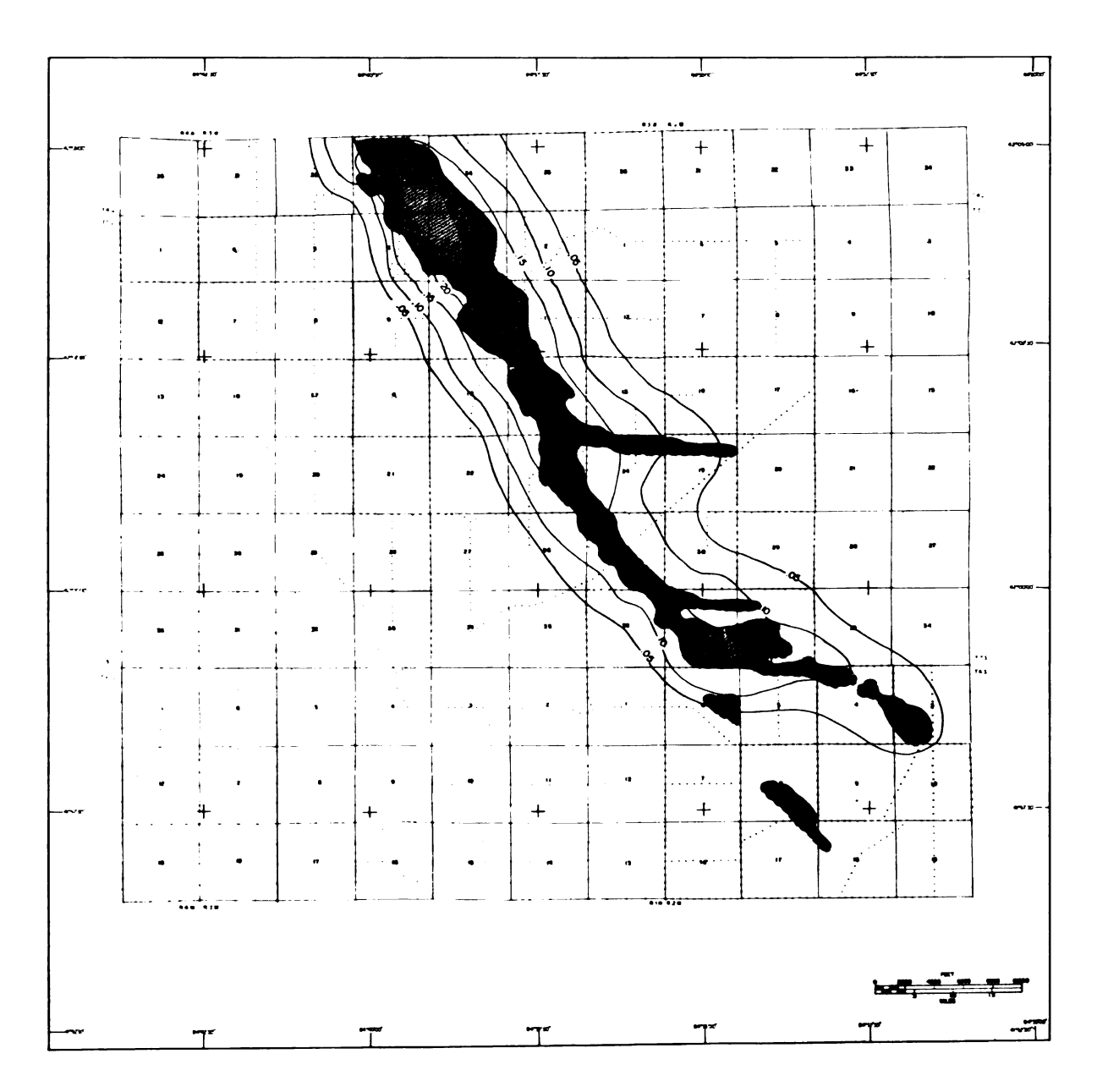


FIGURE 66.--Calculated gravity anomaly of the Scipio Oil Field for a density contrast of 0.125 gm/cc between the dolomite and the dolomitic limestone.

Residual Map Interpretation

Model studies of the Scipio Field indicate anomalies originating within the geological section of the Trenton-Black River sequence will be characterized by E-W anomaly widths between 5,000 and 10,000 feet and range in magnitude from zero to greater than 0.2 milligals.

Least Squares Residuals

Least squares residuals obtained from the seventh degree polynomial approximation to the station gravity values indicate the complexity of the Bouguer surface in the map area excludes the objective use of polynomial analysis. The residual values shown in Figure 44 do not conform to the expected pattern indicated by the model study. The residual pattern is similar to that obtained through high pass filtering methods when anomalies with widths greater than 20,000 feet are removed. This pattern is evidenced by comparing Figures 44 and 58.

<u>Double Fourier Series</u> Residuals

Double Fourier series residuals presented in Figure 46 were also obtained from operating on the station gravity values and begin to display the expected anomaly pattern. Curtailing the N-S wavelength dimension has resulted in the circular anomaly pattern observed in the lower portion of the map. The personal interpretation involved in the hand contouring of the residual

values causes some of the discrepancies observed when comparing this map with the gridded machine contoured residual values resulting from band pass and high pass filtering methods involving similar wavelengths. A re-evaluation of the double Fourier series approach would provide more useful results.

Band Pass Filtering

Band pass filtering with the band pass limited to the expected half wavelength range is successful in delineating linear patterns which coincide with the general pattern of production. E-W anomaly widths between 5,000 and 15,000 feet shown in Figure 50 demonstrate the ability of extracting selected pertinent information from the Bouguer gravity map. Anomalies ranging from 2,500 to 7,500 feet in width shown in Figure 51 further refine the anomaly pattern.

High Pass Filtering

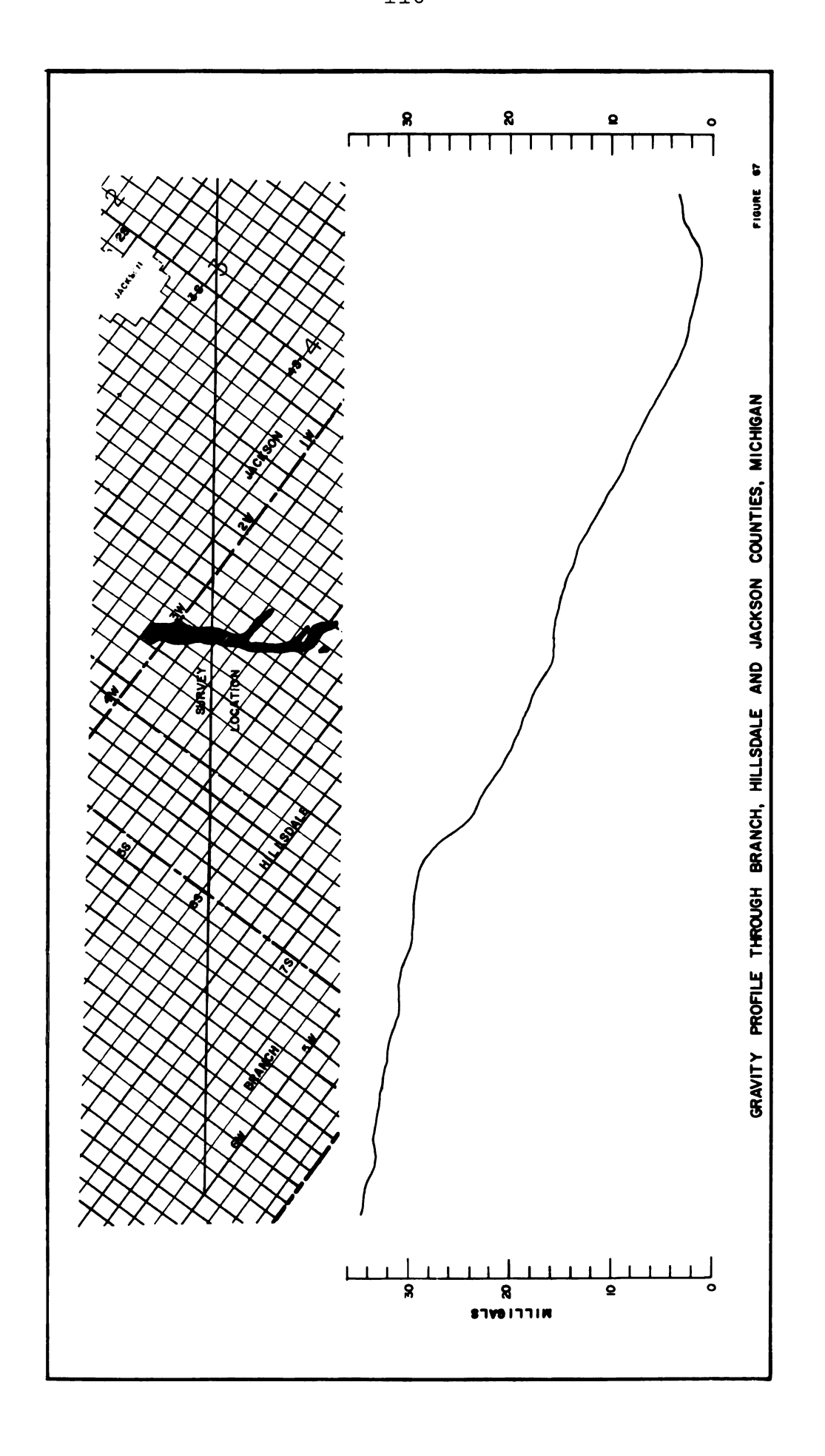
High pass filtering also delineates the linear anomalies associated with the outlined production. Figures 59 and 60 include anomalies up to 10,000 feet and 5,000 feet respectively. The inclusion of the shorter wavelengths has the negative effect of showing non-pertinent information which locally distorts the anomaly pattern.

The geographical distribution of the well data does not permit quantitative evaluation of linear anomalies depicted but not associated with the production. The similarity in magnitude and shape of these anomalies and the anomalies associated with the production indicate that geological conditions exemplifying the producing zone may exist elsewhere in the map area.

Regional Interpretation

Ells (1962, 1966) has speculated that the lineation and interconnection of the synclines associated with the Albion-Scipio Field is controlled by slight lateral movement along a basement fault. Basement control for this same feature is also suggested by Rudman, Summerson, and Hinze (1965) on the basis of correlative regional gravity anomaly trends which primarily originate from structural and lithologic variations within the basement rocks.

In order to investigate the correlation between the basement and the Albion-Scipio Field, a representative regional gravity profile shown in Figure 67 has been drawn from the southern part of Branch County through Hillsdale County to the center of Jackson County. The profile strikes northeast approximately perpendicular to the strike of the "Trend" and the regional gravity contours. The source of the gravity profile is unpublished gravity surveys which have observations at one-fourth mile intervals along all roads.



The dominant aspect of the profile is the negative gradient to the northeast. This negative gradient is on the southwestern edge of the gravity minimum which borders the Mid-Michigan Gravity High. This large positive gravity feature and its bordering negatives has a marked similarity to the Mid-Continent Gravity High which extends from Lake Superior southward into Kansas (Thiruvathukal, 1963). Bacon (1957) on the basis of gravity data and Hinze, O'Hara, Trow, and Secor (1966) from aeromagnetic data suggest that this feature extends through Lake Superior and connects with the Mid-Michigan Gravity High. Thiruvathukal (1963) has modeled several possible geological sources for the regional gravity high and its parallel minimums. He suggests that the gravity lows may be due to clastic wedges similar to those observed associated with the gravity minimums of the Mid-Continent gravity feature at the western end of Lake Superior. An alternative interpretation offered by him involves a downward flexure of the crust beneath the Mid-Michigan gravity feature. White (1966) also suggests this as a possible source for the minimum gravity anomalies associated with the Mid-Continent Gravity High in the Lake Superior region.

The Bouguer gravity anomaly map of the survey area shown in Figure 42 indicates a marked change in the regional gradient along the strike of the outlined production. This is more clearly shown in Figure 53 which

includes gravity anomalies of half wavelengths from 20,000 feet to infinity. This change in gradient is illustrated on the regional gravity profile of Figure 67 as a flattening of the gradient east of the Albion-Scipio Field. Approximately four miles further east the gradient increases and coincides with the gradient observed to the west of the "Trend." Detailed magnetic data is unavailable for this area, but the regional vertical magnetic intensity anomaly map (Hinze, 1963) does not display a similar anomaly.

The decrease in the gravity gradient east of the Albion-Scipio Field is interpreted to be the result of a positive gravity anomaly which interrupts the normal gradient and originates from a semi-infinite slab or fault source. The gradients of the ioslated positive anomaly suggests that the center of the anomalous mass is at a depth of approximately one mile. This depth would place the source of the anomaly at or near the basement surface (Cohee, 1945). This type of anomaly could be attributed to topographic relief on the basement surface with a scarp located approximately one-half mile east of the Albion-Scipio Field. Assuming that the Cambrian sandstones which butt up against and overlie this feature have a density of 2.45 gm/cc and the basement rocks have a density of 2.70 gm/cc, the 2.5 mgal anomaly would necessitate having around 800 feet relief on the basement scarp.

This interpreted basement feature may be either a fault or fault line scarp which parallels the Albion-Scipio Field. Reactivation of this feature in Paleozoic time could have fractured the overlying competent sediments and provided the necessary conditions for the development of the Albion-Scipio reservoir.

Summary of Interpretation

Residual

Three different methods were used in removing the regional effects from the Bouguer anomaly map. The polynomial and double Fourier series methods mathematically approximate the gravity surface, and the residuals are obtained by taking the difference between the station value and the approximated surface at the data point. The complexity of the Bouguer surface in the survey area rendered both of these methods to be unsatisfactory.

Fourier analysis operates on data which has been interpolated onto a uniform spacing. The band pass and high pass filters displayed all data having wavelengths within a predetermined band or range. These filters were successful in delineating linear anomalies coincident with the outlined production. The anomalies are similar to the 0.2 mgal anomalies theoretically calculated from a gravity model of the producing zone.

Regional

All of the regional maps display a change in the regional gravity gradient paralleling the outlined production. A regional profile striking northeast into the basin reveals this to be a displacement in the regional gradient. Basement topographic relief in the form of a fault-line scarp is postulated as the cause of this displacement, and renewed activity associated with this zone may have provided the necessary conditions for the development of the Albion-Scipio Field.

CONCLUSIONS

A detailed gravity survey was conducted in the north central portion of Hillsdale County, Michigan, for the purpose of delineating gravity anomalies associated with the Scipio Oil Field. A method was developed and tested with theoretical model studies, whereby a station elevation factor can be calculated for each station in the survey. This method involved using a polynomial function of the elvation and station coordinates to obtain the desired elevation factor.

Conclusions drawn from the model studies associated with the variable elevation factor:

- 1. Rapid variations in the surface topography do not affect the calculated elevation factor when the topographic expression is not associated with a near-surface density change. This eliminates the possibility of creating anomalies which are topographically associated.
- 2. An intermediate density value is obtained in the immediate vicinity of a sharp near-surface density change.

- 3. Steep gravity gradients caused by near-surface sources have a negative effect on the accuracy.
- 4. The magnitude and lateral extent of the negative effect caused by sharp density changes and steep gravity gradients related to near surface sources is greatly reduced by decreasing the station spacing.
- 5. The calculated elevation factor, being a function of the station elevation differences within the data set, permits the reduction of the data to some geologically significant non-horizontal datum with the calculated elevation factor, and then to a horizontal datum with a pre-selected elevation factor.

Conclusions related to the field data studies:

The field data was corrected with a calculated individual station elevation factor and three different approaches used in removing the regional effects from the Bouguer anomaly map. The polynomial and double Fourier series methods were not effective in adequately removing the complex regional component present in the study area. Band pass and high pass filtering of the gridded Bouguer map effectively isolated elongate discontinuous anomalies coincident with the outline of the production. These anomalies are similar in magnitude and shape to theoretical anomalies calculated from a

gravity model of the producing zone which employs porosity and density values obtained from core analysis.

Conclusions related to the regional profile:

A regional profile striking northeast into the basin reveals a displacement in the uniform gravity gradient. This displacement occurs along the Albion-Scipio Field and is interpreted to originate from basement topographic relief in the form of a fault-line scarp. Renewed activity along the fault associated scarp may have established the conditions necessary for the development of the linear Albion-Scipio Field.

REFERENCES

- BACON, L. O. (1957) Relationship of gravity to geologic structure in Michigan's upper peninsula: Institute on Lake Superior Geology, p. 54.
- BISHOP, W. C. (1967) Study of the Albion-Scipio Field of Michigan: Masters Thesis, Michigan State University.
- BLACKMAN, R. B., and TUKEY, J. W. (1958) Power spectra: New York, Dover.
- COHEE, G. V. (1945) Oil and gas investigation preliminary: U. S. Department of the Interior, Geological Survey, Chart 9.
- DEAN, W. C. (1958) Frequency analysis for gravity and magnetic interpretation: Geophysics, v. 23, p. 97.
- ELLS, G. D. (1962) Structures associated with the Albion-Scipio Oil Field trend: Michigan Department of Conservation, Geological Survey Division.
- FERRIS, C. (1962) Gravity can find another Albion-Scipio: Oil and Gas Journal, October.
- FRASER, D. C., FULLER, B. D., and WARD, S. H. (1966) Some numerical techniques for application in mining exploration: Geophysics, v. 31, no. 6, p. 1066.
- GRANT, F. S., and ELSAHARTY, A. F. (1962) Bouguer gravity corrections using a variable density: Geophysics, v. 27, p. 616.
- HAMMING, R. W. (1962) Numerical methods for scientists and engineers: McGraw-Hill, New York.
- HINZE, W. J., O'HARA, N. W., TROW, J. W., and SECOR, G. B. (1966) Aeromagnetic studies of Eastern Lake Superior: American Geophysical Union Mon. 10, p. 95.

- HINZE, W. J. (1963) Regional gravity and magnetic anomaly maps of the southern peninsula of Michigan: Michigan Geological Survey, Report of Investigation 1.
- IVANHOE, L. F. (1957) Chart to check elevation factor effects on gravity anomalies: Geophysics, v. 22, no. 3, p. 643.
- JAMES, W. R. (1966) Fortran IV program using double Fourier series for surface fitting of irregularly spaced data: Computer Contribution 5, State Geological Survey, The University of Kansas, Lawrence, Kansas.
- JUNG, K. (1953) Some remarks on the interpretation of gravitational and magnetic anomalies: Geophysical Prospecting, v. 1, no. 1, p. 29.
- LEGGE, J. A., Jr. (1944) A proposed least squares method for the determination of the elevation factor: Geophysics, v. 9, p. 175.
- NETTLETON, L. L. (1939) Determination of density for the reduction of gravimeter observations: Geophysics, v. 4, p. 176.
- ROTH, J. N. (1965) A gravitational investigation of fracture zones in Devonian rocks in portions of Arenac and Bay Counties, Michigan: Masters Thesis, Michigan State University.
- SERVOS, G. G. (1965) A gravitational investigation of Niagaran reefs in southeastern Michigan: Ph.D. Thesis, Michigan State University.
- SIEGERT, A. J. F. (1942) Determination of the Bouguer correction constant: Geophysics, v. 7, p. 29.
- TALWANI, M., and EWING, M. (1960) Rapid computation of the gravitational attraction of three-dimensional bodies of arbitrary shape: Geophysics, v. 25, no. 1, p. 203.
- THIRUVATHUKAL, J. V. (1963) A regional study of basement and crystal structures in the southern peninsula of Michigan: Masters Thesis, Michigan State University.
- VAJK, R. (1956) Bouguer corrections with varying surface density: Geophysics, v. 21, p. 1004.
- VEATCH, J. O. Soil survey Hillsdale County, Michigan: United States Department of Agriculture, Series 1924, No. 10.

WHITE, WALTER S. (1966) Geologic evidence for crustal structure in the western Lake Superior basin: American Geophysical Union Mon. 10, p. 28.

MICHIGAN STATE UNIV. LIBRARIES
31293100340524